Universidade Estadual de Campinas
Faculdade de Engenharia Elétrica e de Computação

Gustavo Rodrigues de Lima Tejerina

An extension to the η-μ and to the κ-μ fading models

Uma extensão para os modelos de desvanecimento η-μ e κ-μ

Campinas
2018

Universidade Estadual de Campinas
Faculdade de Engenharia Elétrica e de Computação

Gustavo Rodrigues de Lima Tejerina

An extension to the η-μ and to the κ-μ fading models

Uma extensão para os modelos de desvanecimento η-μ e κ-μ

Doctorate thesis presented to the School of Electrical and Computer Engineering in partial fulfillment of the requirements for the degree of Doctor in Electrical Engineering. Concentration area: Telecommunications and Telematics

Tese de doutorado apresentada à Faculdade de Engenharia Elétrica e de Computação como parte dos requisitos exigidos para a obtenção do título de Doutor em Engenharia Elétrica. Área de concentração: Telecomunicações e Telemática.

Orientador: Prof. Dr. Michel Daoud Yacoub

Este exemplar corresponde à versão final da tese defendida pelo aluno, e orientada pelo Prof. Dr. Michel Daoud Yacoub

Campinas
2018

Agência(s) de fomento e nº(s) de processo(s): CNPq, 141804/2014-9
ORCID: https://orcid.org/0000-0002-7879-0642

Ficha catalográfica
Universidade Estadual de Campinas
Biblioteca da Área de Engenharia e Arquitetura
Luciana Pietrosanto Milla - CRB 8/8129

T235e

Tejerina, Gustavo Rodrigues de Lima, 1987-
An extension to the η-μ and to the κ-μ fading models / Gustavo Rodrigues de Lima Tejerina. – Campinas, SP : [s.n.], 2018.

Orientador: Michel Daoud Yacoub.
Tese (doutorado) – Universidade Estadual de Campinas, Faculdade de Engenharia Elétrica e de Computação.

1. Sistemas de comunicação sem fio. 2. Canal em desvanecimento. 3. Modelos estatísticos. 4. Distribuição (Probabilidades). I. Yacoub, Michel Daoud, 1955-. II. Universidade Estadual de Campinas. Faculdade de Engenharia Elétrica e de Computação. III. Título.

<u>Informações para Biblioteca Digital</u>

Título em outro idioma: Uma extensão para os modelos de desvanecimento η-μ e κ-μ
Palavras-chave em inglês:
Wireless communication systems
Fading channels
Statistical models
Distribution (Probability)
Área de concentração: Telecomunicações e Telemática
Titulação: Doutor em Engenharia Elétrica
Banca examinadora:
Michel Daoud Yacoub [Orientador]
Carlos Eduardo Câmara
Edson Luiz Ursini
Heloisa Peixoto de Barros Pimentel
Iury Bertollo Gomes Pôrto
Data de defesa: 31-07-2018
Programa de Pós-Graduação: Engenharia Elétrica

COMISSÃO JULGADORA - TESE DE DOUTORADO

Candidato: Gustavo Rodrigues de Lima Tejerina
Data de Defesa: 31 de julho de 2018

Título da Tese: "An extension to the η-μ and to the κ-μ fading models".

Título da Tese em Português: "Uma extensão para os modelos de desvanecimento η-μ e κ-μ".

Prof. Dr. Michel Daoud Yacoub (Presidente, FEEC/UNICAMP)
Prof. Dr. Carlos Eduardo Câmara (UniAnchieta)
Prof. Dr. Edson Luiz Ursini (FT/UNICAMP)
Dra. Heloisa Peixoto de Barros Pimentel (Consultora)
Dr. Iury Bertollo Gomes Pôrto (Câmara dos Deputados)

A ata de defesa, com as respectivas assinaturas dos membros da Comissão Julgadora, encontra-se no processo de vida acadêmica do aluno.

To Jacqueline, Gabriela, Chloé
and Leonardo.

Agradecimentos

Há exatos cinco anos, logo após o exame de qualificação do mestrado, eu estava estendendo minha jornada de pesquisador na Unicamp. Entusiasmado com a oportunidade, enfrentei a minha permanência em Campinas como um meio de amadurecimento científico e profissional. Naquela época, não imaginava que conheceria pessoas incríveis ou que reencontraria o amor, apenas sabia que o encerramento se daria por meio de uma tese e uma *soutenance*. De fato, o desfecho idealizado está para acontecer, porém, hoje, percebo que o doutoramento reflete, acima de tudo, o conjunto das minhas experiências e vivências adquiridas neste árduo período. Pensando nelas, serei eternamente grato às pessoas que estavam presentes e acompanharam a minha jornada, em especial,

Ao meu orientador, Prof. Michel, pelos excelentes conselhos, pela paciência e por acreditar no meu trabalho.

À Jacqueline e à Gabriela, por estarem sempre presentes e por saberem que eu nasci assim.

Ao Danilo, por me encorajar e por me mostrar que a vida é feita de encontros e desencontros.

Ao Leonardo e à Chloé, pelo suporte afetivo.

Ao Gabriel, Ivan e Jardel, por serem minha família em Barão Geraldo.

Ao Kaio e à Bruna, pelos nossos encontros, discussões, jantares, e por existirem em minha vida.

À família Carlos, pelas viagens ao redor do mundo e as noites de carteado.

Aos meus colegas de Wisstek, pelo convívio diário.

À FEEC/UNICAMP por proporcionar aos alunos um ambiente único de ensino e pesquisa.

Ao CNPq, por financiar minha pesquisa durante todo o período do doutorado.

A todos que de certa forma colaboraram neste período de dificuldades e aprendizado.

Be wiser.

Michel Daoud Yacoub

I'm on the right track, baby
I was born this way.

Born this way – Stefani J. Germanotta

Abstract

An extension to the η-μ and to the κ-μ fading models is proposed. This is achieved by introducing a parameter that quantifies the clustering imbalance between in-phase and quadrature components. For the η-μ fading model, the introduction of such an imbalance parameter leads to a new fading scenario, with both envelope and phase distributions differing from the original η-μ formulations, rendering this model even more flexible. Interestingly, in spite of introducing a new parameter, the formulations are still given in closed-form expressions. For the κ-μ fading model, the introduction of such an imbalance parameter modifies only the phase of the process, keeping the envelope the same. Interestingly, using some mathematical identities developed along the derivation process, it has been possible to find an excellent approximation for the phase distribution, given in closed-form, avoiding the intricacy of the integral solution. In both fading models, first order and higher order statistics are found in closed-form formulations. In addition, the same approximation procedure is carried out for the α-η-κ-μ phase distribution, resulting in an unprecedented never before seen series expansion expression.

Key-words: wireless fading model, η-μ complex model, κ-μ complex model, α-η-κ-μ complex model, phase-envelope joint distribution, phase distribution, envelope distribution.

Resumo

Este trabalho tem como objetivo apresentar uma extensão para o modelo de desvanecimento η-μ e κ-μ. Para tal, foi necessário introduzir um novo parâmetro que quantifica o desbalanceamento de clusters de multipercurso entre as componentes fase e quadratura. No modelo η-μ, tal parâmetro permitiu explorar novos cenários de desvanecimento em ambas distribuições de fase e envoltória, tornando o modelo mais flexível. Apesar da inserção deste novo parâmetro, as formulações obtidas ainda se encontram em forma fechada. Para o modelo κ-μ, a introdução do parâmetro de desbalanceamento de clusters modificou apenas a distribuição de fase do processo, mantendo a envoltória idêntica ao modelo tradicional. Devido à complexidade do modelo κ-μ, as equações exatas de fase são apresentadas no formato integral. Interessantemente, usando algumas identidades matemáticas obtidas ao longo dos procedimentos, foi possível definir uma excelente aproximação para a distribuição de fase, dada em forma fechada. Este resultado evita qualquer possível complicação decorrente do processo de integração observado na solução exata. Para ambos os modelos, estatísticas de primeira ordem e ordem superior são apresentadas em expressões em forma fechada. Além disso, aproveitando os métodos aqui desenvolvidos, uma aproximação em expansão em série da distribuição de fase do modelo α-η-κ-μ também é apresentada.

Palavras-chave: modelos desvanecimento sem fio, modelo complexo η-μ, modelo complexo κ-μ, modelo complexo α-η-κ-μ, distribuição conjunta de fase-envoltória, distribuição de fase, distribuição da envoltória.

List of Figures

List of Acronyms

ABER	Average Bit Error Rate
AF	Amount of Fading
AFD	Average Fade Duration
ASER	Average Symbol Error Rate
BFSK	Binary Frequency Shift Keying
BPSK	Binary Phase Shift Keying
CDF	Cumulative Density Function
FM	Frequency Modulation
MGF	Moment Generating Function
LCR	Level Crossing Rate
PCR	Phase Crossing Rate
PDF	Probability Density Function
RMS	Root Mean Square
SNR	Signal-to-Noise Ratio

List of Functions

$\mathrm{erf}(z)$	Error function [1, Eq. (7.1.1)]
$H_{p,q}^{m,n}(z)$	Fox's H-function [2, Eq. (8.3.1.1)]
$\Gamma(z)$	Gamma function [1, Eq. (6.1.1)]
$\Gamma(a, z)$	Incomplete Gamma function [1, Eq. (6.5.3)]
$H(z)$	Heaviside step function [1, Eq. (29.1.3)]
${}_1F_1(a; b; z)$	Kummer confluent hypergeometric function [1, Eq. (13.1.2)]
${}_2F_1(a_1, a_2; b; z)$	Gauss hypergeometric function [1, Eq. (15.1.1)]
${}_pF_q((a_p); (b_q); z)$	Generalized hypergeometric function [2, Eq. (7.2.3.1)]
$F_1(a; b_1, b_2; c; w, z)$	Appell hypergeometric function of two variables [2, Eq. (7.2.4.1)]
$\phi_3(b; c; w, z)$	Confluent form of the Appell function [2, Eq. (7.2.4.7)]
$L_n^{\lambda}(z)$	Generalized Laguerre polynomial [1, Eq. (22.3.9)]
$G_{p,q}^{m,n}(z)$	Meijer G-function [2, Eq. (8.2.1.1)]
$I_0(z)$	Modified Bessel function of the first kind and order zero [1, Eq. (9.6.16)]
$I_\nu(z)$	Modified Bessel function of the first kind and arbitrary order ν [1, Eq. 9.6.20]
$(z)_k$	Pochhammer symbol [1, Eq. (6.1.22)]
$\mathrm{sgn}(z)$	Sign function [3]

Contents

Chapter 1

Introduction

Wireless communications are considered the bridge that undeniably connect every person and, soon, every object in the world. Recent predictions estimate a total of 20 billion wireless devices activated by the year 2020 [4]. As the number of daily users constantly increases, new technological demands, such as higher data speed, low latency and energy efficient devices, arise as intricate challenges. With the advent of 5G, some of these problems are expected to be solved, and wider range of applications are to be developed [5], these include: (i) Vehicle-to-vehicle and vehicle-to-infrastructure communication; (ii) autonomous vehicles; (iii) remote health services and health care monitoring; (iv) augmented and virtual reality; and (v) smart cities and smart homes. Hence, to attain such technological development and in order to encompass all possible communication scenarios, the wireless channel has to be properly understood and characterized.

Fading is certainly a phenomenon to be deeply investigated. As well known, wireless signals are characterized by long and short term fadings [6]. The former is defined by the shadowing phenomenon, which occurs due to large scale obstructions between transmitter and receiver, e.g. mountains and buildings, and due to the absence of diffraction at very high frequencies, i.e. 20GHz to 300GHz. The short term fading, by its turn, is related to multipath propagation. This phenomenon is a consequence of the physical singularities that affect electromagnetic waves, such as: (i) reflection; (ii) refraction; (iii) diffraction; and (iv) scattering. As a result, the signal is subjected to constructive and destructive interferences, and delays. Signals affected by multipath fluctuates rapidly, reaching a dynamic range of tens of decibels [7].

In an attempt to better characterize the fading phenomenon, a set of distributions have been proposed to describe the radio channel statistics. It is known that the long-term signal variation is well characterized by the Lognormal distribution. Some alternatives for it, with no physical ground, e.g. Gamma, Nakagami-m, have been used only for the sake of mathematical tractability. The short-term signal variation is well described by several established models, most notably Rayleigh [8], Rice [9], and Hoyt [10]. Such models have been derived jointly in terms of envelope and phase. Even though both envelope and phase probability density functions (PDFs) are obtained in closed-form expressions, the envelope statistics have been more frequently the focus of most researches. Following the intense use of the envelope statistics in wireless communications applications as well as the need for even better descriptions of the channel, new envelope-related models have arisen. These include Nakagami-m [11], followed by more general, yet mathematically easily tractable, models, namely, α-μ [12], κ-μ [13], η-μ [13], α-η-μ [14], α-κ-μ [14]. In order to investigate the phase processes, models for the complex signals in Nakagami-m [15, 16], η-μ [17], and κ-μ [18] scenarios have been proposed, with their corresponding joint phase-envelope PDFs. Even more recently, the α-η-κ-μ model has been proposed [19], comprising all of the mentioned models and Beckmann's distribution [20].

As well known, both envelope and phase statistics are useful in wireless communications systems. The envelope statistics are widely used in the performance analyses of systems involving diversity, modulation, coding, among others [21]. In addition, the level crossing rate (LCR) and average fading duration (AFD) are useful second order statistics for the development of error correcting codes [22] and diversity schemes in mobile systems [7]. The phase statistics are largely used in radar clutter and signal detection [23], and error probability for M-phase signaling over fading channels [24]. Furthermore, the phase crossing rate (PCR) is a necessary statistic introduced in [25] to evaluate noise clicks in FM systems. Other investigations show that the PCR is equally important to: (i) define the average number of noise spikes and slipping events [26, 27]; (ii) measure rate performance of FM receivers using limited-discriminator detector wherein FM random spikes are generated by phase jumps; and (iii) determine the format of noise spikes [28].

In a non-dominant component condition and in a linear environment, the η-μ distribution arises as a very flexible model. This is a general fading model, which has Nakagami-m and Hoyt as special cases. It is known that the η-μ distribution has added flexibility and reliability in the analysis of realistic fading scenarios. Some comparisons, in [13], show that the η-μ distribution is more suitable than the Nakagami-m model in several field measurements scenarios. Moreover, it is noteworthy that its tail portion follows the true field statistics where other distributions fail to yield good fit. The η-μ distribution can also be used to approximate the distribution of the sum of independent non-identically distributed Hoyt variates [29]. More generally, it can also approximate the sum of η-μ random envelopes. Recently, η-μ statistics have been used in several instances, including the following: (i) performance analysis of a mixed radio-frequency and free-space optical system [30]; (ii) performance of energy detection for spectrum sensing in cognitive radio [31]; (iii) performance analysis of relaying networks [32]- [33] and selection combining diversity [34]; and (iv) spatial modulation schemes [35].

The κ-μ model, by its turn, is used in dominant component scenarios, with κ being defined as ratio between the power of dominant components and the scattered components, and with μ representing the number of multipath clusters. In this model, Nakagami-m and Rice distributions arise as particular cases. The κ-μ model is highly flexible and ensures excellent adjust to field data in different scenarios. Some of its statistics have been widely used such as in: (i) the evaluation of outage probability of diversity receivers [36]; (ii) in the analysis of co-channel interference with background noise [37] and its impact in body area network [38]; (iii) the assessment of channel capacity of spectrum aggregation systems [39]; (iv) the analysis of average symbol error rate and diversity gain [40]; and (v) the energy detection scheme of spectrum sensing in cognitive radio systems [41].

More recently, the α-η-κ-μ fading model [19] has been proposed. It captures virtually all fading phenomena reported in the literature for wireless communications, namely nonlinearity of the medium, power of scattered waves, power of dominant components and multipath clustering. With this, the α-η-κ-μ model comprises a multitude of different fading settings, encompassing all of those mentioned before, and some not yet established in the literature. As for its statistics, the joint phase-envelope PDF has been obtained in closed-form formulation, and as for the envelope PDF, a series expansion expression was developed. Unfortunately, no closed-form equation was available for the phase PDF. Although it is still a novelty, the α-η-κ-μ model has already been subject of recent investigations. In [42], the authors obtained some higher order statistics in integral form, and explored its envelope PDF fitting performance over data collected in a mmWave propagation scenario. In [43], the authors investigated the channel capacity under different adaptive transmission techniques operating in α-η-κ-μ fading channel. Finally, in [44], the authors proposed an α-η-κ-μ sample generator and an application which calculates the average bit error rate over BPSK modulation scheme.

Main Contributions

The aim of this thesis is to propose an Extended model for the η-μ and κ-μ complex signals based on the results presented in [19]. This model introduces an imbalance parameter p describing the ratio of the number of multipath clusters of the in-phase and quadrature components. Strikingly, despite the introduction of a new parameter, the formulations for the PDFs of the Extended models are still presented in mathematically tractable closed-form expressions. For the Extended η-μ, it is anticipated that p will have a significant influence on the behavior of both phase and envelope distributions. In addition, new cumulative density functions (CDF) are provided for the envelope and the phase statistics. Other envelope statistics are presented, namely moment generating function (MGF), and average bit error rate (ABER) for binary phase shift keying (BPSK) and binary frequency shift keying (BFSK) modulation schemes in a diversity scenario. Higher order statistics are also derived, which includes level crossing rate, average fading duration and phase crossing rate. As for the Extended κ-μ model, the imbalance parameter affects only the phase PDF. Thence, only phase related statistics are derived, which also includes the phase crossing rate. Based on the elegant method developed in [45], an approximate tight closed-form expression is determined for the phase PDF and PCR. When compared to their exact counterparts, these formulations render excellent results. Finally, by using the same approximation technique, a new expression is obtained for the phase PDF of the α-η-κ-μ fading model. For such a process, a more tractable series representation for the envelope PDF is derived. In addition, interesting outcomes have emerged from all these procedures, which includes new mathematical identities for the modified Bessel function and novel random variables.

Structure

This thesis is organized as follows:

– Chapter 2 provides a statistical guide on all mentioned fading models throughout the thesis, namely Hoyt, Rice, Nakagami-m, η-μ, κ-μ and α-η-κ-μ distributions.

- Chapter 3 proposes a new extension for the η-μ fading model wherein an intriguing new parameter is introduced. This parameter indicates cluster imbalance, and hence, new phase and envelope PDFs are determined. As a consequence, a complete statistical analysis will be carried out, that leads to novel higher order statistics and performance metrics formulations.

- Chapter 4 extends the traditional κ-μ fading model, by introducing the same cluster imbalance parameter. Unlike the Extended η-μ distribution, the new parameter affects only the phase statistics. More importantly, an approximate tight closed-form expression is found for the phase PDF and PCR.

- Chapter 5 develops a new series expression for the envelope PDF of the α-η-κ-μ fading model. With the approximation method employed in Chapter 4, an approximate formulation is also propose for the phase PDF.

- Chapter 6 concludes this thesis with perspectives and future work.

List of Publications

- Tejerina, G. R. L. and Yacoub, M. D. "Efeito de desbalanceamento de *clusters* de multipercurso no modelo η-μ", *XXXIII Simpósio Brasileiro de Telecomunicações (SBrT 2015).* SBrT, Juíz de Fora, MG.

- Tejerina, G. R. L., Rodriguez, A. C. F., García, F. D. A., Fraidenraich, G., Santos Filho, J. C. S., Yacoub, M. D., Miranda, M. A. M., Bertetich, A. and de Macedo, K. A. C. "Modelo de Multipercurso para Sistemas de Radar em Perfis Topográficos Reais", *XXXIV Simpósio Brasileiro de Telecomunicações (SBrT 2016).* SBrT, Santarém, PA.

- Rodriguez, A. C. F., García, F. D. A., Tejerina, G. R. L., Fraidenraich, G., Santos Filho, J. C. S., Yacoub, M. D., Miranda, M. A. M., Bertetich, A. and Moreira Neto, J. R. "Radar Coverage Over Irregular Terrain: a Practical Algorithm for Multipath Propagation", *2018 IEEE Radar Conference (RadarConf 2018).* Oklahoma City, USA.

– da Silva, C. R. N., Tejerina, G. R. L. and Yacoub, M. D. "The α-η-κ-μ Fading Model: New Fundamental Results", *IEEE Transactions on Wireless Communications*, 2018.

Chapter 2

Fading Models Revisited

This chapter revisits first and second order statistics of the consolidated Rice, Hoyt and Nakagami-m fading models, and of the general κ-μ, η-μ and α-η-κ-μ fading distributions. The Rice distribution [9] is commonly used in fading signals with dominant components. The Hoyt distribution [10], in the other hand, is suited for signals with a power imbalance between its in-phase and quadrature components in non-dominant component scenarios. Nakagami-m is a classic wireless communication distribution and is generally applied in moderate fading settings. The κ-μ and η-μ distributions are general fading models and represent small-scale signal variations in non-dominant component and dominant component conditions, respectively. Both distributions have been extensively used for general fading characterizations and as special cases these models enclose Rice, Hoyt and Nakagami-m distributions. More recently, the very general α-η-κ-μ model has been proposed, which comprises all distributions mentioned in this chapter.

2.1 The Rice Fading Model

The Rice complex signal is given as

$$S = (X + p) + j(Y + q), \tag{2.1}$$

wherein X and Y are Gaussian distributed random variables with zero mean and equal variance σ^2, and p and q are the mean values of the in-phase (X) and quadrature (Y) components, respectively. The envelope R and phase Θ joint distribution is found as [9]

$$f_{R,\Theta}(r,\theta) = \frac{(1+k)}{\pi}\frac{r}{\hat{r}^2}\exp\left(-k-(1+k)\frac{r^2}{\hat{r}^2}+2\sqrt{k(1+k)}\cos(\theta-\phi)\frac{r}{\hat{r}}\right), \tag{2.2}$$

in which $r \geq 0$ and $-\pi < \theta \leq \pi$ holds, $k = (p^2+q^2)/(2\sigma^2)$ is the Ricean parameter, $\sigma^2 = \hat{r}^2/(2(1+k))$, $\hat{r}^2 = E(R^2)$ is the mean value of the envelope, and $\phi = \arg(p+jq)$.

By integrating (2.2) in terms of θ, the envelope PDF is obtained as

$$f_R(r) = \frac{2(1+k)r}{\hat{r}^2} \exp\left(-k - (1+k)\frac{r^2}{\hat{r}^2}\right) I_0\left(2\sqrt{k(k+1)}\frac{r}{\hat{r}}\right), \tag{2.3}$$

where $I_0(z)$ is the modified Bessel function of the first kind and order zero [1, Eq. (9.6.16)].

After integrating (2.2) in respect to r, the marginal phase PDF is calculated as

$$\begin{aligned} f_\Theta(\theta) &= \left(1 + \sqrt{\pi k}\cos(\theta-\phi)\exp\left(k\cos^2(\theta-\phi)\right)\left(1 + \operatorname{erf}\left(\sqrt{k}\cos(\theta-\phi)\right)\right)\right) \\ &\quad \times \frac{\exp(-k)}{2\pi}, \end{aligned} \tag{2.4}$$

where $\operatorname{erf}(z)$ is the error function [1, Eq. (7.1.1)].

The level crossing rate is defined as

$$N_R(r) = \int_0^\infty \dot{r} f_{R,\dot{R}}(r,\dot{r})\,\mathrm{d}\dot{r}. \tag{2.5}$$

with $f_{R,\dot{R}}(r,\dot{r})$ denoting the joint PDF of R and its time derivative $\dot{R}$. For the Rice fading model, the LCR is expressed as [9]

$$N_R(r) = \frac{\sqrt{2\pi(1+k)}f_m r}{\hat{r}^2} \exp\left(-k - (1+k)\frac{r^2}{\hat{r}^2}\right) I_0\left(2\sqrt{k(k+1)}\frac{r}{\hat{r}}\right). \tag{2.6}$$

In similar fashion, the phase crossing rate is established as

$$N_\Theta(\theta) = \int_0^\infty \dot{\theta} f_{\Theta,\dot{\Theta}}(\theta,\dot{\theta})\,\mathrm{d}\dot{\theta}. \tag{2.7}$$

where $f_{\Theta,\dot{\Theta}}(\theta,\dot{\theta})$ is the the joint PDF of Θ and its time derivative $\dot{\Theta}$. Thus, the Ricean PCR is obtained as

$$N_\Theta(\theta) = \frac{f_m}{2\sqrt{2}}\left(1 + \operatorname{erf}\left(\sqrt{k}\cos(\theta-\phi)\right)\right)\exp\left(-k\sin^2(\theta-\phi)\right), \tag{2.8}$$

with f_m denoting the maximum Doppler shift in hertz.

2.2 The Hoyt Fading Model

The Hoyt complex signal is given as

$$S = X + jY, \tag{2.9}$$

where X and Y are the in-phase and quadrature components, with each following a Gaussian process with zero mean and arbitrary variances σ_x and σ_y, respectively. The envelope R and phase Θ joint PDF is found as [10, Eq. (2.15)]

$$f_{R,\Theta}(r,\theta) = \frac{r}{\pi\sqrt{1-b^2}} \exp\left(-\frac{r^2}{1-b^2}(1 - b\cos(2\theta))\right), \tag{2.10}$$

in which $r \geq 0$, $-\pi < \theta \leq \pi$, and $b = \left(\sigma_x^2 - \sigma_y^2\right) / \left(\sigma_x^2 + \sigma_y^2\right)$ is the Hoyt parameter.

The envelope PDF can be evaluated as [10, Eq. (3.4)]

$$f_R(r) = \frac{2r}{\sqrt{1-b^2}} \exp\left(-\frac{r^2}{1-b^2}\right) I_0\left(\frac{br^2}{1-b^2}\right). \tag{2.11}$$

The phase PDF is obtained by integrating (2.10) with respect to r from 0 to ∞ [10, Eq. (6.3)],

$$f_\Theta(\theta) = \frac{\sqrt{1-b^2}}{2\pi(1 - b\cos(2\theta))}. \tag{2.12}$$

The LCR of the Hoyt distribution is found in integral-form as given in [46]

$$N_R(r) = \frac{2^{\frac{3}{2}} f_m r}{\sqrt{\pi(1-b^2)}} \int_{-\pi}^{\pi} \sqrt{1 + b\cos(2\theta)} \exp\left(-\frac{r^2(1 - b\cos(2\theta))}{(1-b^2)}\right) \mathrm{d}\theta. \tag{2.13}$$

And the Hoyt's PCR is calculates as [47]

$$N_\Theta(\theta) = \frac{f_m}{2\sqrt{2}}, \tag{2.14}$$

wherein f_m is defined as the maximum Doppler shift in hertz.

The Hoyt fading distribution is also known as the Nakagami-q model. As special cases, when $b \to 0$, the Rayleigh fading model is obtained, and by properly manipulating b in terms of σ_x and σ_y, the unilateral Gaussian model is also attained. Moreover, Hoyt statistics are widely used to describe the signal amplitude distribution over a satellite link subjected to ionospheric scintillation [48, 49], and in wireless link performance investigation [50–54].

2.3 The Generalized Nakagami-m Fading Model

The Nakagami-m model was first derived empirically in [11]. Since then, it has been extensively used due to its mathematical tractability and accurate descritive power of real world fading scenarios. Nevertheless, a physical model contemplating the envelope distribution was proposed in [55]. On the other hand, its phase distribution, first assumed uniform, was then found to be non-uniform, arising from a physically-based fading model [15]. More recently a generalized model was presented in [16], in which a phase parameter was introduced by allowing different number of in-phase and quadrature multipath cluster in the fading channel.

A Nakagami-m signal is given as

$$S = X + jY, \tag{2.15}$$

in which

$$X^2 = \sum_{i=1}^{m_x} X_i^2 \quad \text{and} \quad Y^2 = \sum_{i=1}^{m_y} Y_i^2, \tag{2.16}$$

where X_i and Y_i are Gaussian distributed random variables with zero mean and equal variances, and m_x and m_y are the number of cluster multipath in the in-phase and quadrature components, respectively. In addition, m_x and m_y are related as follows

$$2m = m_x + m_y, \tag{2.17}$$

in which m is the original Nakagami-m parameter.

The phase parameter $-1 \leq p \leq 1$ is defined as

$$p = \frac{m_X - m_Y}{m_X + m_Y}, \tag{2.18}$$

in which: (i) $p = 0$ stands for the balanced condition where the number of multipath clusters are equally distributed within the in-phase and quadrature components; $p \neq 0$ stands for the unbalanced condition; and (ii) $p = 1$ or $p = -1$ signifies that all Gaussian components are either concentrated in the in-phase or quadrature component.

The phase-envelope joint PDF is found as [56]

$$f_{R,\Theta}(r,\theta) = \frac{m^m \left|\sin\theta\cos\theta\right|^{m-1} r^{2m-1}}{\Omega^m \Gamma\left(\frac{1+p}{2}m\right)\Gamma\left(\frac{1-p}{2}m\right)\left|\tan\theta\right|^{pm}} \exp\left(-\frac{mr^2}{\Omega}\right), \tag{2.19}$$

wherein $r \geq 0$ and $-\pi < \theta \leq \pi$, $\Gamma(z)$ is the Gamma function [1, Eq. (6.1.1)], and $\Omega = E\left(R^2\right)$ is the mean value of the envelope.

By integrating(2.19) in terms of θ, the envelope PDF is calculated as

$$f_R(r) = \frac{2m^m r^{2m-1}}{\Omega^m \Gamma(m)} \exp\left(-\frac{mr^2}{\Omega}\right). \tag{2.20}$$

Similarly, the phase PDF is obtained, after integrating (2.19) with respect to θ, as

$$f_\Theta(\theta) = \frac{\Gamma(m)\left|\sin\theta\right|^{m-1}}{2^m \Gamma\left(\frac{1+p}{2}m\right)\Gamma\left(\frac{1-p}{2}m\right)\left|\tan\theta\right|^{pm}}. \tag{2.21}$$

Finally, the LCR [55] and PCR [16] are found as

$$N_R(r) = \frac{\sqrt{2}\pi f_m m^{m-\frac{1}{2}} r^{2m-1}}{\Omega^m \Gamma(m)} \exp\left(-\frac{r^2}{\Omega}\right) \tag{2.22}$$

and

$$N_\Theta(\theta) = \frac{\sqrt{\pi} f_m \left|\sin(2\theta)\right|^{m-1} \Gamma\left(m - \frac{1}{2}\right)}{2^{m+\frac{1}{2}} \Gamma\left(m\frac{1+p}{2}\right)\Gamma\left(m\frac{1-p}{2}\right)\left|\tan\theta\right|^{pm}} \tag{2.23}$$

where f_m is the maximum Doppler shift in hertz.

Note that when $p = 0$, the balanced case is attained, and all equations presented here for the Generalized Nakagami-m reduce to their classic approach. Moreover, for $p = 1$ and $m = 1$, the Rayleigh fading model arises as a special case.

2.4 The η-μ Fading Model

The η-μ distribution is a fading model used to represent the small-scale variation of the signal in a non-dominant condition [13]. As implied, the distribution is known to describe two different physical phenomena based on the definition of the parameter η. In Format 1, the in-phase and quadrature components of the signal are independent from each other and have different powers. In addition, $0 < \eta < \infty$ is defined as the scattered-wave power ratio between the in-phase and quadrature components of each multipath cluster. In Format 2, the in-phase and quadrature signals have identical power and are correlated with each other. In such a case, $-1 < \eta < 1$ is the correlation coefficient between the scattered-wave in the in-phase and quadrature components of each cluster of multipath. In both formats, the parameter $\mu > 0$ is defined as the number of multipath clusters.

The η-μ complex signal is described as follows,

$$S = X + jY, \tag{2.24}$$

in which the real (X) and imaginary (Y) parts of the signal are represented by

$$X^2 = \sum_{i=1}^{2\mu} X_i^2 \quad \text{and} \quad Y^2 = \sum_{i=1}^{2\mu} Y_i^2 \tag{2.25}$$

wherein X_i and Y_i are random Gaussian variables with zero mean and arbitrary variances σ_x^2 and σ_y^2. In Format 1, X_i and Y_i are independent and $\eta = \sigma_x^2/\sigma_y^2$. In Format 2, X_i and Y_i are correlated processes and their variances are defined as $\sigma_x^2 = \sigma_y^2 = \hat{r}^2$, and $\eta = E\left(X_i, Y_i\right)/\hat{r}^2$ indicates the correlation between clusters. An η-μ signal with envelope R and phase Θ has a joint phase-envelope PDF $f_{R,\Theta}(r,\theta)$ defined as [17]

$$f_{R,\Theta}(r,\theta) = \frac{2\mu^{2\mu} h^{2\mu} r^{4\mu-1} \left|\sin\left(2\theta\right)\right|^{2\mu-1}}{\left(h^2 - H^2\right)^{\mu} \hat{r}^{4\mu} \Gamma^2\left(\mu\right)} \exp\left(-\frac{2\mu h r^2}{\hat{r}^2\left(h^2 - H^2\right)}\left(h + H\cos\left(2\theta\right)\right)\right), \tag{2.26}$$

where: (i) $\hat{r} = \sqrt{E(R^2)}$ is the RMS value of R; (ii) h and H are functions of η and provide different relations for each format; (iii) $\mu > 0$, the number of multipath clusters, is given by $\mu = (E^2(R^2)/2\mathrm{Var}(R^2))\left(1+(H/h)^2\right)$; and (iv) $E(\cdot)$ and $\mathrm{Var}(\cdot)$ indicate the expectation and variance operators, respectively. In Format 1, the terms h and H are defined, respectively, as

$$h = \frac{(2+\eta^{-1}+\eta)}{4} \quad \text{and} \quad H = \frac{\eta^{-1}-\eta}{4}, \tag{2.27}$$

and in Format 2, they are described, respectively, as

$$h = \frac{1}{1-\eta^2} \quad \text{and} \quad H = \frac{\eta}{1-\eta^2}. \tag{2.28}$$

Thus, from these relations, it is possible to obtain one format from the other by applying

$$\eta_1 = \frac{1-\eta_2}{1+\eta_2} \tag{2.29}$$

or

$$\eta_2 = \frac{1-\eta_1}{1+\eta_1}, \tag{2.30}$$

where η_1 and η_2 are the parameter η for Format 1 and Format 2, respectively.

From (2.26), envelope [13] and phase [17] marginal PDFs are obtained, respectively, as

$$f_R(r) = \frac{4\sqrt{\pi}\mu^{\mu+\frac{1}{2}}h^{\mu}}{\Gamma(\mu)\,H^{\mu-\frac{1}{2}}\hat{r}}\left(\frac{r}{\hat{r}}\right)^{2\mu}\exp\left(-2\mu h\left(\frac{r}{\hat{r}}\right)^2\right)I_{\mu-\frac{1}{2}}\left(2\mu H\left(\frac{r}{\hat{r}}\right)^2\right) \tag{2.31}$$

and

$$f_\Theta(\theta) = \frac{(h^2-H^2)^{\mu}\,\Gamma(2\mu)\,|\sin(2\theta)|^{2\mu-1}}{2^{2\mu}\Gamma(\mu)^2\,(h+H\cos(2\theta))^{2\mu}} \tag{2.32}$$

where $I_\nu(z)$ is the modified Bessel function of the first kind and arbitrary order ν [1, Eq. 9.6.20]. Note that, in Format 1, η is symmetrical around $\eta = 1$. In other words, within $0 < \eta \leq 1$, the envelope PDF yields the same values as for within $0 < \eta^{-1} \leq 1$. On the other hand, within $0 < \eta \leq 1$, in Format 2, the envelope PDF yields the same value as for within $-1 < \eta \leq 0$, which means it is symmetrical around $\eta = 0$.

As indicated in [57], the LCR for Format 1 is represented in an integral-form as

$$\begin{aligned} N_R(r) &= \frac{f_m\sqrt{\pi}\,((1+\eta)\,\mu)^{2\mu-\frac{1}{2}}\,r^{4\mu-1}}{2^{2\mu-2}\eta^{\mu}\Gamma(\mu)^2\,\hat{r}^{4\mu-1}}\int_0^{\frac{\pi}{2}}\sin(2\theta)^{2\mu-1}\sqrt{1+\eta-(1-\eta)\cos(2\theta)} \\ &\quad\times\exp\left(\left((1+\eta)^2+(1-\eta^2)\cos(2\theta)\right)\frac{\mu r^2}{2\eta\hat{r}^2}\right)\mathrm{d}\theta. \end{aligned} \tag{2.33}$$

The PCR is obtained in closed-form expression as [57]

$$N_\Theta(\theta) = \frac{f_m\sqrt{\pi}\eta^{\mu-\frac{1}{2}}\Gamma(2\mu-\frac{1}{2})|\sin(2\theta)|^{2\mu-1}}{2^{\frac{3}{2}}\Gamma^2(\mu)\,(1+\eta+(1-\eta)\cos(2\theta))^{2\mu-1}}. \tag{2.34}$$

wherein f_m is the maximum Doppler shift in hertz.

Finally, for all formulations presented in this sections, the original Nakagami-m distribution can be obtained in an exact manner by setting $\mu = m/2$ and $\eta \to 1$ in Format 1, or $\eta \to 0$ in Format 2. Also, the Hoyt distribution can be attained by setting $\mu = 0.5$ and $\eta = (1+b)/(1-b)$ in Format 1, or $\eta = -b$, parameter in Format 2, where b is the Hoyt parameter. Other special cases consist of the unilateral Gaussian distribution, by setting $\eta \to 0$ or $\eta \to \infty$ in Format 1, or $\eta \to \pm 1$, in Format 2, and the Rayleigh distribution for $\mu = 1/2$ and adjusting $\eta = 1$, in Format 1, or $\eta = 0$, in Format 2 [13].

2.4.1 The Generalized η-μ Fading Model

Following the same approach as in [16], the authors of [58] introduced cluster imbalance with the phase parameter p to the η-μ model. According to the Nakagami-m model, the generalized η-μ distribution is related to its classic counterpart by setting $p = 0$. Also, when $\eta = 1$ and $\mu = m/2$ in Format 1, or $\eta \to 0$ and $\mu = m/2$ in Format 2, the expressions for the generalized Nakagami-m model are obtained. Thus, the joint phase-envelope PDF for Format 1 is revealed as

$$\begin{aligned} f_{R,\Theta}(r,\theta) &= \frac{(1+p)^{\mu(1+p)}(1-p)^{\mu(1-p)}(1+\eta)^{2\mu}\mu^{2\mu}}{\eta^{\mu(1+p)}\Gamma\left(\mu\left(1+p\right)\right)\Gamma\left(\mu\left(1-p\right)\right)} \left|\cos\theta\right|^{2\mu(1+p)-1} \left|\sin\theta\right|^{2\mu(1-p)-1} \frac{r^{4\mu-1}}{\hat{r}^{4\mu}} \\ &\quad \times \exp\left(-\frac{(1+\eta)\mu}{\eta}\left((1+p)\cos^2\theta + (1-p)\eta\sin^2\theta\right)\frac{r^2}{\hat{r}^2}\right), \end{aligned} \tag{2.35}$$

with $r \geq 0$ and $-\pi < \theta \leq \pi$.

As hinted in [59], the envelope marginal PDF is indicated in integral-form as

$$f_R(r) = \int_{-\pi}^{\pi} f_{R,\Theta}(r,\theta)\,\mathrm{d}\theta. \tag{2.36}$$

The phase PDF for Format 1 is given as

$$\begin{aligned} f_\Theta(\theta) &= \frac{\Gamma\left(2\mu\right)(1-p)^{\mu(1-p)}(1+p)^{\mu(1+p)}\eta^{\mu(1-p)}}{\Gamma\left(\mu(1+p)\right)\Gamma\left(\mu(1-p)\right)\left(1+p+\eta(-p)+\left((1+p)-\eta(1-p)\right)\cos(2\theta)\right)^{2\mu}} \\ &\quad \times \frac{\left|\sin(2\theta)\right|^{2\mu-1}}{\left|\tan\theta\right|^{2\mu p}}. \end{aligned} \tag{2.37}$$

The PCR for Format 1 is found as [59]

$$\begin{aligned} N_\Theta(\theta) &= \frac{\sqrt{\pi} f_m \Gamma\left(2\mu - \frac{1}{2}\right)(1+p)^{\mu(1+p)}(1-p)^{\mu(1-p)}\eta^{\mu(1-p)-\frac{1}{2}}}{2^{\frac{3}{2}}\sqrt{1-p^2}\,\Gamma(\mu(1+p))\Gamma(\mu(1-p))} \frac{\left|\sin(2\theta)\right|^{2\mu-1}}{\left|\tan\theta\right|^{2\mu p}} \\ &\quad \times \left(1+p+\eta(1-p)+\left((1+p)-\eta(1-p)\right)\cos(2\theta)\right)^{1-2\mu}. \end{aligned} \tag{2.38}$$

Note that Format 2 is attainable from (2.35), (2.37) and (2.38) by setting the parameter η as

$$\eta_1 = \frac{(1-\eta_2)(1+p)}{(1+\eta_2)(1-p)}, \tag{2.39}$$

in which η_1 and η_2 are the parameter η in Formats 1 and 2, respectively. The Format 2 counterpart is given as

$$\eta_2 = \frac{(1+p)-(1-p)\eta_1}{(1+p)+(1-p)\eta_1}. \tag{2.40}$$

2.5 The κ-μ Fading Model

The κ-μ distribution is a general fading model which has been used to represent small scale variation in a linear medium and with dominant components [13]. As can be seen, the distribution has two important parameters: (i) $\kappa > 0$, indicating the ratio between the power of all dominant components to the power of the scattered waves; and (ii) $\mu > 0$, representing the number of multipath clusters of the received signal.

The complex κ-μ signal is defined as

$$S = X + jY, \tag{2.41}$$

in which the in-phase (X) and quadrature (Y) components are defined as

$$X^2 = \sum_{i=1}^{\mu} (X_i + p_i)^2 \quad \text{and} \quad Y^2 = \sum_{i=1}^{\mu} (Y_i + q_i)^2, \tag{2.42}$$

wherein X_i and Y_i are independent Gaussian distributed random variables with zero mean and equal variances σ^2, p_i and q_i indicate the mean values of the in-phase and quadrature signals of the multipath waves of clusters with index i, and μ represents the number of multipath clusters. The power of the in-phase and quadrature components are defined as

$$p^2 = \sum_{i=1}^{2\mu} p_i^2 \quad \text{and} \quad q^2 = \sum_{i=1}^{2\mu} q_i^2. \tag{2.43}$$

Then, κ is represented as the ratio between the total power of dominant components to the power of scattered waves, as indicated in

$$\kappa = \frac{p^2 + q^2}{2\mu\sigma^2}. \tag{2.44}$$

The variance σ^2 is written in terms of κ, μ and the RMS value of the envelope $\hat{r} = \sqrt{E\left(R^2\right)}$, leading to

$$\sigma^2 = \frac{\hat{r}^2}{2\mu(1+\kappa)}. \tag{2.45}$$

Now, by defining the phase parameter $\phi = \arg(p+jq)$, p and q can be rewritten as

$$p = \sqrt{\frac{\kappa}{1+\kappa}}\hat{r}\cos\phi \tag{2.46}$$

and

$$q = \sqrt{\frac{\kappa}{1+\kappa}}\hat{r}\sin\phi. \tag{2.47}$$

With this in mind, the envelope R and the phase Θ joint PDF can be properly calculated as

$$\begin{aligned} f_{R,\Theta}(r,\theta) &= \frac{1}{2}\kappa^{1-\frac{\mu}{2}}(1+\kappa)^{\frac{\mu}{2}+1}\mu^2\frac{r^{\mu+1}}{\hat{r}^{\mu+2}}\left|\sin 2\theta\right|^{\frac{\mu}{2}}\left|\sin 2\phi\right|^{1-\frac{\mu}{2}} \\ &\times I_{\frac{\mu}{2}-1}\left(2\sqrt{\kappa(1+\kappa)}\mu\left|\cos\theta\cos\phi\right|\frac{r}{\hat{r}}\right)\operatorname{sech}\left(2\sqrt{\kappa(1+\kappa)}\mu\cos\theta\cos\phi\frac{r}{\hat{r}}\right) \\ &\times I_{\frac{\mu}{2}-1}\left(2\sqrt{\kappa(1+\kappa)}\mu\left|\sin\theta\sin\phi\right|\frac{r}{\hat{r}}\right)\operatorname{sech}\left(2\sqrt{\kappa(1+\kappa)}\mu\sin\theta\sin\phi\frac{r}{\hat{r}}\right) \\ &\times \exp\left(-\kappa\mu-(1+\kappa)\mu\frac{r^2}{\hat{r}^2}+2\sqrt{\kappa(1+\kappa)}\mu\cos(\theta-\phi)\frac{r}{\hat{r}}\right) \end{aligned} \tag{2.48}$$

in which $r \geq 0$ and $-\pi < \theta \leq \pi$. An indeterminacy is encountered in (2.48) when $\phi = n\pi$ or $\phi = (2n+1)\pi/2$ with $n \in \mathbb{Z}$. However, these can be easily solved resulting, respectively, in

$$\begin{aligned} f_{R,\Theta}(r,\theta)_{\phi=n\pi} &= \frac{1}{\Gamma\left(\frac{\mu}{2}\right)}\mu^{1+\frac{\mu}{2}}\kappa^{\frac{1}{2}-\frac{\mu}{4}}(1+\kappa)^{\frac{1}{2}+\frac{3\mu}{4}}\frac{r^{\frac{3\mu}{2}}}{\hat{r}^{\frac{3\mu}{2}+1}}\left|\sin\theta\right|^{\mu-1}\left|\cos\theta\right|^{\frac{\mu}{2}} \\ &\times I_{\frac{\mu}{2}-1}\left(2\sqrt{\kappa(1+\kappa)}\mu\left|\cos\theta\right|\frac{r}{\hat{r}}\right)\operatorname{sech}\left(2\sqrt{\kappa(1+\kappa)}\mu\cos\theta\frac{r}{\hat{r}}\right) \\ &\times \exp\left(-(1+\kappa)\mu\frac{r^2}{\hat{r}^2}-\kappa\mu+2\sqrt{\kappa(1+\kappa)}\mu\cos\theta\cos\phi\frac{r}{\hat{r}}\right) \end{aligned} \tag{2.49}$$

and

$$\begin{aligned} f_{R,\Theta}(r,\theta)_{\phi=\frac{(2n+)\pi}{2}} &= \frac{1}{\Gamma\left(\frac{\mu}{2}\right)}\mu^{1+\frac{\mu}{2}}\kappa^{\frac{1}{2}-\frac{\mu}{4}}(1+\kappa)^{\frac{1}{2}+\frac{3\mu}{4}}\frac{r^{\frac{3\mu}{2}}}{\hat{r}^{\frac{3\mu}{2}+1}}\left|\cos\theta\right|^{\mu-1}\left|\sin\theta\right|^{\frac{\mu}{2}} \\ &\times I_{\frac{\mu}{2}-1}\left(2\sqrt{\kappa(1+\kappa)}\mu\left|\sin\theta\right|\frac{r}{\hat{r}}\right)\operatorname{sech}\left(2\sqrt{\kappa(1+\kappa)}\mu\sin\theta\frac{r}{\hat{r}}\right) \\ &\times \exp\left(-(1+\kappa)\mu\frac{r^2}{\hat{r}^2}-\kappa\mu+2\sqrt{\kappa(1+\kappa)}\mu\sin\theta\sin\phi\frac{r}{\hat{r}}\right). \end{aligned} \tag{2.50}$$

By integrating (2.48) in terms of θ, the envelope PDF is found in closed-form as

$$f_R(r) = \frac{2\mu(1+\kappa)^{\frac{\mu+1}{2}}r^{\mu}}{\kappa^{\frac{\mu-1}{2}}\hat{r}^{\mu+1}\exp(\mu\kappa)}\exp\left(-\mu(1+\kappa)\left(\frac{r}{\hat{r}}\right)^2\right)I_{\mu-1}\left(2\mu\sqrt{\kappa(1+\kappa)}\frac{r}{\hat{r}}\right). \tag{2.51}$$

Then, by integrating (2.48), (2.49) or (2.50) in respect to R, the marginal phase PDF is obtained as

$$f_\Theta(\theta) = \int_0^\infty f_{R,\Theta}(r,\theta)\,\mathrm{d}r. \tag{2.52}$$

However, as indicated in [18], no closed-form expressions were found for this statistics. Hence, in order to fill this gap, [45] derived a new approximation method leading to a tight-closed approximation for the κ-μ phase PDF. This expression was shown to be very accurate by maintaining all original properties of the exact phase PDF, including minimum and maximum values, occurring at values of θ close to these of the exact PDF. The tight closed-form approximation of the phase PDF $f_{\mathbb{O}}(\theta)$ is given as

$$\begin{aligned} f_\Theta(\theta) \approx f_{\mathbb{O}}(\theta) =& \frac{\sqrt{\kappa(1+\kappa)}\mu}{4I_{\mu-1}\left(2\sqrt{\kappa(1+\kappa)}\mu\right)} |\sin 2\theta|^{\frac{\mu}{2}} |\sin 2\phi|^{1-\frac{\mu}{2}} \exp\left(2\sqrt{\kappa(1+\kappa)}\mu\cos(\theta-\phi)\right) \\ &\times I_{\frac{\mu}{2}-1}\left(2\sqrt{\kappa(1+\kappa)}\mu\,|\sin\theta\sin\phi|\right) I_{\frac{\mu}{2}-1}\left(2\sqrt{\kappa(1+\kappa)}\mu\,|\cos\theta\cos\phi|\right) \\ &\times \operatorname{sech}\left(2\sqrt{\kappa(1+\kappa)}\mu\cos\theta\cos\phi\right) \operatorname{sech}\left(2\sqrt{\kappa(1+\kappa)}\mu\sin\theta\sin\phi\right), \end{aligned} \tag{2.53}$$

where $\mathbb{O}$ is the new phase random variable.

The particular cases for $\phi = n\pi$ or $\phi = (2n+1)\pi/2$ are represented as follows in

$$\begin{aligned} f_{\mathbb{O}}(\theta)_{\phi=n\pi} =& \frac{\sqrt{\kappa(1+\kappa)}\mu}{2\Gamma\left(\frac{\mu}{2}\right) I_{\mu-1}\left(2\sqrt{\kappa(1+\kappa)}\mu\right)} |\sin\theta|^{\mu-1} |\cos\theta|^{\frac{\mu}{2}} \exp\left(2\sqrt{\kappa(1+\kappa)}\mu\cos\theta\cos\phi\right) \\ &\times I_{\frac{\mu}{2}-1}\left(2\sqrt{\kappa(1+\kappa)}\mu\,|\cos\theta|\right) \operatorname{sech}\left(2\sqrt{\kappa(1+\kappa)}\mu\cos\theta\right) \end{aligned} \tag{2.54}$$

and

$$\begin{aligned} f_{\mathbb{O}}(\theta)_{\phi=\frac{(2n+1)\pi}{2}} =& \frac{\sqrt{\kappa(1+\kappa)}\mu}{2\Gamma\left(\frac{\mu}{2}\right) I_{\mu-1}\left(2\sqrt{\kappa(1+\kappa)}\mu\right)} |\cos\theta|^{\mu-1} |\sin\theta|^{\frac{\mu}{2}} \\ &\times I_{\frac{\mu}{2}-1}\left(2\sqrt{\kappa(1+\kappa)}\mu\,|\sin\theta|\right) \operatorname{sech}\left(2\sqrt{\kappa(1+\kappa)}\mu\sin\theta\right) \\ &\times \exp\left(2\sqrt{\kappa(1+\kappa)}\mu\sin\theta\sin\phi\right). \end{aligned} \tag{2.55}$$

Surprisingly, (2.53) has as particular cases: (i) the exact Nakagami-m phase distribution which is obtainable by setting $\kappa \to 0$ and $\mu = m$; and (ii) the von Mises distribution for $\kappa = k$ and $\mu = 1$.

The LCR of the κ-μ model is described in closed-form as [60]

$$N_R(r) = \frac{\sqrt{2\pi\mu}(1+\kappa)^{\frac{\mu}{2}} f_m}{\kappa^{\frac{\mu-1}{2}}} \frac{r^\mu}{\hat{r}^{\mu+1}} \exp\left(-\kappa\mu - (1+\kappa)\mu\frac{r^2}{\hat{r}^2}\right) I_{\mu-1}\left(2\sqrt{\kappa(1+\kappa)}\mu\frac{r}{\hat{r}}\right). \tag{2.56}$$

Finally, the PCR is written in integral-form as follows [45]

$$N_{\Theta}(\theta)=\frac{\sqrt{\pi}f_m}{2\sqrt{2}}\kappa^{1-\frac{\mu}{2}}(1+\kappa)^{\frac{\mu+1}{2}}\mu^{\frac{3}{2}}\left|\sin 2\theta\right|^{\frac{\mu}{2}}\left|\sin 2\phi\right|^{1-\frac{\mu}{2}}\exp\left(-\kappa\mu\right)$$
$$\int_0^{\infty}\frac{r^{\mu}}{\hat{r}^{\mu+1}}\exp\left(-(1+\kappa)\mu\frac{r^2}{\hat{r}^2}+2\sqrt{\kappa(1+\kappa)}\mu\cos\left(\theta-\phi\right)\frac{r}{\hat{r}}\right)$$
$$\times I_{\frac{\mu}{2}-1}\left(2\sqrt{\kappa(1+\kappa)}\mu\left|\sin\theta\sin\phi\right|\frac{r}{\hat{r}}\right)I_{\frac{\mu}{2}-1}\left(2\sqrt{\kappa(1+\kappa)}\mu\left|\cos\theta\cos\phi\right|\frac{r}{\hat{r}}\right)$$
$$\times\ \mathrm{sech}\left(2\sqrt{\kappa(1+\kappa)}\mu\cos\theta\cos\phi\frac{r}{\hat{r}}\right)\mathrm{sech}\left(2\sqrt{\kappa(1+\kappa)}\mu\sin\theta\sin\phi\frac{r}{\hat{r}}\right)\mathrm{d}r. \quad (2.57)$$

Here again, the authors in [45] proposed a closed-form approximation which is represented below as

$$N_{\Theta}(\theta)\approx N_{\mathbb{O}}(\theta)=\frac{\sqrt{\pi}f_m\sqrt{\kappa(1+\kappa)}\mu\Gamma\left(\mu-\frac{1}{2}\right)\ {}_1F_1\left(\frac{1}{2};\mu;-\kappa\mu\right)}{2^{\frac{5}{2}}\Gamma\left(\mu\right)I_{\mu-1}\left(2\sqrt{\kappa(1+\kappa)}\mu\right)}\left|\sin(2\theta)\right|^{\frac{\mu}{2}}\left|\sin(2\phi)\right|^{1-\frac{\mu}{2}}$$
$$\times I_{\frac{\mu}{2}-1}\left(2\sqrt{\kappa(1+\kappa)}\mu\left|\sin\theta\sin\phi\right|\right)I_{\frac{\mu}{2}-1}\left(2\sqrt{\kappa(1+\kappa)}\mu\left|\cos\theta\cos\phi\right|\right)$$
$$\times\,\mathrm{sech}\left(2\sqrt{\kappa(1+\kappa)}\mu\cos\theta\cos\phi\right)\mathrm{sech}\left(2\sqrt{\kappa(1+\kappa)}\mu\sin\theta\sin\phi\right)$$
$$\times\exp\left(2\sqrt{\kappa(1+\kappa)}\mu\cos(\theta-\phi)\right). \quad (2.58)$$

In a similar fashion, particular cases for $\phi=n\pi$ and $\phi=(2n+1)\pi/2$ can also be calculated, resulting in

$$N_{\mathbb{O}}(\theta)_{\phi=\pm n\pi}=\frac{\sqrt{\pi}f\mu^{\frac{\mu}{2}}\kappa^{\frac{\mu}{4}}(1+\kappa)^{\frac{\mu}{4}}\Gamma\left(\mu-\frac{1}{2}\right)\ {}_1F_1\left(\frac{1}{2};\mu;-\kappa\mu\right)}{2^{\frac{3}{2}}\Gamma\left(\frac{\mu}{2}\right)\Gamma\left(\mu\right)I_{\mu-1}\left(2\sqrt{\kappa(1+\kappa)}\mu\right)}\left|\sin\theta\right|^{\mu-1}\left|\cos\theta\right|^{\frac{\mu}{2}}$$
$$\times\,\mathrm{sech}\left(2\sqrt{\kappa(1+\kappa)}\mu\cos\theta\right)I_{\frac{\mu}{2}-1}\left(2\sqrt{\kappa(1+\kappa)}\mu\left|\cos\theta\right|\right)$$
$$\times\exp\left(2\sqrt{\kappa(1+\kappa)}\mu\cos\theta\cos\phi\right) \quad (2.59)$$

and

$$N_{\mathbb{O}}(\theta)_{\phi=\pm\frac{(2n+1)\pi}{2}}=\frac{\sqrt{\pi}f\mu^{\frac{\mu}{2}}\kappa^{\frac{\mu}{4}}(1+\kappa)^{\frac{\mu}{4}}\Gamma\left(\mu-\frac{1}{2}\right)\ {}_1F_1\left(\frac{1}{2};\mu;-\kappa\mu\right)}{2^{\frac{3}{2}}\Gamma\left(\frac{\mu}{2}\right)\Gamma\left(\mu\right)I_{\mu-1}\left(2\sqrt{\kappa(1+\kappa)}\mu\right)}\left|\cos\theta\right|^{\mu-1}\left|\sin\theta\right|^{\frac{\mu}{2}}$$
$$\times\,\mathrm{sech}\left(2\sqrt{\kappa(1+\kappa)}\mu\sin\theta\right)I_{\frac{\mu}{2}-1}\left(2\sqrt{\kappa(1+\kappa)}\mu\left|\sin\theta\right|\right)$$
$$\times\exp\left(2\sqrt{\kappa(1+\kappa)}\mu\sin\theta\sin\phi\right). \quad (2.60)$$

It is important to reiterate that all κ-μ statistics, including both exact and approximate cases, are reducible to the classic Nakagami-m model ($p=0$) when $\kappa\to 0$

and $\mu = m$. Also, for all exact κ-μ statistics, Rice fading model arises as special cases by setting $\kappa = k$ and $\mu = 1$. For all approximate κ-μ formulations, the von Mises distribution is obtainable as an approximation to Rice distribution, where $\kappa = k$ and $\mu = 1$.

2.6 The α-η-κ-μ Fading Model

The α-η-κ-μ distribution is a very general complex fading model derived to encompass all relevant short-term propagation phenomena depicted in the literature [19].

The complex α-η-κ-μ signal model can be described as

$$S = X + jY \tag{2.61}$$

where X and Y correspond to in-phase and quadrature signals whose PDFs $f_X(x)$ and $f_Y(y)$ follow that in (2.64), by substituting the parameters σ_z, λ_z and μ_z by the parameters σ_x, λ_x and μ_x, or σ_y, λ_y and μ_y, as required. The envelope R and phase Θ are defined as

$$R^\alpha = X^2 + Y^2 \tag{2.62}$$

and

$$\Theta = \arg(X + jY) \tag{2.63}$$

wherein $\alpha > 0$ represents the nonlinearity parameter.

The building block for such a complex model is entrusted to a general quadrature PDF indicated, as follows, by the general process Z [19]

$$f_Z(z) = \frac{|z|^{\frac{\mu_z}{2}} \exp\left(-\frac{(z-\lambda_z)^2}{2\sigma_z^2}\right) I_{\frac{\mu_z}{2}-1}\left(\frac{|z\lambda_z|}{\sigma_z^2}\right)}{2\sigma_z^2 |\lambda_z|^{\frac{\mu_z}{2}-1} \cosh\left(\frac{z\lambda_z}{\sigma_z^2}\right)}, \tag{2.64}$$

in which: (i) $-\infty < z < \infty$; (ii) σ_z^2 is the power of one multipath cluster and $\sigma_z > 0$; (iii) λ_z^2 is the power of dominant component of all clusters and $-\infty < \lambda_z < \infty$; and (iv) $\mu_z > 0$ is the number of multipath clusters.

In addition, let $W = Z^2$ be the corresponding power random variable. The PDF of W, $f_W(w)$, is represented as

$$f_W(w) = \frac{|w|^{\frac{\mu_w}{4}-\frac{1}{2}} \exp\left(-\frac{w-\lambda_w^2}{2\sigma_w^2}\right) I_{\frac{\mu_w}{2}-1}\left(\frac{\lambda_w\sqrt{w}}{\sigma_w^2}\right)}{2\sigma_w^2 \lambda_w^{\frac{\mu_w}{2}-1}} \tag{2.65}$$

with $\mu_w = \mu_z$, $\lambda_w = |\lambda_z|$ and $\sigma_w = \sigma_z$.

Before proceeding to the model PDFs, let us discuss some of the many parametrizations available for the α-η-κ-μ distribution [19], denominated: (i) Parametrization-0 (raw parametrization); (ii) Parametrization-1 (local parametrization); and (iii) Parametrization-2 (global parametrization). Each format has its uniqueness and represents a set of physical parameters. For Parametrization-0, the PDFs make use of already defined in-phase (X) and quadrature (Y) parameters, which are σ_x and σ_y, λ_x and λ_y, and μ_x and μ_y. In Parametrization-1, the parameters are switched out to local conventional parameters known as: (i) κ_x and κ_y, representing the ratio between the total power of the dominant components and the total power of scattered waves, i.e. $\kappa_x = \lambda_x^2/\left(\mu_x\sigma_x^2\right)$ and $\kappa_y = \lambda_y^2/\left(\mu_y\sigma_y^2\right)$; and (ii) $\hat{r}_x^2 = E\left(X^2\right)$ and $\hat{r}_y^2 = E\left(Y^2\right)$, indicating the mean value, and $\hat{r}_x^2 = \mu_x\sigma_x^2 + \lambda_x^2$. and $\hat{r}_y^2 = \mu_z\sigma_y^2 + \lambda_y^2$. Finally, in Parametrization-2, the PDFs are described in terms of comparative parameters, namely: (i) $\hat{r}^\alpha > 0$, denoting the mean value $E\left(R^\alpha\right)$, i.e. $\hat{r}^\alpha = \mu_x\sigma_x^2 + \lambda_x^2 + \mu_y\sigma_y^2 + \lambda_y^2$; (ii) $\eta > 0$, defining the ratio of the total power of in-phase and quadrature scattered waves of the multipath clusters, i.e. $\eta = \sigma_x^2/\sigma_y^2$; (iii) $\kappa > 0$, indicating the ratio of the total power of the dominant components and the total power of scattered waves, i.e. $\kappa = (\lambda_x^2 + \lambda_y^2)/(\mu_x\sigma_x^2 + \mu_y\sigma_y^2)$; (iv) $\mu > 0$, representing the total number of multipath clusters, i.e. $\mu = (\mu_x + \mu_y)/2$; (v) $p > 0$, portraying the ratio of the number of multipath clusters of in-phase and quadrature signals, i.e. $p = \mu_x/\mu_y$; and (vi) $q > 0$, giving the ratio of two ratios: (a) the ratio of the power of the dominant components to the power of the scattered waves of the in-phase signal to (b) its quadrature counterpart, i.e. $q = \lambda_x^2/\lambda_y^2$. As can be observed, all Parametrizations are intrinsically linked. For completeness, three other relations are shown below as follows: (i) in (2.66), the raw parameters are rewritten in terms of global parameters ; (ii) in (2.67), the local parameters are redefined as global parameters; and (iii) in (2.68), the global parameters are represented in terms of local parameters.

$$
\begin{aligned}
\sigma_x &= \left(\frac{\eta(1+p)\hat{r}^\alpha}{2(1+\eta)(1+\kappa)\mu p}\right)^{\frac{1}{2}} & \sigma_y &= \left(\frac{(1+p)\hat{r}^\alpha}{2(1+\eta)(1+\kappa)\mu}\right)^{\frac{1}{2}} \\
\lambda_x &= \left(\frac{\eta\kappa q\hat{r}^\alpha}{(1+\kappa)(q\eta+1)}\right)^{\frac{1}{2}} & \lambda_y &= \left(\frac{\kappa\hat{r}^\alpha}{(1+\kappa)(q\eta+1)}\right)^{\frac{1}{2}} \\
\mu_x &= \frac{2p\mu}{1+p} & \mu_y &= \frac{2\mu}{1+p}
\end{aligned}
\tag{2.66}
$$

$$\begin{aligned}
\kappa_x &= \frac{(1+\eta)q\kappa}{1+q\eta} & \kappa_y &= \frac{(1+\eta)\kappa}{1+q\eta} \\
\hat{r}_x &= \left(\frac{\eta(1+q(\eta+\kappa+\eta\kappa))\hat{r}^\alpha}{(1+\eta)(1+\kappa)(1+q\eta)}\right)^{\frac{1}{2}} & \hat{r}_y &= \left(\frac{(1+\kappa+\eta(q+\kappa)\hat{r}^\alpha}{(1+\eta)(1+\kappa)(1+q\eta)}\right)^{\frac{1}{2}} \\
\mu_x &= \frac{2p\mu}{1+p} & \mu_y &= \frac{2\mu}{1+p}
\end{aligned} \tag{2.67}$$

$$\begin{aligned}
\kappa &= \frac{\kappa_x(1+\kappa_x)\hat{r}_x^2+\kappa_y(1+\kappa_y)\hat{r}_y^2}{(1+\kappa_x)\hat{r}_x^2+(1+\kappa_y)\hat{r}_y^2} & \eta &= \frac{(1+\kappa_y)\hat{r}_y^2}{(1+\kappa_x)\hat{r}_x^2} \\
\hat{r}^\alpha &= \hat{r}_x^2+\hat{r}_x^2 & q &= \frac{\kappa_x}{\kappa_y}
\end{aligned} \tag{2.68}$$

With these in mind, and considering Parametrization-2, the α-η-κ-μ signal has a joint phase-envelope PDF $f_{R,\Theta}(r,\theta)$ given as

$$\begin{aligned}
f_{R,\Theta}(r,\theta) = {} & \frac{\alpha\mu^2 p(1+\eta)^2(1+\kappa)^{\frac{\mu}{2}+1}(1+q\eta)^{\frac{\mu}{2}-1}}{2\eta(1+p)^2(q\eta)^{\frac{\mu p}{2(1+p)}-\frac{1}{2}}\kappa^{\frac{\mu}{2}-1}}\,|\sin\theta|^{\frac{\mu}{1+p}}\,|\cos\theta|^{\frac{\mu p}{1+p}}\,\frac{r^{\frac{\alpha}{2}(\mu+2)-1}}{\hat{r}^{\frac{\alpha}{2}(\mu+2)}} \\
& \times\exp\left(-\frac{(1+\eta)\kappa\mu(1+pq)}{(1+p)(1+q\eta)}-\frac{(1+\eta)(1+\kappa)\mu\left(\eta\sin^2\theta+p\cos^2\theta\right)}{\eta(1+p)}\frac{r^\alpha}{\hat{r}^\alpha}\right) \\
& \times\exp\left(\frac{2(1+\eta)\mu\cos(\theta-\phi)}{\eta(1+p)}\sqrt{\frac{\eta\kappa(1+\kappa)\left(\eta+p^2q\right)}{1+q\eta}}\frac{r^{\frac{\alpha}{2}}}{\hat{r}^{\frac{\alpha}{2}}}\right) \\
& \times\frac{I_{\frac{\mu}{1+p}-1}\left(\frac{2(1+\eta)\mu|\sin\theta|}{1+p}\sqrt{\frac{\kappa(1+\kappa)}{1+q\eta}}\frac{r^{\frac{\alpha}{2}}}{\hat{r}^{\frac{\alpha}{2}}}\right)I_{\frac{\mu p}{1+p}-1}\left(\frac{2(1+\eta)\mu p|\cos\theta|}{\eta(1+p)}\sqrt{\frac{\eta\kappa q(1+\kappa)}{1+q\eta}}\frac{r^{\frac{\alpha}{2}}}{\hat{r}^{\frac{\alpha}{2}}}\right)}{\cosh\left(\frac{2(1+\eta)\mu|\sin\theta|}{1+p}\sqrt{\frac{\kappa(1+\kappa)}{1+q\eta}}\frac{r^{\frac{\alpha}{2}}}{\hat{r}^{\frac{\alpha}{2}}}\right)\cosh\left(\frac{2(1+\eta)\mu p|\cos\theta|}{\eta(1+p)}\sqrt{\frac{\eta\kappa q(1+\kappa)}{1+q\eta}}\frac{r^{\frac{\alpha}{2}}}{\hat{r}^{\frac{\alpha}{2}}}\right)},
\end{aligned} \tag{2.69}$$

wherein $r \geq 0$, $-\pi < \theta \leq \pi$ and $\phi = \tan^{-1}\left((1/p)\,(\eta/q)^{\frac{1}{2}}\right)$.

From (2.69), the phase and envelope marginal PDFs can be promptly obtained by performing an integration with respect to R and Θ, respectively. Note that (2.69) is rather elaborate, and therefore, no closed-form formulations for the marginal PDFs could be found from this approach. In order to fill this gap, [19] developed an envelope-based approach, where the relation between the envelope R and in-phase and quadrature components X and Y given in (2.62) was used, in which X^2 and Y^2 denoting the power of two independent κ-μ variables, with their respective PDFs being indicated in (2.64). As defined in [19], with $U = X^2$ and $V = Y^2$, the PDF of α-η-κ-μ envelope can be evaluated as

$$f_R(r) = \alpha r^\alpha \int_0^{r^\alpha} f_U(u) f_V(r^\alpha - u)\,\mathrm{d}u \tag{2.70}$$

or

$$f_R(r) = \alpha r^\alpha \int_0^{r^\alpha} f_U(r^\alpha - v) f_V(v)\,\mathrm{d}v, \tag{2.71}$$

wherein $f_U(u)$ and $f_V(v)$ follow the PDF in (2.65) with $\mu_u = \mu_x$, $\lambda_u = |\lambda_x|$, $\sigma_u = \sigma_x$, $\mu_v = \mu_y$, $\lambda_v = |\lambda_y|$ and $\sigma_v = \sigma_y$.

To solve these integrals, the author in [19] proposed a series expansion formulation. This equation, however, is quite complicated to implement due to its recursive nature, and its convergence is largely dependent on parameters.

The exact LCR and PCR are given in integral-form, respectively, as [42]

$$\begin{aligned}
N_R(r) = &\frac{\sqrt{2\pi} f_m \kappa^{1-\frac{\mu}{2}}(1+\kappa)^{\frac{1+\mu}{2}}(1+\eta)^{\frac{3}{2}}\mu^{\frac{3}{2}}q^{\frac{1}{2}\left(1-\frac{\mu p}{1+p}\right)}}{(1+d)\eta^{\frac{1}{2}\left(1+\frac{\mu p}{1+p}\right)}(1+p)^{3/2}(1+q\eta)^{1-\frac{\mu}{2}}} \frac{r^{\frac{1}{2}\alpha(\mu+2)}}{\hat{r}^{\frac{1}{2}\alpha(\mu+2)}} \int_{-\pi}^{\pi} |\sin\theta|^{\frac{\mu}{1+p}} |\cos\theta|^{\frac{\mu p}{1+p}} \\
&\times \sqrt{p\left(d^2\eta\cos^2\theta + p\sin^2\theta\right)} \exp\left(-\frac{(1+\eta)\kappa\mu(1+pq)}{(1+p)(1+q\eta)}\right) \\
&\times \exp\left(\frac{2(1+\eta)\mu}{1+p}\frac{\sqrt{\kappa(1+\kappa)}}{\sqrt{\eta(1+q\eta)}}\left(\sqrt{\eta}\sin\theta + p\sqrt{q}\cos\theta\right)\frac{r^{\alpha/2}}{\hat{r}^{\alpha/2}}\right) \\
&\times \exp\left(-\frac{(1+\eta)(1+\kappa)\mu}{\eta(1+p)}\left(\eta\sin^2\theta + p\cos^2\theta\right)\frac{r^{\alpha}}{\hat{r}^{\alpha}}\right) \\
&\times I_{\frac{\mu p}{1+p}-1}\left(\frac{2(1+\eta)(1+\kappa)\mu p}{\eta(1+p)}\sqrt{\frac{\eta\kappa q}{(1+\kappa)(1+q\eta)}}|\cos\theta|\frac{r^{\frac{\alpha}{2}}}{\rho^{\frac{\alpha}{2}}}\right) \\
&\times I_{\frac{\mu}{1+p}-1}\left(\frac{2(1+\eta)(1+\kappa)\mu}{1+p}\sqrt{\frac{\kappa}{(1+\kappa)(1+q\eta)}}|\sin\theta|\frac{r^{\frac{\alpha}{2}}}{\rho^{\frac{\alpha}{2}}}\right) \\
&\times \operatorname{sech}\left(\frac{2(1+\eta)(1+\kappa)\mu p}{\eta(1+p)}\sqrt{\frac{\eta\kappa q}{(1+\kappa)(1+q\eta)}}\cos\theta\frac{r^{\frac{\alpha}{2}}}{\rho^{\frac{\alpha}{2}}}\right) \\
&\times \operatorname{sech}\left(\frac{2(1+\eta)(1+\kappa)\mu}{1+p}\sqrt{\frac{\kappa}{(1+\kappa)(1+q\eta)}}\sin\theta\frac{r^{\frac{\alpha}{2}}}{\hat{r}^{\frac{\alpha}{2}}}\right) \mathrm{d}\theta
\end{aligned} \tag{2.72}$$

and

$$
\begin{aligned}
N_\Theta(\theta) = {} & \frac{\sqrt{\pi}\alpha f_m(1+\eta)^{3/2}\mu^{3/2}\sqrt{p}\kappa^{1-\frac{\mu}{2}}(1+\kappa)^{\frac{\mu+1}{2}}q^{\frac{1}{2}\left(1-\frac{\mu p}{1+p}\right)}}{(1+d)(1+p)^{3/2}\eta^{\frac{1}{2}\left(\frac{\mu p}{1+p}+1\right)}(1+\eta q)^{1-\frac{\mu}{2}}\sqrt{d^2\eta+\cos(2\theta)\left(p-d^2\eta\right)+p}} \\
& \times |\sin\theta|^{\frac{\mu}{1+p}}\,|\cos\theta|^{\frac{\mu p}{1+p}}\left(d^2\eta\sin^2(\theta)+p\cos^2(\theta)\right)\exp\left(-\frac{(1+\eta)\kappa\mu(1+pq)}{(1+p)(1+q\eta)}\right) \\
& \times \int_0^\infty \frac{r^{\frac{1}{2}(\alpha\mu+\alpha-2)}}{\hat{r}^{\frac{1}{2}\alpha(\mu+1)}}\exp\left(-\frac{(1+\eta)(1+\kappa)\mu}{\eta(1+p)}\left(\eta\sin^2\theta+p\cos^2\theta\right)\frac{r^\alpha}{\hat{r}^\alpha}\right) \\
& \times \exp\left(\frac{4(1+\eta)\mu}{1+p}\frac{\sqrt{\kappa(1+\kappa)}}{\sqrt{\eta(1+q\eta)}}\left(\sqrt{\eta}\sin\theta+p\sqrt{q}\cos\theta\right)\frac{r^{\alpha/2}}{\hat{r}^{\alpha/2}}\right) \\
& \times I_{\frac{\mu p}{1+p}-1}\left(\frac{2(1+\eta)(1+\kappa)\mu p}{\eta(1+p)}\sqrt{\frac{\eta\kappa q}{(1+\kappa)(1+q\eta)}}\,|\cos\theta|\,\frac{r^{\frac{\alpha}{2}}}{\rho^{\frac{\alpha}{2}}}\right) \\
& \times I_{\frac{\mu}{1+p}-1}\left(\frac{2(1+\eta)(1+\kappa)\mu}{1+p}\sqrt{\frac{\kappa}{(1+\kappa)(1+q\eta)}}\,|\sin\theta|\,\frac{r^{\frac{\alpha}{2}}}{\rho^{\frac{\alpha}{2}}}\right) \\
& \times \operatorname{sech}\left(\frac{2(1+\eta)(1+\kappa)\mu p}{\eta(1+p)}\sqrt{\frac{\eta\kappa q}{(1+\kappa)(1+q\eta)}}\cos\theta\frac{r^{\frac{\alpha}{2}}}{\rho^{\frac{\alpha}{2}}}\right) \\
& \times \operatorname{sech}\left(\frac{2(1+\eta)(1+\kappa)\mu}{1+p}\sqrt{\frac{\kappa}{(1+\kappa)(1+q\eta)}}\sin\theta\frac{r^{\frac{\alpha}{2}}}{\hat{r}^{\frac{\alpha}{2}}}\right)\mathrm{d}r,
\end{aligned}
\tag{2.73}
$$

wherein f is the mean Doppler frequency defined as $f \triangleq (f_x+f_y)/2$, and f_x and f_y are the in-phase and quadrature Doppler frequencies, respectively, and d is the ratio of Doppler frequencies between in-phase and quadrature components, i.e. $d = f_x/f_y$.

As mentioned earlier, the α-η-κ-μ model is very general; therefore, an enormous number of distributions can be mapped from its expressions. Considering Parametrization-2, the following general distributions can be obtained: (i) α-μ with $\alpha=\alpha$, $\mu=\mu$, $\kappa\to 0$, $\eta=p$ and $\hat{r}=\hat{r}$; (ii) η-μ model with $\alpha=2$, $\mu=2\mu$, $\kappa\to 0$, $\eta=\eta$, $p=1$ and $\hat{r}=\hat{r}$; (iii) κ-μ model wherein $\alpha=2$, $\mu=\mu$, $\kappa=\kappa$, $\eta=p$, $q=q$ and $\hat{r}=\hat{r}$; (iv) Beckmann model with $\alpha=2$, $\mu=1$, $\kappa=\kappa$, $\eta=\eta$, $p=1$, $q=q$ and $\hat{r}=\hat{r}$; (v) α-η-μ $\alpha=\alpha$, $\mu=2\mu$, $\kappa\to 0$, $\eta=\eta$, $p=1$; and (vi) α-κ-μ model wherein $\alpha=\alpha$, $\mu=\mu$, $\kappa=\kappa$, $\eta=p$, $q=q$ and $\hat{r}=\hat{r}$. As previously specified, the η-μ fading distribution has Hoyt and Nakagami-m models as particular cases, and the κ-μ fading distribution reduces to both Rice and Nakagami-m models.

Chapter 3

The Extended η-μ Fading Model

Cluster imbalance was first introduced in [16] for the Nakagami-m phase-envelope joint distribution. In that case, the Nakagami-m complex model was redefined by inserting a new parameter p which affected only its phase PDF formulation. Furthermore, the same parameter was inserted in [58] for the η-μ fading model. Surprisingly, for this particular case, the envelope statistics were also affected by the cluster imbalance phenomenon, although no closed-form expression was found to depict its behavior. Later on, the imbalance parameter was reinvented in [19] for the α-η-κ-μ model. Despite its novelty and possible potential for delivering new closed-form expressions for both phase and envelope, little attention has been given to p concerning its influence on first order statistics and on other mapped models.

With that in mind, the aim of this chapter is to partially fill this gap, by proposing an Extended η-μ complex model, as a particular case of the α-η-κ-μ fading model. Unlike the original η-μ model, this proposal explores the difference in the number of multipath clusters between the in-phase and quadrature components, by introducing the parameter p.

This chapter offers a thorough statistical study for the Extended model and is structured as follows:

– Section 3.1 introduces the Extended η-μ physical model and derives the joint phase-envelope distribution;

– Section 3.2 derives the envelope PDF and CDF, and depicts their behavior with some plots;

– Section 3.3 proposes expressions for both phase PDF and CDF, which are accompanied with some curves;

- Section 3.4 develops formulations for the Extended η-μ higher order statistics, such as LCR and PCR;

- Section 3.5 derives the moment generating function for the instantaneous SNR, and indicates possible applications in wireless channels;

- Finally, Section 3.6 explores some of its particular cases.

3.1 Joint Phase-Envelope Statistics

As discussed in [19], the complex fading models of the well established fading models, namely, Rayleigh, Rice, Hoyt, and Beckmann, have made use of a quadrature Gaussian. Such a paradigm was broken in the complex models for Nakagami-m, η-μ, κ-μ, and α-η-κ-μ. On the latter, the author proposed a general quadrature PDF which encompasses all previously mentioned fading models. For the Extended η-μ, the general process $-\infty < Z < \infty$ indicated in (2.64) is considered, wherein due to the absence of dominant components $\lambda_z \to 0$. With this, the PDF of Z is redefined as

$$f_Z(z) = \frac{|z|^{2\mu_z-1}}{2^{\mu_z}\sigma_z^{2\mu_z}\Gamma(\mu_z)} \exp\left(-\frac{z^2}{2\sigma_z^2}\right), \tag{3.1}$$

in which $\sigma_z^2 > 0$ is the power of one multipath cluster, $\mu_z > 0$ is the number of multipath clusters and $\Gamma(x)$ is the Gamma function [1, Eq. (6.1.1)]. In addition, let $V = Z^2$ be the corresponding power. Its PDF is found as

$$f_V(v) = \frac{v^{\mu_v-1}}{2^{\mu_v}\sigma_v^{2\mu_v}\Gamma(\mu_v)} \exp\left(-\frac{v}{2\sigma_v^2}\right), \tag{3.2}$$

with $\mu_v = \mu_z$ and $\sigma_v = \sigma_z$.

Let the complex Extended η-μ signal be defined as

$$S = X + jY, \tag{3.3}$$

in which X and Y denote the in-phase and quadrature signals whose PDFs $f_X(x)$ and $f_Y(y)$ follow that in (3.1), with respective parameters μ_x and σ_x, and μ_y and σ_y. The resulting complex signal can be rewritten as

$$S = R\exp(j\Theta), \tag{3.4}$$

wherein R is the envelope and Θ is the phase. By making the variable transformations $X = R\cos\Theta$ and $Y = R\sin\Theta$, the joint PDF is found as

$$f_{R,\Theta}(r,\theta) = r f_X(r\cos\theta) \times f_Y(r\sin\theta). \tag{3.5}$$

For the following development, let us consider only the Format 1 of the η-μ model. Thus, $0 < \eta < \infty$ is defined as the ratio of the total power of in-phase and quadrature scattered waves of the multipath clusters, i.e. $\eta = \mu_x\sigma_x^2/\left(\mu_y\sigma_y^2\right)$, and σ_x and σ_y are obtained, respectively, as

$$\sigma_x = \left(\frac{\hat{r}^2\eta}{2\mu_x(1+\eta)}\right)^{\frac{1}{2}} \tag{3.6}$$

and

$$\sigma_y = \left(\frac{\hat{r}^2}{2\mu_y(1+\eta)}\right)^{\frac{1}{2}}. \tag{3.7}$$

Now, consider an imbalance parameter $p > 0$ defined as the ratio of the number of multipath clusters of in-phase and quadrature signals given as

$$p = \frac{\mu_x}{\mu_y}, \tag{3.8}$$

in which $p = 1$ stands for the balanced condition. Finally, let $\mu > 0$ be defined as the total number of multipath clusters as in

$$\mu_x + \mu_y = 2\mu. \tag{3.9}$$

Then, from (3.8) and (3.9), μ_x and μ_y can be represented in terms of μ and p as given in

$$\mu_x = \frac{2\mu p}{1+p} \tag{3.10}$$

and

$$\mu_y = \frac{2\mu}{1+p}. \tag{3.11}$$

Substituting (3.1), (3.6), (3.7), (3.10) and (3.11) in (3.5), the phase-envelope joint distribution is obtained as

$$\begin{aligned} f_{R,\Theta}(r,\theta) = {} & \frac{2^{2\mu}(1+\eta)^{2\mu}\mu^{2\mu}p^{\frac{2\mu p}{1+p}}}{\eta^{\frac{2\mu p}{1+p}}(1+p)^{2\mu}\Gamma\left(\frac{2\mu}{1+p}\right)\Gamma\left(\frac{2\mu p}{1+p}\right)} |\sin\theta|^{\frac{4\mu}{1+p}-1} |\cos\theta|^{\frac{4\mu p}{1+p}-1} \frac{r^{4\mu-1}}{\hat{r}^{4\mu}} \\ & \times \exp\left(-\frac{2(1+\eta)\mu}{(1+p)}\left(\sin^2\theta + \frac{p}{\eta}\cos^2\theta\right)\frac{r^2}{\hat{r}^2}\right), \end{aligned} \tag{3.12}$$

wherein $r \geq 0$ and $-\pi < \theta \leq \pi$. Note that (3.12) reduces to (2.26) for $p = 1$ (balanced case). Although only Format 1 formulations are shown, Format 2 can be obtained by means of

$$\eta_1 = \frac{(1-\eta_2)}{(1+\eta_2)}. \tag{3.13}$$

3.2 Envelope Statistics

3.2.1 Envelope PDF

Given the phase-envelope joint PDF, the marginal PDF of one variable can be obtained by simple integration of this joint PDF with respect to the other variable. For instance, the envelope PDF can be calculated by

$$f_R(r) = \int_{-\pi}^{\pi} f_{R,\Theta}(r,\theta)\,\mathrm{d}\theta. \tag{3.14}$$

However, in the present case (Eq. (3.12)), only the phase PDF can be found in closed-form by direct integration (discussed later on Section 3.3). Then, to obtain a closed-form solution for the envelope PDF, another convenient statistical approach is needed.

Let the power of the envelope be defined as $W = U + Q$, wherein $W = R^2$, and $U = X^2$ and $Q = Y^2$ are the powers of both in-phase and quadrature signals X and Y, with their PDFs detailed in (3.2). Then, to obtain the PDF of W, $f_W(w)$, we follow the standard convolution procedure for adding two independent random variables which is defined as

$$f_W(w) = f_U(u) * f_Q(q). \tag{3.15}$$

In this case, to solve (3.15), the Laplace transform operation is carried out, converting the convolution procedure into a multiplication, as pointed below by

$$\mathcal{L}_w\left[f_W(w)\right](s) = \mathcal{L}_u\left[f_U(u)\right](s) \times \mathcal{L}_q\left[f_Q(q)\right](s), \tag{3.16}$$

wherein $\mathcal{L}\left[\cdot\right](s)$ is the Laplace transform operator [1, Eq. (29.1.1)], s is the Laplace variable, and the Laplace transform of (3.2) is given as

$$\mathcal{L}_w\left[f_V(v)\right](s) = \left(2\sigma_v^2 s + 1\right)^{-\mu_v}. \tag{3.17}$$

Using (3.17), Equation (3.16) can be rewritten as

$$\mathcal{L}_w\left[f_W(w)\right](s) = \left(2\sigma_x^2 s + 1\right)^{-\mu_x}\left(2\sigma_y^2 s + 1\right)^{-\mu_y}, \tag{3.18}$$

where $\sigma_u = \sigma_x$ and $\mu_u = \mu_x$, and $\sigma_q = \sigma_y$ and $\mu_q = \mu_y$.

Now, consider the following variable transformation $s = 2\pi j f$, in which f is the Fourier variable. Thus, the Laplacian operator can be substituted by the Fourier transform operator leading to

$$\begin{aligned}\mathcal{F}_w\left[f_W(w)\right](f) &= \mathcal{L}_w\left[f_W(w)\right](s)|_{s=2\pi jf} \\ &= \left(\frac{1}{4\pi\sigma_x^2}+jf\right)^{-\mu_x}\left(\frac{1}{4\pi\sigma_y^2}+jf\right)^{-\mu_y}\left(\frac{1}{4\pi\sigma_x^2}\right)^{\mu_x}\left(\frac{1}{4\pi\sigma_y^2}\right)^{\mu_y}, \quad (3.19)\end{aligned}$$

where $\mathcal{F}\left[\cdot\right](f)$ is the Fourier transform operator [3, Eq. (17.21)].

To obtain the PDF of W, the inverse Fourier transform of (3.19) must be carried out, leading to

$$\begin{aligned}f_W(w) = &\left(\frac{1}{4\pi\sigma_x^2}\right)^{\mu_x}\left(\frac{1}{4\pi\sigma_y^2}\right)^{\mu_y}\int_{-\infty}^{\infty}\left(\frac{1}{4\pi\sigma_x^2}+jf\right)^{-\mu_x} \\ &\times\left(\frac{1}{4\pi\sigma_y^2}+jf\right)^{-\mu_y}\exp\left(2\pi jwf\right)\mathrm{d}f. \quad (3.20)\end{aligned}$$

Equation (3.20) can be solved by using the following mathematical identity [61, Eq. (2.3.6.18)],

$$\int_{-\infty}^{\infty}\frac{(y+jx)^{-\rho}(z+jx)^{-\sigma}}{\exp\left(-2\pi jwx\right)}\mathrm{d}x = \frac{2\pi(2\pi w)^{\rho+\sigma-1}\,{}_1F_1(\rho;\rho+\sigma;2\pi w(z-y))}{\Gamma(\rho+\sigma)\exp\left(2\pi wz\right)}, \quad (3.21)$$

wherein ${}_1F_1\left(a;b;z\right)$ is the Kummer confluent hypergeometric function [1, Eq. (13.1.2)]. Therefore, the envelope power PDF, $f_W(w)$, is given as in

$$\begin{aligned}f_W(w) = &\frac{w^{\mu_x+\mu_y-1}}{2^{\mu_x+\mu_y}\sigma_x^{2\mu_x}\sigma_y^{2\mu_y}\Gamma(\mu_x+\mu_y)}\,{}_1F_1\left(\mu_x;\mu_x+\mu_y;\frac{1}{2}w\left(\frac{1}{\sigma_y^2}-\frac{1}{\sigma_x^2}\right)\right) \\ &\times\exp\left(-\frac{w}{2\sigma_y^2}\right) \quad (3.22)\end{aligned}$$

or equivalently,

$$\begin{aligned}f_W(w) = &\frac{w^{\mu_x+\mu_y-1}}{2^{\mu_x+\mu_y}\sigma_x^{2\mu_x}\sigma_y^{2\mu_y}\Gamma(\mu_x+\mu_y)}\,{}_1F_1\left(\mu_y;\mu_x+\mu_y;\frac{1}{2}w\left(\frac{1}{\sigma_x^2}-\frac{1}{\sigma_y^2}\right)\right) \\ &\times\exp\left(-\frac{w}{2\sigma_x^2}\right). \quad (3.23)\end{aligned}$$

Replacing (3.6), (3.7), (3.10) and (3.11) in (3.22) (or (3.23)), the PDF of W can be rewritten as

$$\begin{aligned}f_W(w) = &\frac{2^{2\mu+1}w^{2\mu-1}p^{\frac{2\mu p}{1+p}}(1+\eta)^{2\mu}\mu^{2\mu}}{\eta^{\frac{2\mu p}{1+p}}\left(1+p\right)^{2\mu}\hat{r}^{4\mu}\Gamma(2\mu)}\,{}_1F_1\left(\frac{2\mu p}{1+p};2\mu;-\frac{2(p-\eta)(1+\eta)\mu w}{\hat{r}^2(1+p)\eta}\right) \\ &\times\exp\left(-\frac{2(1+\eta)\mu w}{\hat{r}^2\left(1+p\right)}\right). \quad (3.24)\end{aligned}$$

Finally, with $W = R^2$, the envelope PDF, $f_R(r)$, is obtained as

$$f_R(r) = \frac{2^{2\mu+1} r^{4\mu-1} p^{\frac{2\mu p}{1+p}} (1+\eta)^{2\mu} \mu^{2\mu}}{\eta^{\frac{2\mu p}{1+p}} (1+p)^{2\mu} \hat{r}^{4\mu} \Gamma(2\mu)} \, {}_1F_1\left(\frac{2\mu p}{1+p}; 2\mu; -\frac{2(p-\eta)(1+\eta)\mu r^2}{\hat{r}^2(1+p)\eta}\right)$$
$$\times \exp\left(-\frac{2(1+\eta)\mu r^2}{\hat{r}^2(1+p)}\right). \tag{3.25}$$

Observe that with $p = 1$, (3.25) reduces to (2.31), and accordingly to both Nakagami-m and Hoyt distributions, depending on the value of η [13]. Interestingly, for any given η and p, (3.25) yields the same value for η/p and for p/η. This can be observed from the definition of these parameters. In addition, the Nakagami-m distribution can be directly obtained from it by using $\eta = p$.

Figure 3.1 depicts the plots of the envelope PDF for different values of p and some arbitrary values for the other parameters. As can be seen, the imbalance factor has great influence over the envelope PDF. Moreover, observe that as p grows from near zero towards the value of η, the PDF mode shifts rightwards, meaning a better fading condition. Interestingly, as p surpasses η, i.e. increases further towards infinity, the PDF mode shifts back leftwards, meaning a worse fading condition. This can be directly inferred from Figure 3.1 by noticing that the PDF is the same for η/p and p/η. Also, this pattern is noted for different settings of η, μ and p.

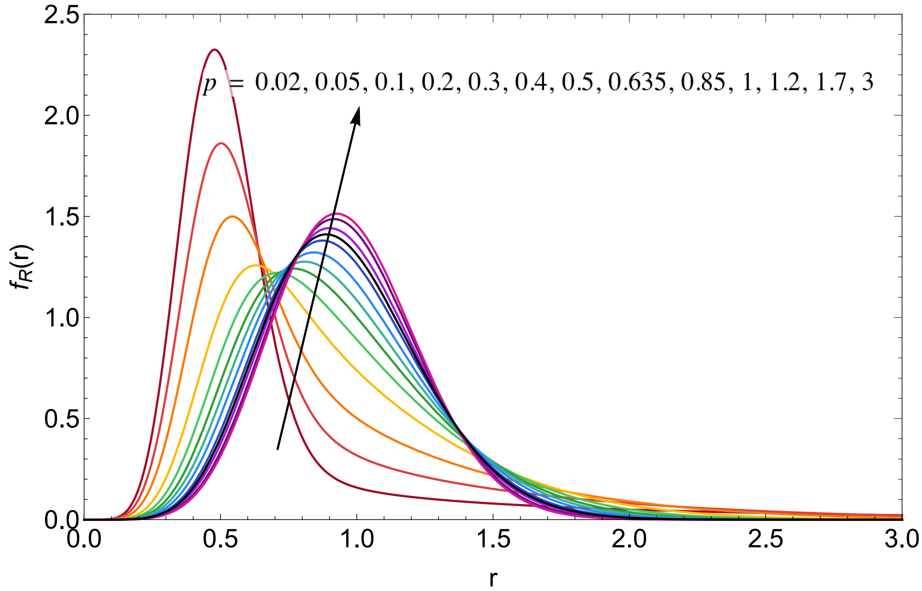

Figure 3.1: Envelope PDF for varying values of p ($\eta = 3.0$, $\mu = 1.75$ and $\hat{r} = 1$).

Figure 3.2 and 3.3 illustrate the behavior of envelope PDF for varying values of η and μ, respectively. Interestingly, in Figure 3.2, as observed earlier, as η approximates

p, the PDF mode shift grows rightwards, indicating better fading scenario. After η outstrips p, an inferior fading condition takes over, and the PDF grows indefinitely, shifting leftwards. As already expected, in Figure 3.3, the PDF mass dislocates towards superior fading scenario as μ grows.

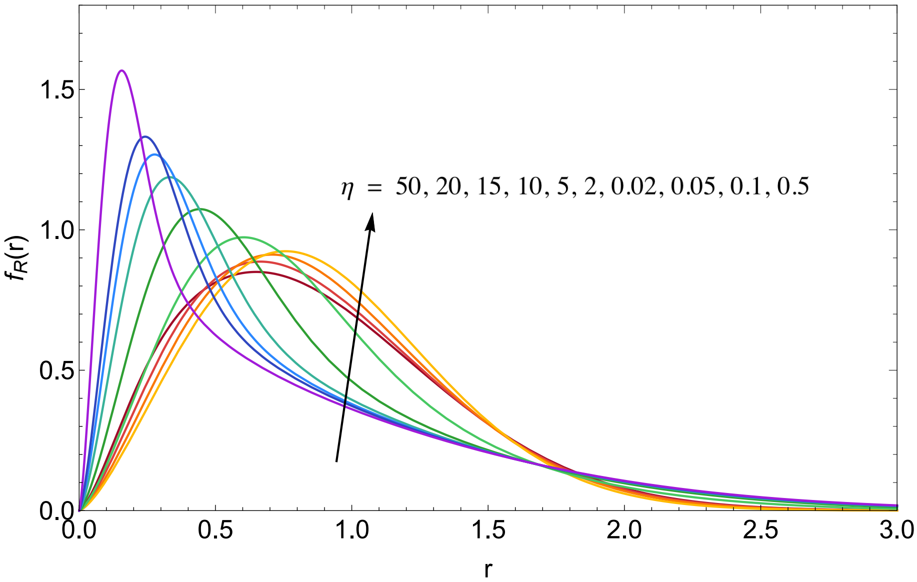

Figure 3.2: Envelope PDF for varying values of η ($\mu = 0.6$, $p = 0.35$ and $\hat{r} = 1$).

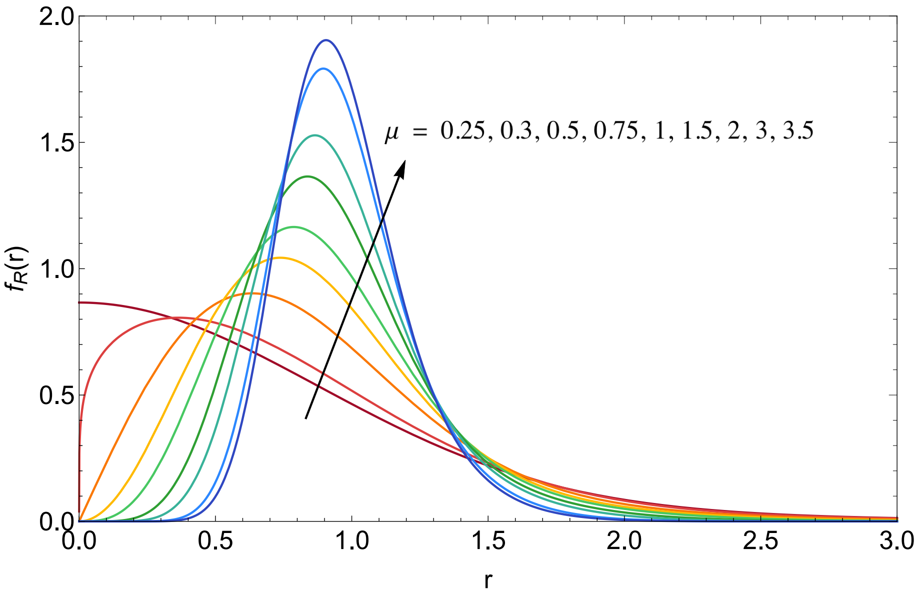

Figure 3.3: Envelope PDF for varying values of μ ($\eta = 0.5$, $p = 0.1$ and $\hat{r} = 1$).

3.2.2 Envelope CDF

The envelope CDF, $F_R(r)$, is given as

$$F_R(r) = 1 - \int_r^{\infty} f_R(x) \, \mathrm{d}x. \tag{3.26}$$

Therefore, the CDF for the Extended η-μ envelope is obtained by substituting (3.25) in (3.26). In order to arrive at a more tractable expression, a series expansion formulation for the CDF is now proposed. Let us rewrite the hypergeometric function in (3.25) as defined in [2, Eq. (2.20)],

$$ {}_1F_1\left(\frac{2\mu p}{1+p}; 2\mu; \frac{2(\eta-p)(1+\eta)\mu x^2}{(1+p)\eta\hat{r}^2}\right) = \sum_{k=0}^{\infty} \frac{\left(\frac{2\mu p}{1+p}\right)_k}{k!(2\mu)_k} \left(\frac{2(\eta-p)(1+\eta)\mu x^2}{(1+p)\eta\hat{r}^2}\right)^k, \quad (3.27) $$

with $(z)_k$ being the Pochhammer symbol [1, Eq. (6.1.22)].

Replacing (3.27) in (3.25), the envelope PDF is rewritten as

$$ f_R(r) = \sum_{k=0}^{\infty} \frac{2^{k+2\mu+1}\mu^{k+2\mu}p^{\frac{2\mu p}{1+p}}(\eta+1)^{k+2\mu}(\eta-p)^k r^{2k+4\mu-1}}{k!\Gamma(2\mu)(1+p)^{k+2\mu}(2\mu)_k \eta^{k+\frac{2\mu p}{1+p}}\hat{r}^{2k+4\mu}} \left(\frac{2\mu p}{1+p}\right)_k \times \exp\left(-\frac{2(1+\eta)\mu r^2}{(1+p)\hat{r}^2}\right). \quad (3.28) $$

And then, by replacing (3.28) in (3.26), the integral is formally solved, as given in

$$ F_R(r) = 1 - t^{\frac{2\mu p}{1+p}} \sum_{k=0}^{\infty} (1-t)^k \left(\frac{2\mu p}{1+p}\right)_k \frac{\Gamma\left(k+2\mu, \frac{2r^2(1+\eta)\mu}{(1+p)\hat{r}^2}\right)}{\Gamma(k+1)\Gamma(k+2\mu)}, \quad (3.29) $$

wherein $\Gamma(a,z)$ is the incomplete Gamma function [1, Eq. (6.5.3)] and $t = \min\{p/\eta, \eta/p\}$.

Figure 3.4 illustrates the envelope CDF of both integral and series expansion solutions for the same set of parameters as before, showing their equivalence. Here again the influence of p on the fading conditions is clearly observed: the closer p is to η the better the fading scenario. Note that there is no distinction between the integral and series expansion solutions.

3.2.3 Higher Order Moments

The n$^{\text{th}}$ moment of the envelope is defined as

$$ E(R^n) = \int_0^{\infty} r^n f_R(r)\,\mathrm{d}r. \quad (3.30) $$

By substituting (3.25) in (3.30), the n$^{\text{th}}$ moment of the envelope is found formally as

$$ E(R^n) = \frac{\hat{r}^n(1+p)^{\frac{n}{2}}p^{\frac{2\mu p}{1+p}}\Gamma\left(\frac{n}{2}+2\mu\right)}{2^{\frac{n}{2}}\eta^{\frac{2\mu p}{1+p}}(1+\eta)^{\frac{n}{2}}\mu^{\frac{n}{2}}\Gamma(2\mu)} {}_2F_1\left(\frac{2\mu p}{1+p}, \frac{1}{2}(n+4\mu); 2\mu; 1-\frac{p}{\eta}\right), \quad (3.31) $$

where ${}_2F_1(a_1, a_2; b; z)$ is the Gauss hypergeometric function [1, Eq. (15.1.1)].

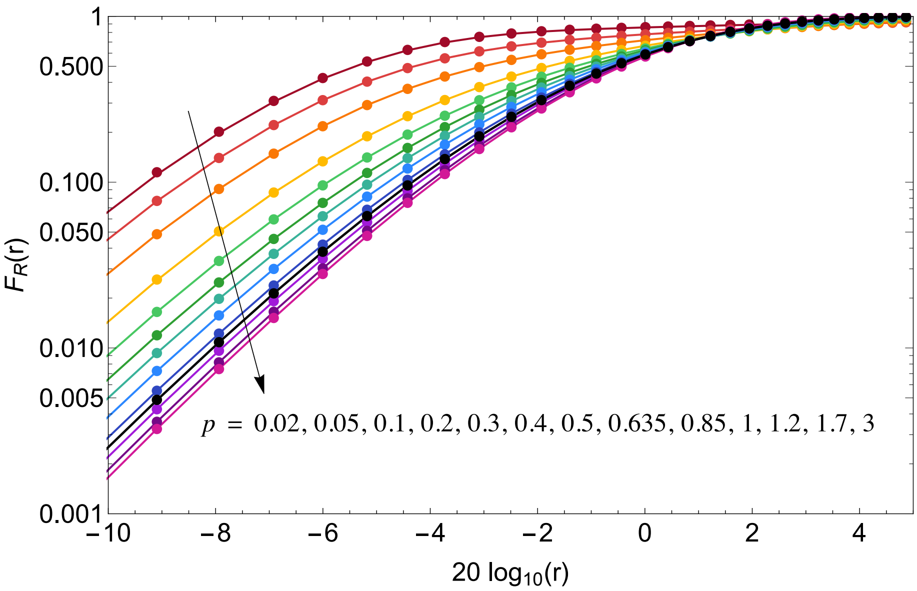

Figure 3.4: Envelope CDF for varying values of p ($\eta = 3.0$, $\mu = 1.75$ and $\hat{r} = 1$). Solid lines indicate integral solution and dot markers indicate series expansion solution.

3.2.4 Amount of Fading

The amount of fading (AF), also known as fading figure, is a unified measure of the severity of the fading [21]. It is defined as

$$AF \triangleq \frac{\mathrm{Var}(R^2)}{E(R^2)^2}, \tag{3.32}$$

wherein $\mathrm{Var}(R^2) = E\left(R^4\right) - E\left(R^2\right)^2$ is the variance operation.

Hence, using the higher order moment expression obtained in (3.31), the AF of the Extended η-μ model is obtained as

$$AF = \frac{(1+p)\left(\eta^2 + p\right)}{2\left(1+\eta\right)^2 \mu p}. \tag{3.33}$$

In Figure 3.5, the amount of fading is depicted as a function of the parameter η for varying p, and fixed $\mu = 2.35$. As can be seen in this particular scenario, the severity of the fading decreases until it reaches its minimum value wherein $p = \eta$. As η grows, i.e. $\eta > p$, the AF slowly start to increase again, indefinitely. Interestingly, the parameter μ dictates the behavior of the minimum value of the function, whereas cluster imbalance shifts its position along the abscissa. In other words, in fading scenarios where the number of multipath are equal, the AF minimum value is the same, for any given η and p.

Figure 3.6 illustrate the behavior of the AF as a function of μ for different values of p, and fixed $\eta = 2.35$. As expected, in different scenarios of cluster imbalance,

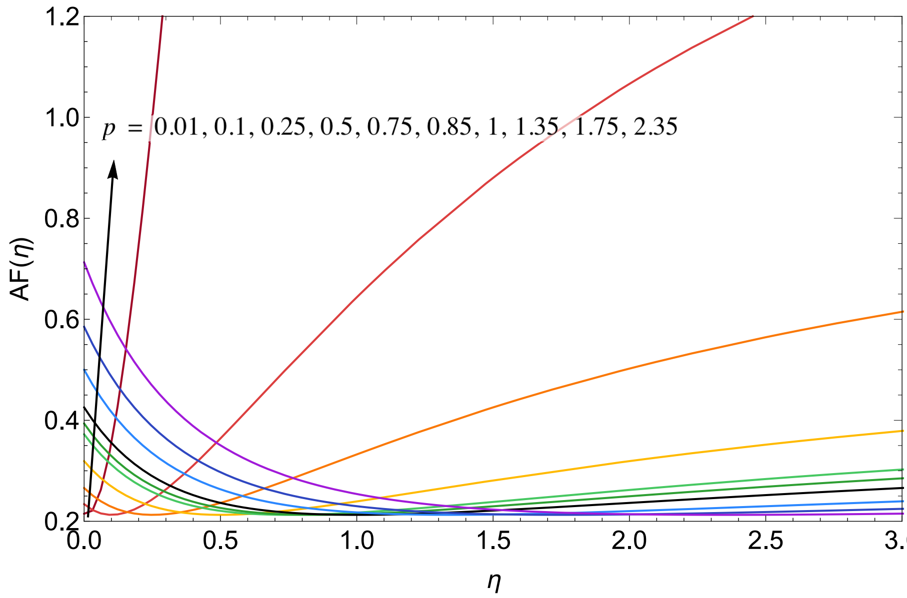

Figure 3.5: Amount of fading for varying values of η and p ($\mu = 2.35$).

fading severity decreases as μ increases. Also, as $p < \eta$ grows, the severity of the fading is drastically attenuated. However, the opposite is observed when the threshold $p = \eta$ is surpassed. This can be verified by taking the partial derivatives of (3.33) in respect to p, η and μ, and equating it to zero.

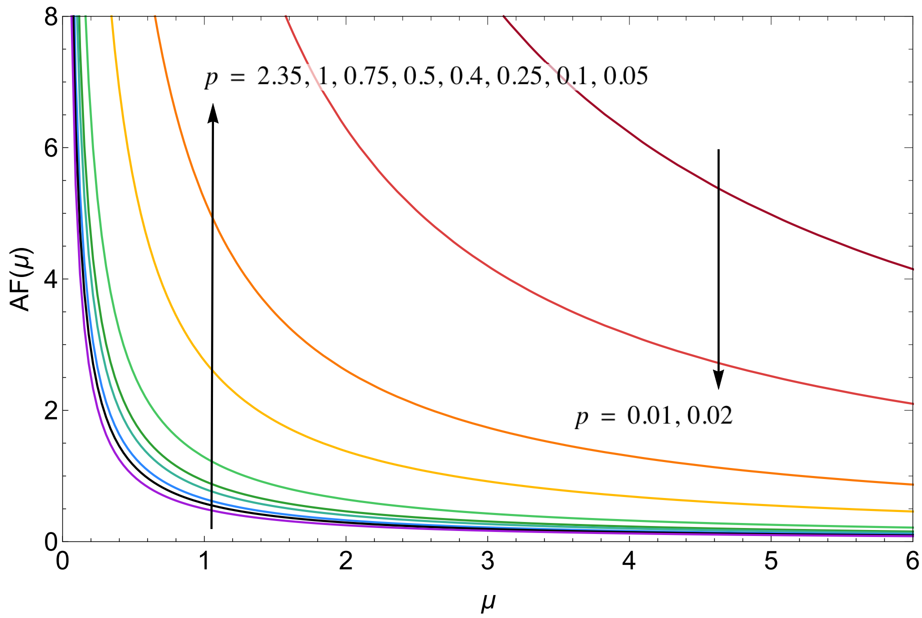

Figure 3.6: Amount of fading for varying values of μ and p ($\eta = 2.35$).

3.2.5 The Extended η-μ for a Fixed m

As seen in [21], the amount of fading of the Nakagami-m process is given as $AF = 1/m$. With this, [13] proposed an interesting alternative for parameter estimation by equaling both η-μ and Nakagami-m AFs. Then, for a given m, the parameters η and μ can be determined in order to yield the best fit. Note that some restrictions were imposed, i.e. $m/2 \leq \mu \leq m$, to guarantee that, for a fixed m and varying μ, a corresponding $\eta = (1-a)/(1+a)$ can be properly calculated, wherein $a = \sqrt{(2\mu/m)-1}$. Thus, in this section, a similar approach is carried on for the Extended η-μ model.

First, let us express the m parameter in respect to the Extended η-μ parameters,

$$m = \frac{2\left(1+\eta\right)^2 \mu p}{(1+p)(\eta^2+p)}, \tag{3.34}$$

so that $AF = 1/m$.

For a given m, the parameters η, μ and p are then selected to yield the best fit. The maximum and minimum values of m can be calculated by substituting the limiting values of η in (3.34), which are, for the Format 1 of the Extended η-μ model $\eta = 0$ and $\eta = \infty$, leading to $m = 2\mu/(1+p)$ and $m = 2\mu p/(1+p)$, respectively. Consequently, with $p \pm 1$, both scenarios lead to $m = \mu$, and with $p \to 0$ or $p \to \infty$, $m = 2\mu$. Therefore, for any given m, the parameter μ has to obey the following range

$$\frac{m}{2} < \mu < m. \tag{3.35}$$

Finally, considering (3.35), (3.34) can be solved in η, leading to

$$\eta = \frac{2\mu p}{m(1+p)-2\mu p} + \sqrt{\frac{mp(1+p)^2(2\mu-m)}{(m(1+p)-2\mu p)^2}}. \tag{3.36}$$

As observed in the traditional η-μ model, when $\mu = m/2$, (3.36) reduces to the Nakagami-m process with $\eta = p$. Surprisingly, when $\mu = m$, the Nakagami-m model is only attained if $p = 1$, and for $p \neq 1$, (3.36) simplifies to

$$\eta = \frac{2p}{1-p} + \sqrt{\frac{p(1+p)^2}{(p-1)^2}}. \tag{3.37}$$

As can be seen from (3.36), for a fixed m, the Extended η-μ model renders a myriad of different fading scenarios. Figure 3.7 illustrates one of the cases for the envelope PDF, wherein $m = 1.25$, $\mu = 1.245$ and p assumes varying values.

3.2.6 New Fading Scenarios

After exploring all these new statistics of the Extended η-μ model, some questions about the applicability of cluster imbalance on real fading scenarios still remain

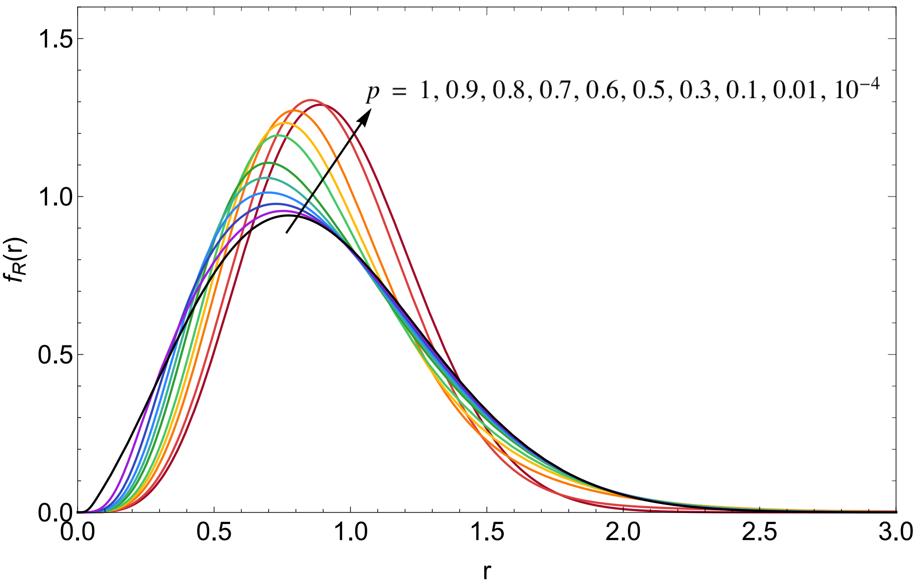

Figure 3.7: Envelope PDF for fixed $m = 1.25$, $\mu = 1.245$ and varying values of p ($\hat{r} = 1$).

unanswered. Having worked with the generalized phase Nakagami-m process, the authors in [62] showed real world propagation measurements that are best fit by taking into account cluster imbalance. Figure 3.8 illustrates some of the new fading scenarios possibilities attained with cluster imbalance. For such, the extent of the envelope CDF of the Extended η-μ model is depicted alongside the classic η-μ and Nakagami-m models, with $m = 1.25$ and μ obeying the relation found in (3.35), and $0 < p \leq 1$. As inferred earlier, the Nakagami-m process, indicated by the black line, is obtained when $\mu = m/2$, or when $\mu = m$ and $p = 1$, and the classic η-μ model is found as $p = 1$, represented by the green line. Whence, the green shade denotes all fading scenarios available for the classic η-μ model (as illustrated in [13]), and the blue shade adds the potential new fading settings.

3.3 Phase Statistics

3.3.1 Phase PDF

The phase distribution is obtained by integrating (3.12) with respect to r, i.e.

$$f_\Theta(\theta) = \int_0^\infty f_{R,\Theta}(r,\theta)\,\mathrm{d}r. \tag{3.38}$$

By solving the integral, the phase PDF is obtained as

$$f_\Theta(\theta) = \frac{2^{2\mu-1}\Gamma(2\mu)\eta^{\frac{2\mu}{1+p}}p^{\frac{2\mu p}{1+p}}}{\Gamma\left(\frac{2\mu}{1+p}\right)\Gamma\left(\frac{2\mu p}{1+p}\right)\left((p-\eta)\cos(2\theta)+\eta+p\right)^{2\mu}}\left|\sin\theta\right|^{\frac{4\mu}{1+p}-1}\left|\cos\theta\right|^{\frac{4\mu p}{1+p}-1}. \tag{3.39}$$

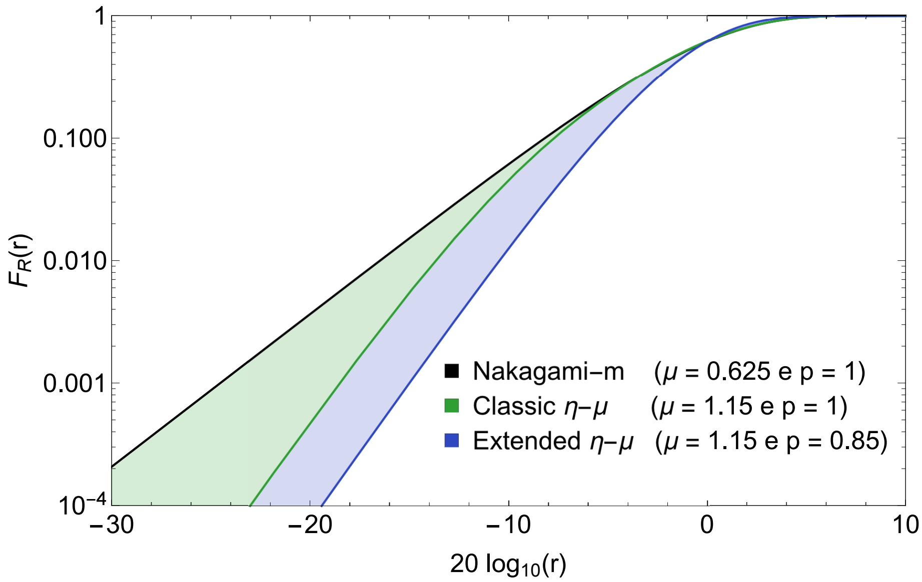

Figure 3.8: Extent of the Extended η-μ distribution with fixed $m = 1.25$.

As expected, for the balanced case ($p = 1$), (3.39) reduces to (2.32) and as seen in [17], R and Θ are not independent from each other. It is noteworthy that in making the appropriate substitutions, $\mu = m/2$ and $\eta = 1$, the generalized Nakagami-m phase distribution in (2.21) is obtained.

Figure 3.9 illustrates the behavior of the phase PDF in polar coordinates for different values of p and arbitrary η and μ. Note that, as one of the quadrature fading components degrades into the Gaussian condition, i.e. $p = \mu/2$, the PDF is led to move from a bimodal to a quadrimodal characteristic. Also, it has been observed that, unlike the envelope statistics, the phase PDF shows no symmetry as that observed for the envelope case with respect to the ratios η/p and p/η. In fact, in such conditions, a shift of $\pi/2$ in the phase occurs. Such pattern is also noticed in Figure 3.10, in which η is varying, p and μ are fixed. Note, however, in this case, that $\eta = 1$ (black line) is the turning point for the phase shift. Finally, Figure 3.11 illustrates again the PDF's bimodal to quadrimodal characteristics wherein μ is varying, and arbitrary η and p.

3.3.2 Phase CDF

The phase CDF can be obtained in a straightforward manner by performing the following integration

$$F_\Theta(\theta) = \int_{-\pi}^{\theta} f_\Theta(x)\,\mathrm{d}x, \tag{3.40}$$

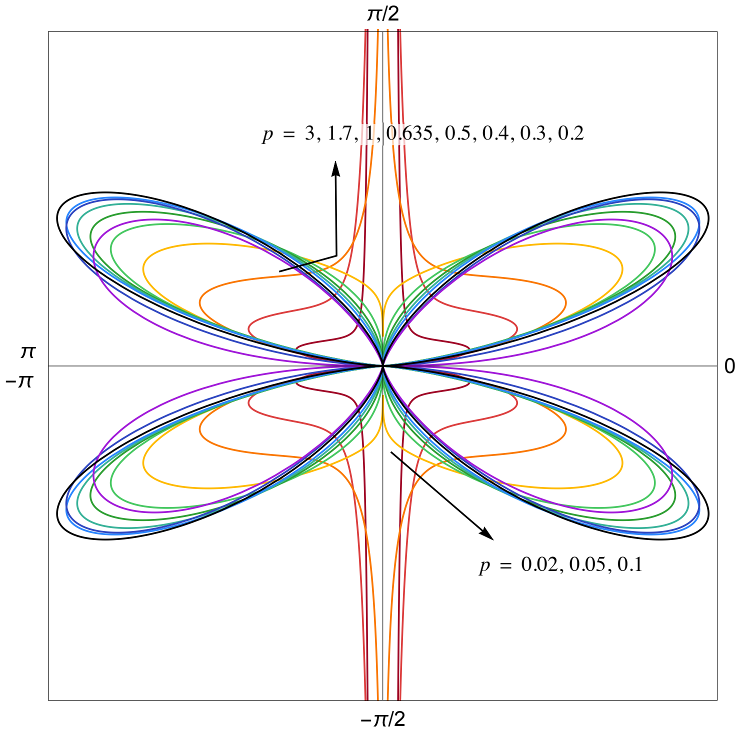

Figure 3.9: Phase PDF in polar coordinates with p varying, $\eta = 3.0$ and $\mu = 1.75$.

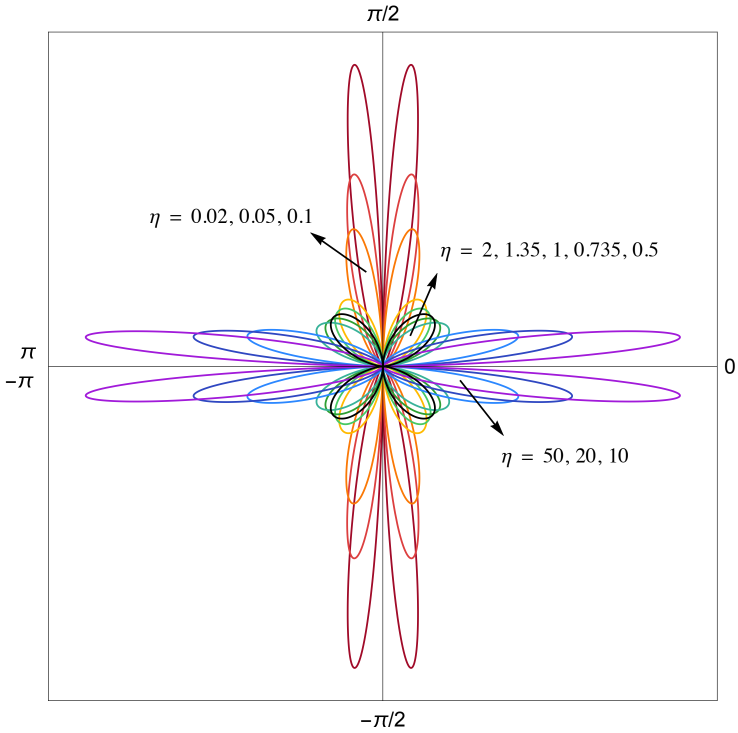

Figure 3.10: Phase PDF in polar coordinates, for varying values of η ($\mu = 1.375$ and $p = 0.735$).

in which $f_\Theta(x)$ is represented by (3.39). This procedure, however, does not result in any closed-form expression due to its complicated background with the modulus operator, present in the equation of the phase PDF. Having bumped in this same issue for the

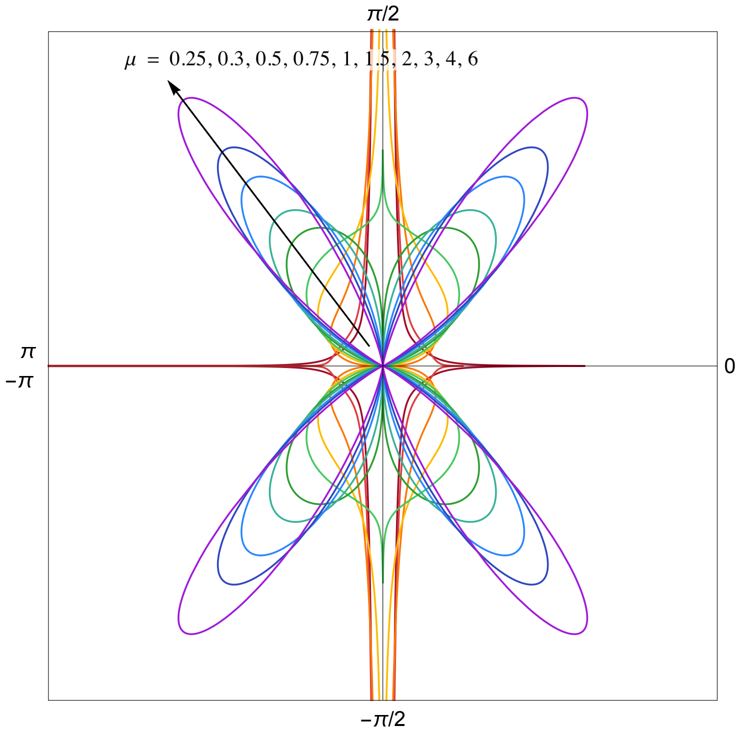

Figure 3.11: Phase PDF in polar coordinates, for varying values of μ ($\eta = 1.375$ and $p = 0.735$).

Nakagami-m phase distribution, the authors in [62] elegantly circumvented this situation with a new method. Succinctly, the following procedure is used: (i) the function's domain is divided in pieces in which the modulus operator signal is invariant; (ii) the integral for one specific domain piece is evaluated; and finally, (iii) the results are applied to the whole domain by taking advantage of symmetries and periodicities of the phase PDF.

With this in mind, our first task is to identify possible periodicities in the phase PDF. From (3.39), it can be seen that the phase distribution is an even function and has period π. Furthermore, over the interval $[0, \pi/2)$, the modulus operator is ineffective and thus, the phase PDF can be rewritten as

$$f_\Theta(\theta) = \frac{2^{2\mu-1}\Gamma(2\mu)\eta^{\frac{2\mu}{1+p}}p^{\frac{2\mu p}{1+p}}}{\Gamma\left(\frac{2\mu}{1+p}\right)\Gamma\left(\frac{2\mu p}{1+p}\right)\left((p-\eta)\cos(2\theta)+\eta+p\right)^{2\mu}}(\sin\theta)^{\frac{4\mu}{1+p}-1}(\cos\theta)^{\frac{4\mu p}{1+p}-1}. \quad (3.41)$$

Now, to enhance comprehensiveness, consider the auxiliary function $u_1(\theta)$, and its mirrored version $u_2(\theta)$, defined over the interval $[0, \pi/2)$ as

$$u_1(\theta) = \begin{cases} f_\Theta(\theta), & \text{if} \quad 0 \leq \theta < \dfrac{\pi}{2} \\ 0, & \text{otherwise} \end{cases} \quad (3.42)$$

and

$$u_2(\theta) = \begin{cases} f_\Theta\left(\frac{\pi}{2} - \theta\right), & \text{if } \quad 0 \leq \theta < \frac{\pi}{2} \\ 0, & \text{otherwise,} \end{cases} \tag{3.43}$$

in which $f_\Theta(\theta)$ is expressed as in (3.41). It can be easily observed that both auxiliary functions are related to each other as

$$u_2(\theta) = u_1\left(\frac{\pi}{2} - \theta\right). \tag{3.44}$$

Then, by performing the same integral operation as in (3.40) over the interval $[0, \pi/2)$, the CDF for both $u_1(\theta)$ and $u_2(\theta)$ are obtained, respectively, in closed-form as in

$$\begin{aligned} U_1(\theta) = {} & F_1\left(\frac{2\mu}{1+p}; 1 - \frac{2\mu p}{1+p}, 2\mu; \frac{2\mu}{1+p} + 1; \sin^2\theta, \frac{(p-\eta)}{p}\sin^2\theta\right) \\ & \times \frac{\Gamma(2\mu)\eta^{\frac{2\mu}{1+p}}}{2^2 p^{\frac{2\mu}{1+p}}\Gamma\left(\frac{2\mu p}{1+p}\right)\Gamma\left(\frac{2\mu}{1+p}+1\right)}\left(\sin^2\theta\right)^{\frac{2\mu}{1+p}} \end{aligned} \tag{3.45}$$

and

$$\begin{aligned} U_2(\theta) = {} & \frac{1}{4} - \left(F_1\left(\frac{2\mu}{1+p}; 1 - \frac{2\mu p}{1+p}, 2\mu; \frac{2\mu}{1+p} + 1; \sin^2\theta, \frac{(p-\eta)}{p}\sin^2\theta\right)\right. \\ & \left.\times \frac{\Gamma(2\mu)\eta^{\frac{2\mu}{1+p}}}{2^2 p^{\frac{2\mu}{1+p}}\Gamma\left(\frac{2\mu p}{1+p}\right)\Gamma\left(\frac{2\mu}{1+p}+1\right)}\left(\sin^2\theta\right)^{\frac{2\mu}{1+p}}\right), \end{aligned} \tag{3.46}$$

wherein $F_1(a; b_1, b_2; c; w, z)$ is the Appell hypergeometric function of two variables [2, Eq. (7.2.4.1)]. From the definitions of $u_1(\theta)$ and $u_2(\theta)$, it can be easily seen that the following relation holds

$$U_2(\theta) = \frac{1}{4} - U_1\left(\frac{\pi}{2} - \theta\right). \tag{3.47}$$

More importantly, when $\theta = \pi/2$, (3.45) and (3.46) evaluate, respectively, as $U_1(\pi/2) = 1/4$ and $U_2(\pi/2) = 1/4$.

Having defined these, let strip down the original phase PDF (Eq. (3.39)) in four distinct pieces, wherein

$$f_\Theta(\theta) = \begin{cases} u_1(\theta + \pi) & \text{if } \quad -\pi \leq \theta < -\frac{\pi}{2} \\ u_2\left(\theta + \frac{\pi}{2}\right) & \text{if } \quad -\frac{\pi}{2} \leq \theta < 0 \\ u_1(\theta) & \text{if } \quad 0 \leq \theta < \frac{\pi}{2} \\ u_2\left(\theta - \frac{\pi}{2}\right) & \text{if } \quad \frac{\pi}{2} \leq \theta < \pi. \end{cases} \tag{3.48}$$

Next, the phase CDF is promptly calculated by integrating each term of (3.48), resulting in

$$F_\Theta(\theta) = \begin{cases} 0, & \text{if} \quad \theta < -\pi \\ U_1\left(\theta + \pi\right), & \text{if} \quad -\pi \leq \theta < -\dfrac{\pi}{2} \\ U_2\left(\theta + \dfrac{\pi}{2}\right) + \dfrac{1}{4}, & \text{if} \quad -\dfrac{\pi}{2} \leq \theta < 0 \\ U_1\left(\theta\right) + \dfrac{1}{2}, & \text{if} \quad 0 \leq \theta < \dfrac{\pi}{2} \\ U_2\left(\theta - \dfrac{\pi}{2}\right) + \dfrac{3}{4}, & \text{if} \quad \dfrac{\pi}{2} \leq \theta < \pi \\ 1, & \text{if} \quad \theta > \pi. \end{cases} \tag{3.49}$$

As mentioned earlier, $U_1(\theta)$ is defined over the interval $[0, \pi/2)$. However, the domain can be expanded to $[-\pi, \pi)$, by noting that

$$U_1(\theta) = U_1(\theta + \pi) \tag{3.50}$$

and

$$U_1(\theta) = U_1(-\theta). \tag{3.51}$$

With (3.50), (3.51) and (3.44), (3.49) can be rewritten in terms of $U_1(\theta)$ as

$$F_\Theta(\theta) = \begin{cases} 0 & \text{if} \quad \theta < -\pi \\ U_1\left(\theta\right) & \text{if} \quad -\pi \leq \theta < -\dfrac{\pi}{2} \\ U_1\left(\theta\right) + \dfrac{1}{2} & \text{if} \quad -\dfrac{\pi}{2} \leq \theta < 0 \\ U_1\left(\theta\right) + \dfrac{1}{2} & \text{if} \quad 0 \leq \theta < \dfrac{\pi}{2} \\ U_1\left(\theta\right) + 1 & \text{if} \quad \dfrac{\pi}{2} \leq \theta < \pi \\ 1 & \text{if} \quad \theta > \pi. \end{cases} \tag{3.52}$$

Finally, to comprise all cases observed in (3.52), the phase CDF of the Extended η-μ model is determined as

$$F_\Theta(\theta) = \frac{1}{2}\left(H\left(\theta + \frac{\pi}{2}\right) + H\left(\theta - \frac{\pi}{2}\right)\right) + S\left(\frac{\theta}{\pi}\right) U_1(\theta), \tag{3.53}$$

in which $H(z)$ is the Heaviside step function [1, Eq. (29.1.3)], $S(z) \triangleq \operatorname{sgn}\left(\sin(2\pi z)\right)$ is the square wave function and $\operatorname{sgn}(z)$ is the sign function [3]. As far as we know, this formulation has never be seen for any η-μ model. In addition, (3.53) comprises the traditional η-μ phase CDF (with $p = 1$), and more importantly, with appropriate substitutions, the generalized Nakagami-m phase CDF obtained in [62, Eq. (15)].

The phase CDF characterization is presented in the following three plots. In Figure 3.12, the CDF is depicted considering the cluster imbalance scenario, in which p is varying, η and μ follow arbitrary values. As can be seen, the influence of p is unquestionable, and as $p \to 0$ or $p \to \infty$, the CDF assumes a more impulsive response around $\pm\pi$, $\pm\pi/2$ and 0. In these limits, either the in-phase or quadrature components cease to exist, and therefore, there is a phase concentration at the indicated angles. Interestingly, in such a scenario, the CDF has a rotational symmetry around the coordinates $(0, 0.5)$, naturally, associated to the ratio p/η and η/p. This pattern can also be observed in Figure 3.13, wherein η is the varying parameter. Finally, Figure 3.14 portrays the phase CDF with different values of μ.

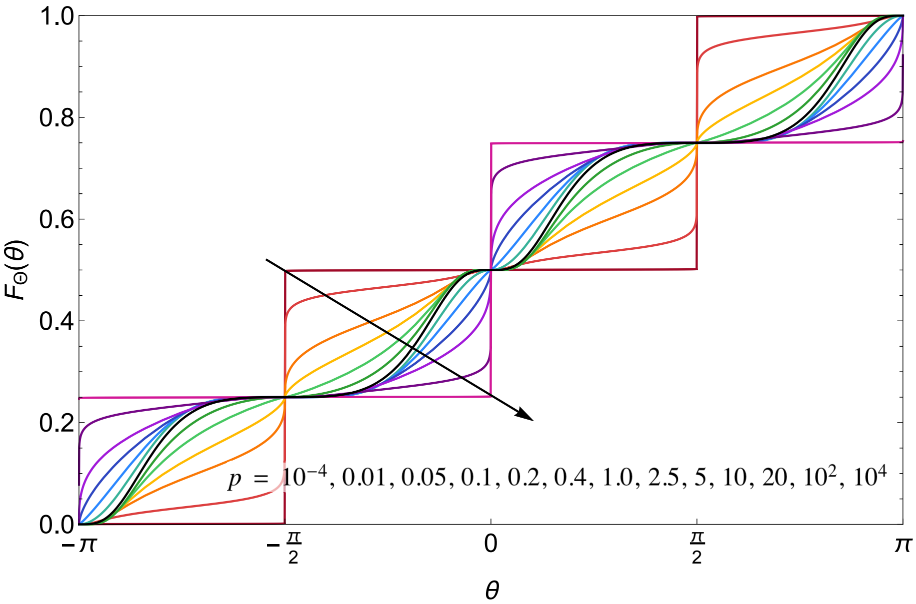

Figure 3.12: Phase CDF for varying values of p ($\eta = 3.0$ and $\mu = 1.75$).

3.4 Higher Order Statistics

The higher order statistics derived here for the Extended η-μ model are dependent of the time derivative of in-phase and quadrature signals. For such, we firstly obtain the joint distribution X, $\dot{X}$, Y and $\dot{Y}$, in which the dot notation characterizes the temporal derivation of the random variable. Next, the joint PDF of R, $\dot{R}$, Θ and $\dot{\Theta}$ is derived, by means of a common transformation of variables. Finally, important metrics such as level crossing rate and phase crossing rate are determined.

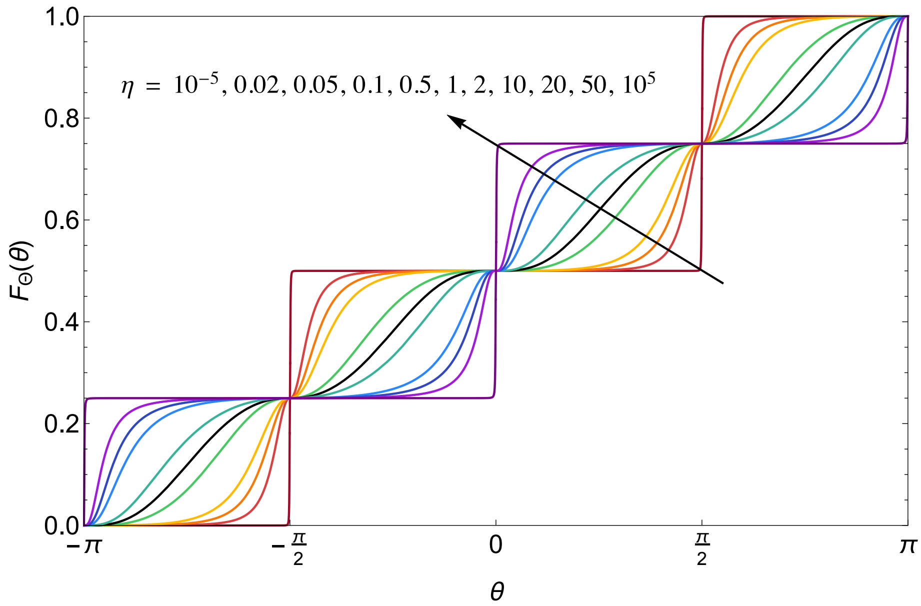

Figure 3.13: Phase CDF for varying values of η ($\mu = 1.375$ and $p = 0.735$).

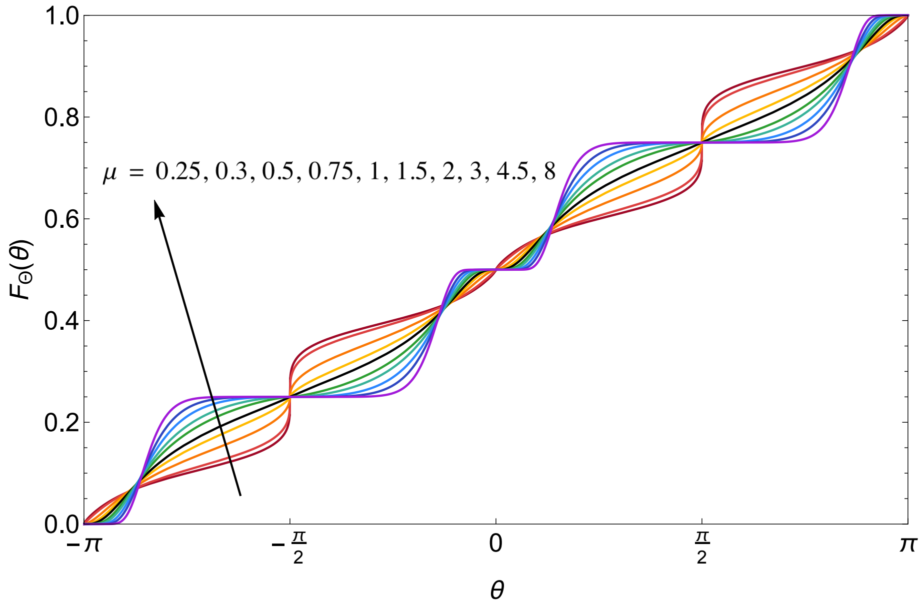

Figure 3.14: Phase CDF for varying values of μ ($\eta = 4.0$ and $p = 0.3$).

3.4.1 Joint PDF of X, Y, $\dot{X}$ and $\dot{Y}$

Let us reconsider the general process Z, which PDF follows (3.1), and its time derivative $\dot{Z}$. As widely investigated in [15, 45, 57, 59], $\dot{Z}$ is independent of Z and is Gaussian distributed with zero mean and variance $\dot{\sigma}^2$, as indicated below

$$f_{\dot{Z}}(\dot{z}) = \frac{1}{\sqrt{2\pi\dot{\sigma}^2}} \exp\left(-\frac{\dot{z}^2}{2\dot{\sigma}^2}\right), \tag{3.54}$$

in which, for an isotropic environment,

$$\dot{\sigma}_z^2 = 2\pi^2 f_m^2 \sigma_z^2, \tag{3.55}$$

wherein f_m is maximum Doppler shift and σ_z^2 is the variance of Z.

Since X and Y are independent process, it follows that X, Y, $\dot{X}$ and $\dot{Y}$ are independent from each other, which allows their joint PDF to be written as

$$f_{X,\dot{X},Y,\dot{Y}}(x,\dot{x},y,\dot{y}) = f_X(x)f_{\dot{X}}(\dot{x})f_Y(y)f_{\dot{Y}}(\dot{y}). \tag{3.56}$$

Then, by making the appropriate substitutions of Z by X and Y, and $\dot{Z}$ by $\dot{X}$ and $\dot{Y}$, the joint PDF is expressed as

$$\begin{aligned} f_{X,\dot{X},Y,\dot{Y}}(x,\dot{x},y,\dot{y}) = &\frac{4^{\mu}\mu^{2\mu+1}(\eta+1)^{2\mu+1}p^{\frac{2\mu p}{p+1}+\frac{1}{2}}|x|^{\frac{4\mu p}{p+1}-1}|y|^{\frac{4\mu}{p+1}-1}}{\pi^3 f_m^2\hat{r}^{4\mu+2}(p+1)^{2\mu+1}\eta^{\frac{2\mu p}{p+1}+\frac{1}{2}}\Gamma\left(\frac{2\mu}{p+1}\right)\Gamma\left(\frac{2\mu p}{p+1}\right)} \\ &\times \exp\left(-\frac{(1+\eta)\mu\left(2\pi^2 f_m^2\left(x^2p+\eta y^2\right)+\dot{x}^2p+\eta\dot{y}^2\right)}{\pi^2 f_m^2\eta\hat{r}^2(p+1)}\right). \end{aligned} \tag{3.57}$$

3.4.2 Joint PDF of R, $\dot{R}$, Θ and $\dot{\Theta}$

Now, the joint PDF of R, Θ and their respective time derivative is determined by

$$f_{P,\dot{P},\Theta,\dot{\Theta}(\rho,\dot{\rho},\theta,\dot{\theta})} = |J|\, f_{X,\dot{X},Y,\dot{Y}}(x,\dot{x},y,\dot{y}), \tag{3.58}$$

wherein by performing a transformation of variables, $|J| = R^2$ is the Jacobian of the transformation and $X = R\cos\Theta$, $Y = R\sin\Theta$, $\dot{X} = \dot{R}\cos\Theta - R\dot{\Theta}\sin\Theta$ e $\dot{Y} = \dot{R}\sin\Theta + R\dot{\Theta}\cos\Theta$. With the proper substitutions, we find that

$$\begin{aligned} f_{R,\dot{R},\Theta,\dot{\Theta}}(r,\dot{r},\theta,\dot{\theta}) = &\frac{2^{2\mu}\mu^{2\mu+1}(\eta+1)^{2\mu+1}p^{\frac{2\mu p}{1+p}+\frac{1}{2}}}{\pi^3 f_m^2(1+p)^{2\mu+1}\eta^{\frac{2\mu p}{1+p}+\frac{1}{2}}\Gamma\left(\frac{2\mu}{1+p}\right)\Gamma\left(\frac{2p\mu}{1+p}\right)}|\sin\theta|^{\frac{4\mu}{1+p}-1}|\cos\theta|^{\frac{4\mu p}{1+p}-1} \\ &\times\frac{r^{4\mu}}{\hat{r}^{4\mu+2}}\exp\left(-\frac{(1+\eta)\mu p}{\pi^2 f_m^2\eta(1+p)\hat{r}^2}(\dot{r}\cos\theta - r\dot{\theta}\sin\theta)^2\right) \\ &\times\exp\left(-\frac{(1+\eta)\mu}{\pi^2 f_m^2(1+p)\hat{r}^2}(r\dot{\theta}\cos\theta+\dot{r}\sin\theta)^2\right) \\ &\times\exp\left(-\frac{(1+\eta)\mu}{\eta(1+p)}(p+\eta+(p-\eta)\cos(2\theta))\frac{r^2}{\hat{r}^2}\right). \end{aligned} \tag{3.59}$$

3.4.3 Other Joint PDFs

Having defined (3.59) and after the proper integration procedure, a series of new closed-form expressions arise for different combinations of R, $\dot{R}$, Θ and $\dot{\Theta}$.

The joint PDF of R, $\dot{R}$ and Θ is defined by integrating (3.59) in terms of $\dot{\Theta}$,

$$
\begin{aligned}
f_{R,\dot{R},\Theta}(r,\dot{r},\theta)=&\int_{-\infty}^{\infty} f_{R,\dot{R},\Theta,\dot{\Theta}}(r,\dot{r},\theta,\dot{\theta})\,\mathrm{d}\dot{\theta}\\
=&\frac{2^{2\mu+\frac{1}{2}}\mu^{2\mu+\frac{1}{2}}(\eta+1)^{2\mu+\frac{1}{2}}p^{\frac{2\mu p}{1+p}+\frac{1}{2}}\left|\sin\theta\right|^{\frac{4\mu}{1+p}-1}\left|\cos\theta\right|^{\frac{4\mu p}{1+p}-1}}{\pi^{\frac{3}{2}}f_m(1+p)^{2\mu+\frac{1}{2}}\eta^{\frac{2\mu p}{1+p}}\Gamma\left(\frac{2\mu}{1+p}\right)\Gamma\left(\frac{2p\mu}{1+p}\right)(p+\eta+\cos(2\theta)(\eta-p))^{\frac{1}{2}}}\frac{r^{4\mu-1}}{\hat{r}^{4\mu+1}}\\
&\times\exp\left(-\frac{\mu\left(\pi^2f_m^2r^2\left(\eta^2+p^2-\cos(4\theta)(p-\eta)^2+6\eta p\right)+4\eta p\dot{r}^2\right)}{2\pi^2f_m^2\eta(\eta+1)^{-1}\mu(1+p)\hat{r}^2(\eta+\cos(2\theta)(\eta-p)+p)}\right).
\end{aligned}
\tag{3.60}
$$

The joint PDF for R, Θ, $\dot{\Theta}$ is calculated by integrating (3.59) with respect to $\dot{R}$,

$$
\begin{aligned}
f_{R,\Theta,\dot{\Theta}}(r,\theta,\dot{\theta})=&\int_{-\infty}^{\infty} f_{R,\dot{R},\Theta,\dot{\Theta}}(r,\dot{r},\theta,\dot{\theta})\,\mathrm{d}\dot{r}\\
=&\frac{2^{2\mu+\frac{1}{2}}\mu^{2\mu+\frac{1}{2}}(\eta+1)^{2\mu+\frac{1}{2}}p^{\frac{2\mu p}{1+p}+\frac{1}{2}}\left|\sin\theta\right|^{\frac{4\mu}{1+p}-1}\left|\cos\theta\right|^{\frac{4\mu p}{1+p}-1}}{\pi^{\frac{3}{2}}f_m(1+p)^{2\mu+\frac{1}{2}}\eta^{\frac{2\mu p}{1+p}}\Gamma\left(\frac{2\mu}{1+p}\right)\Gamma\left(\frac{2p\mu}{1+p}\right)(p+\eta+(p-\eta)\cos(2\theta))^{\frac{1}{2}}}\frac{r^{4\mu}}{\hat{r}^{4\mu+2}}\\
&\times\ \exp\left(-\frac{(1+\eta)\mu r^2\left(3\pi^2f_m^2\eta^2+3\pi^2f_m^2p^2+2\pi^2f_m^2\eta p+4\eta p\dot{\theta}^2\right)}{2\pi^2f_m^2\eta(1+p)\hat{r}^2(p+\eta+\cos(2\theta)(p-\eta))}\right)\\
&\times\ \exp\left(-\frac{(1+\eta)\mu r^2\left(4\cos(2\theta)\left(p^2-\eta^2\right)+\cos(4\theta)(p-\eta)^2\right)}{2\eta(1+p)\hat{r}^w(p+\eta+(p-\eta)\cos(2\theta))}\right).
\end{aligned}
\tag{3.61}
$$

The joint PDF for $\dot{R}$, Θ, $\dot{\Theta}$ is determined below by integrating with respect to R,

$$
\begin{aligned}
f_{\dot{R},\Theta,\dot{\Theta}}(\dot{r},\theta,\dot{\theta})=&\int_{0}^{\infty} f_{R,\dot{R},\Theta,\dot{\Theta}}(r,\dot{r},\theta,\dot{\theta})\,\mathrm{d}r\\
=&\frac{2^{2\mu-1}\pi^{4\mu-3}f_m^{4\mu}p^{\frac{2\mu p}{1+p}+\frac{1}{2}}\eta^{\frac{2\mu}{1+p}-\frac{1}{2}}\left|\sin\theta\right|^{\frac{4\mu}{1+p}-1}\left|\cos\theta\right|^{\frac{4\mu p}{1+p}-1}}{\Gamma\left(\frac{2\mu}{1+p}\right)\Gamma\left(\frac{2p\mu}{1+p}\right)\exp\left(\frac{(1+\eta)\mu\dot{r}^2}{\pi^2f_m^2\eta(1+p)}\left(\eta\sin^2\theta+p\cos^2\theta\right)\right)}\\
&\times\ \left(\pi^2f_m^2(p+\eta+\cos(2\theta)(p-\eta))+\dot{\theta}^2\left(\eta\cos^2\theta+p\sin^2\theta\right)\right)^{-2\mu-1}\\
&\times\left[\left(\pi^2f_m^2(\eta+\cos(2\theta)(p-\eta)+p)+\dot{\theta}^2\left(\eta\cos^2\theta+p\sin^2\theta\right)\right)^{\frac{1}{2}}\right.\\
&\times\ \frac{\pi\Gamma(\mu+1)}{f_m}\sqrt{\frac{\eta\mu(1+\eta)}{(1+p)}}\\
&\times{}_1F_1\left(2\mu+\frac{1}{2};\frac{1}{2};\frac{2^{-2}\pi^{-2}f_m^{-2}\eta^{-1}(1+p)^{-1}(1+\eta)\mu\dot{\rho}^2\dot{\theta}^2\sin^2(2\theta)(p-\eta)^2}{\pi^2f_m^2(\eta+\cos(2\theta)(p-\eta)+p)+\dot{\theta}^2\left(\eta\cos^2\theta+p\sin^2\theta\right)}\right)\\
&+{}_1F_1\left(2\mu+1;\frac{3}{2};\frac{2^{-2}\pi^{-2}f_m^{-2}\eta^{-1}(1+p)^{-1}(1+\eta)\mu\dot{\rho}^2\dot{\theta}^2\sin^2(2\theta)(p-\eta)^2}{\pi^2f_m^2(\eta+\cos(2\theta)(p-\eta)+p)+\dot{\theta}^2\left(\eta\cos^2\theta+p\sin^2\theta\right)}\right)\\
&\left.\quad\times\frac{(1+\eta)\mu(p-\eta)\Gamma(2\mu+1)}{f_m^2(1+p)}\dot{\rho}\dot{\theta}\sin(2\theta)\right].
\end{aligned}
\tag{3.62}
$$

Now, by integrating (3.60) with respect to R, the joint PDF of $\dot{R}$ and Θ is calculated as

$$
\begin{aligned}
f_{\dot{R},\Theta}(\dot{r},\theta) =& \int_0^\infty f_{R,\dot{R},\Theta}(r,\dot{r},\theta)\,\mathrm{d}r \\
=& \frac{2^{2\mu-\frac{1}{2}}\Gamma(2\mu)p^{\frac{2\mu p}{1+p}+\frac{1}{2}}\eta^{\frac{2\mu}{1+p}}\,|\sin\theta|^{\frac{4\mu}{1+p}-1}\,|\cos\theta|^{\frac{4\mu p}{1+p}-1}}{\pi^{\frac{3}{2}}f_m\mu^{\frac{1}{2}}\,(\eta+1)^{\frac{1}{2}}\,(1+p)^{\frac{1}{2}}\,\Gamma\left(\frac{2\mu}{1+p}\right)\Gamma\left(\frac{2p\mu}{1+p}\right)(\eta+\cos(2\theta)(\eta-p)+p)^{2\mu+\frac{1}{2}}} \\
&\times\,\exp\left(-\frac{2(1+\eta)\mu p\dot{\rho}^2}{\pi^2 f_m^2(1+p)(p+\eta+\cos(2\theta)(\eta-p))}\right). \qquad (3.63)
\end{aligned}
$$

Equivalently, (3.63) is obtainable by integrating (3.62) in terms of $\dot{\Theta}$. Also, when performing the integral in respect to $\dot{R}$, the phase PDF (3.39) is achieved.

Finally, the joint PDF of $\dot{\Theta}$ and Θ is derived with (3.61) and its integral in respect to R,

$$
\begin{aligned}
f_{\Theta,\dot{\Theta}}(\theta,\dot{\theta}) =& \int_0^\infty f_{R,\Theta,\dot{\Theta}}(r,\theta,\dot{\theta})\,\mathrm{d}r \\
=& \frac{2^{4\mu}\pi^{4\mu-\frac{1}{2}}f_m^{4\mu}p^{\frac{2\mu p}{1+p}+\frac{1}{2}}\eta^{\frac{2\mu}{1+p}+\frac{1}{2}}\,|\sin\theta|^{\frac{4\mu}{1+p}-1}\,|\cos\theta|^{\frac{4\mu p}{1+p}-1}\,(\eta+\cos(2\theta)(p-\eta)+p)^{2\mu}}{\left(\pi^2 f_m^2\left(3\eta^2+4\cos(2\theta)\left(p^2-\eta^2\right)+3p^2+\cos(4\theta)(p-\eta)^2+2\eta p\right)+4\eta p\dot{\theta}^2\right)^{2\mu+\frac{1}{2}}} \\
&\times\,\frac{\Gamma\left(2\mu+\frac{1}{2}\right)}{\Gamma\left(\frac{2\mu}{1+p}\right)\Gamma\left(\frac{2p\mu}{1+p}\right)}. \qquad (3.64)
\end{aligned}
$$

The expression in (3.64) is also obtainable by integrating (3.62) with respect to $\dot{R}$. Note that, (3.39) can also be attained by integrating (3.64) in terms of $\dot{\Theta}$.

3.4.4 Level Crossing Rate and Average Fading Duration

The Level Crossing Rate is defined as

$$N_R(r) \triangleq \int_0^\infty \dot{r} f_{R,\dot{R}}(r,\dot{r})\,\mathrm{d}\dot{r}, \qquad (3.65)$$

in which $f_{R,\dot{R}}(r,\dot{r})$ stands for the joint PDF of R and its time derivative $\dot{R}$. Theoretically, this expression can be obtained by integrating (3.60) in respect to Θ. However, this procedure does not lead to a closed-form formulation. Therefore, the LCR has to be evaluated as

$$N_R(r) = \int_0^\infty \int_{-\pi}^{\pi} \dot{r} f_{R,\dot{R},\Theta}(r,\dot{r},\theta)\,\mathrm{d}\theta\,\mathrm{d}\dot{r}. \qquad (3.66)$$

This procedure can become quite a burden if performed repeatedly. To overcome this complication, the integral order in (3.66) can be rearranged to

$$N_R(r) = \int_{-\pi}^{\pi} \int_0^\infty \dot{r} f_{R,\dot{R},\Theta}(r,\dot{r},\theta)\,\mathrm{d}\dot{r}\,\mathrm{d}\theta. \qquad (3.67)$$

An auxiliary LCR function is determined by performing first the integral with respect to $\dot{R}$, leading to

$$
\begin{aligned}
N_R(r,\theta) &= \int_0^\infty \dot{r} f_{R,\dot{R},\Theta}(r,\dot{r},\theta)\,\mathrm{d}\dot{r} \\
&= \frac{\sqrt{\pi} f_m 2^{2\mu-\frac{3}{2}} \mu^{2\mu-\frac{1}{2}} (\eta+1)^{2\mu-\frac{1}{2}} p^{\frac{2\mu p}{1+p}-\frac{1}{2}} \rho^{4\mu-1} \left|\sin\theta\right|^{\frac{4\mu}{1+p}-1} \left|\cos\theta\right|^{\frac{4\mu p}{1+p}-1}}{(1+p)^{2\mu-\frac{1}{2}} \eta^{\frac{2\mu p}{1+p}} \Gamma\left(\frac{2\mu}{1+p}\right) \Gamma\left(\frac{2p\mu}{1+p}\right) (p+\eta-\cos(2\theta)(p-\eta))^{-\frac{1}{2}}} \\
&\quad \times \exp\left(-\frac{(1+\eta)\mu\rho^2}{\eta(1+p)}(p+\eta+\cos(2\theta)(p-\eta))\right),
\end{aligned}
\tag{3.68}
$$

so that

$$
N_R(r) = \int_{-\pi}^{\pi} N_R(r,\theta)\,\mathrm{d}\theta. \tag{3.69}
$$

With (3.68), the LCR in (3.69) can be written in a single integral as

$$
\begin{aligned}
N_R(r) = \int_{-\pi}^{\pi} & \frac{\sqrt{\pi} f_m 2^{2\mu-\frac{3}{2}} \mu^{2\mu-\frac{1}{2}} (\eta+1)^{2\mu-\frac{1}{2}} p^{\frac{2\mu p}{1+p}-\frac{1}{2}} \rho^{4\mu-1} \left|\sin\theta\right|^{\frac{4\mu}{1+p}-1} \left|\cos\theta\right|^{\frac{4\mu p}{1+p}-1}}{(1+p)^{2\mu-\frac{1}{2}} \eta^{\frac{2\mu p}{1+p}} \Gamma\left(\frac{2\mu}{1+p}\right) \Gamma\left(\frac{2p\mu}{1+p}\right) (p+\eta-\cos(2\theta)(p-\eta))^{-\frac{1}{2}}} \\
& \times \exp\left(-\frac{(1+\eta)\mu\rho^2}{\eta(1+p)}(p+\eta+\cos(2\theta)(p-\eta))\right)\mathrm{d}\theta.
\end{aligned}
\tag{3.70}
$$

The Average Fading Duration is defined as

$$
T_R(r) \triangleq \frac{F_R(r)}{N_R(r)}, \tag{3.71}
$$

in which $F_R(r)$ and $N_R(r)$ are indicated respectively by the equations in (3.29) and (3.70).

In Figures 3.15 and 3.16, the LCR and AFD are portrayed for different values of p, to illustrate the influence of cluster imbalance in such statistics.

3.4.5 Phase Crossing Rate

The Phase Crossing Rate is defined as

$$
N_\Theta(\theta) = \int_0^\infty \dot{\theta} f_{\Theta,\dot{\Theta}}(\theta,\dot{\theta})\,\mathrm{d}\dot{\theta}, \tag{3.72}
$$

in which $f_{\Theta,\dot{\Theta}}(\theta,\dot{\theta})$ is represented in (3.64). Thus, a closed-form expression is attained in a straightforward manner by substituting (3.64) in (3.72) and by performing the integration, leading to

$$
N_\Theta(\theta) = \frac{2^{2\mu-\frac{3}{2}} \sqrt{\pi} f_m \Gamma\left(2\mu+\frac{1}{2}\right) p^{\frac{2\mu p}{1+p}-\frac{1}{2}} \eta^{\frac{2\mu}{1+p}-\frac{1}{2}} \left|\sin\theta\right|^{\frac{4\mu}{1+p}-1} \left|\cos\theta\right|^{\frac{4\mu p}{1+p}-1}}{(4\mu-1)\Gamma\left(\frac{2\mu}{1+p}\right)\Gamma\left(\frac{2p\mu}{1+p}\right)(\eta+\cos(2\theta)(p-\eta)+p)^{2\mu-1}}. \tag{3.73}
$$

Figures 3.17 depicts the phase crossing rate of the Extended η-μ model in different cluster imbalance scenarios.

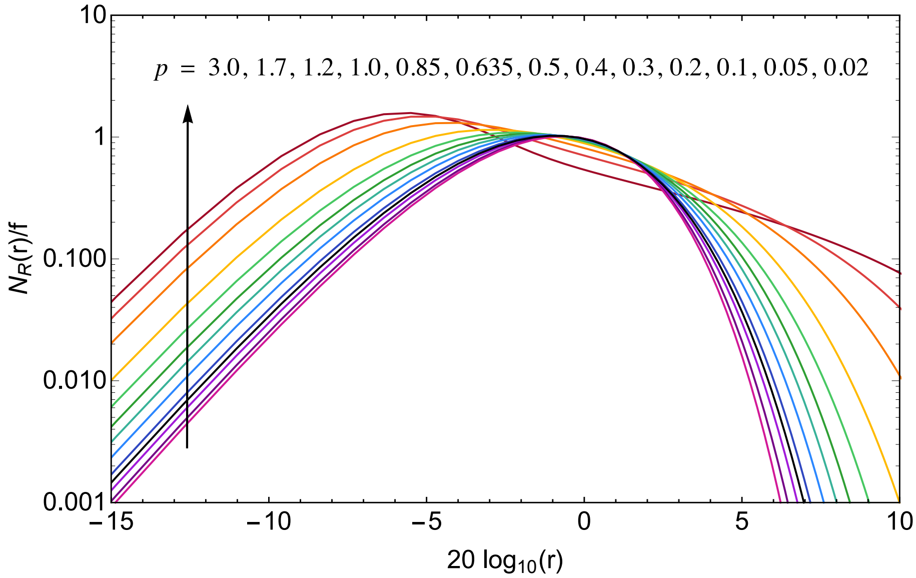

Figure 3.15: LCR for varying values of p ($\mu = 1.75$ and $\eta = 3.0$).

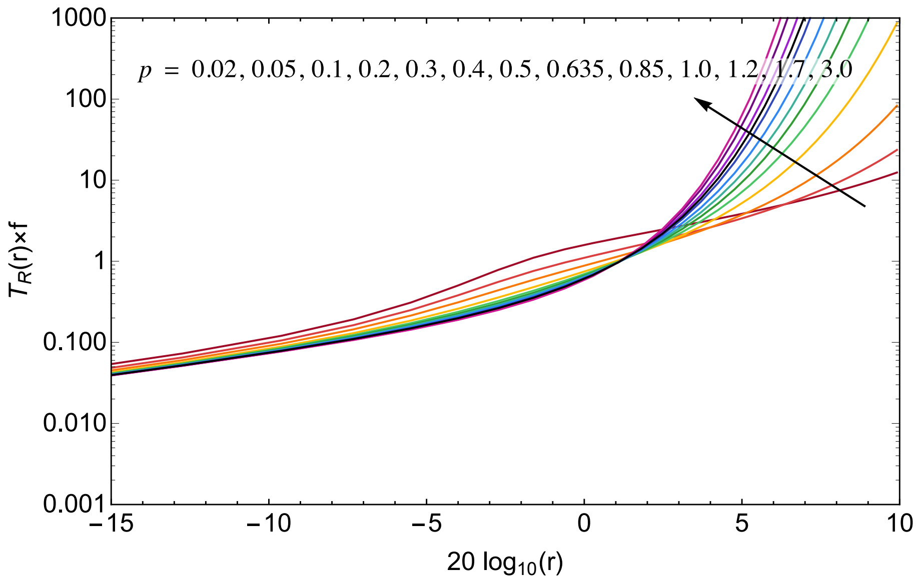

Figure 3.16: AFD for varying values of p ($\mu = 1.75$ and $\eta = 3.0$).

3.5 Moment Generating Function and Applications

Moment generating functions can be used to obtain the average symbol and bit error rates (ASER and ABER) expressions for different modulation schemes. As indicated in [21], such performance measurements can be put in terms of a single finite-range integral, with integrands corresponding to the MGF of the instantaneous signal-to-noise ratio (SNR). Therefore, in order to obtain a more tractable expression, thus circumventing the burden of an integration procedure, a MGF series expansion for the Extended η-μ will be presented. Also, formulations for a maximal ratio combining scheme will be provided.

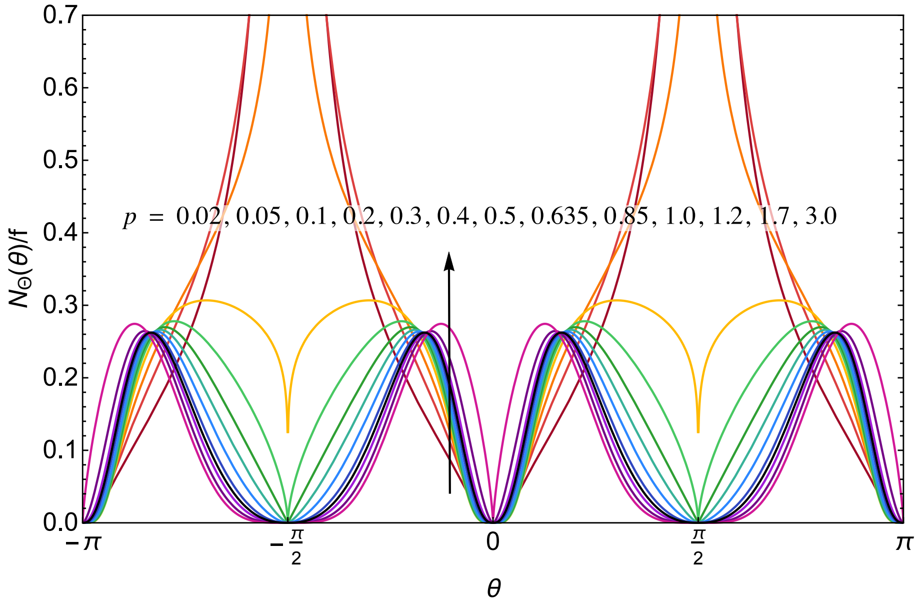

Figure 3.17: PCR for varying values of p ($\mu = 1.75$ and $\eta = 3.0$).

Hence, an ABER expression concerning coherent BPSK and BFSK shall be derived.

Let $\Upsilon = R^2$ represent the instantaneous SNR. After performing this variable transformation, the PDF $f_\Upsilon(\gamma)$ can be calculated from (3.25), leading to

$$f_\Upsilon(\gamma) = \frac{2^{2\mu}\mu^{2\mu}\gamma^{2\mu-1}(1+\eta)^{2\mu}p^{\frac{2\mu p}{1+p}}}{\bar{\gamma}^{2\mu}\Gamma(2\mu)(1+p)^{2\mu}\eta^{\frac{2\mu p}{1+p}}}\,{}_1F_1\left(\frac{2\mu p}{1+p}; 2\mu; \frac{2\gamma(\eta-p)(1+\eta)\mu}{(1+p)\eta\bar{\gamma}}\right) \times \exp\left(-\frac{2\gamma(1+\eta)\mu}{(1+p)\bar{\gamma}}\right), \tag{3.74}$$

in which is the average SNR given as $\bar{\gamma} = E(\Upsilon)$. The MGF of the instantaneous SNR, $M_\Upsilon(s)$, is defined as

$$M_\Upsilon(s) = \int_0^\infty \exp(-s\gamma) f_\Upsilon(\gamma)\, \mathrm{d}\gamma. \tag{3.75}$$

Following [57], in order to obtain the MGF, the hypergeometric function in (3.74) must be rewritten as in (3.27) and substituted in (3.75), leading to

$$M_\Upsilon(s) = \int_0^\infty \frac{2^{2\mu}\mu^{2\mu}\gamma^{2\mu-1}(1+\eta)^{2\mu}p^{\frac{2\mu p}{1+p}}}{\bar{\gamma}^{2\mu}\Gamma(2\mu)(1+p)^{2\mu}\eta^{\frac{2\mu p}{1+p}}} \exp\left(-\frac{2\gamma(1+\eta)\mu}{(1+p)\bar{\gamma}}\right)\exp(-s\gamma) \times \sum_{k=0}^{\infty} \frac{\left(\frac{2\mu p}{1+p}\right)_k}{k!(2\mu)_k}\left(\frac{2(\eta-p)(1+\eta)\mu\gamma}{(1+p)\eta\bar{\gamma}}\right)^k \mathrm{d}\gamma. \tag{3.76}$$

From (3.76), the summation operator and every multiplicative terms not related to γ can be rearranged before the integral, obtaining the auxiliary function L as follows

$$L = \int_0^\infty \gamma^{2\mu+k-1} \exp(-s\gamma)\exp\left(-\frac{2\mu(1+\eta)\gamma}{(1+p)\bar{\gamma}}\right)\mathrm{d}\gamma. \tag{3.77}$$

Now, the exponential functions in (3.77) can be replaced by [2, Eq. (8.4.3.1)],

$$\exp(-z) = G_{0,1}^{1,0}\left(z \,\middle|\, \begin{matrix} - \\ 0 \end{matrix} \right), \tag{3.78}$$

leading to

$$L = \int_0^\infty \gamma^{k+2\mu-1}\, G_{0,1}^{1,0}\left(\frac{2(1+\eta)\mu\gamma}{(1+p)\bar{\gamma}} \,\middle|\, \begin{matrix} - \\ 0 \end{matrix} \right) G_{0,1}^{1,0}\left(s\gamma \,\middle|\, \begin{matrix} - \\ 0 \end{matrix} \right) \mathrm{d}\gamma, \tag{3.79}$$

in which $G_{p,q}^{m,n}(z)$ is the Meijer G-function [2, Eq. (8.2.1.1)]. Finally, (3.79) can be solved with [2, Eq. (2.24.1.1)], resulting in

$$L = \left(\frac{2(1+\eta)\mu}{(1+p)\bar{\gamma}} \right)^{-k-2\mu} G_{1,1}^{1,1}\left(\frac{(1+p)s\bar{\gamma}}{2(1+\eta)\mu} \,\middle|\, \begin{matrix} 1-k-2\mu \\ 0 \end{matrix} \right), \tag{3.80}$$

Then, using the property given in [2, Eq. (8.2.2.14)],

$$G_{p,q}^{m,n}\left(z \,\middle|\, \begin{matrix} (a_p) \\ (b_q) \end{matrix} \right) = G_{q,p}^{n,m}\left(\frac{1}{z} \,\middle|\, \begin{matrix} 1-(b_q) \\ 1-(a_p) \end{matrix} \right), \tag{3.81}$$

in (3.80), the MGF of the Extended η-μ channel is found as

$$M_\Upsilon(s) = \frac{p^{\frac{2\mu p}{1+p}}}{\eta^{\frac{2\mu p}{1+p}}\Gamma\left(\frac{2\mu p}{1+p}\right)} \sum_{k=0}^{\infty} \left(1-\frac{p}{\eta}\right)^k \frac{\Gamma\left(k+\frac{2p\mu}{1+p}\right)}{k!\Gamma(k+2\mu)} G_{1,1}^{1,1}\left(\frac{2(1+\eta)\mu}{(1+p)s\bar{\gamma}} \,\middle|\, \begin{matrix} 1 \\ k+2\mu \end{matrix} \right). \tag{3.82}$$

Maximal Ratio Combining Scheme

Now, considering a diversity scenario with maximal ratio combining, the total SNR is given as [21]

$$\gamma = \sum_{m=1}^{M} \gamma_m, \tag{3.83}$$

in which γ_m is the instantaneous SNR for each m branch, and M is the number of branches of the multichannel receiver.

By taking into account that all instantaneous SNR are identically distributed random variables with PDF described in (3.74) with the same fading parameters and the same average SNR, the PDF for the total SNR can be calculated after a simple sum of M random variables, leading to

$$\begin{aligned} f_\Upsilon(\gamma) = {} & \frac{2^{2\mu M}\mu^{2\mu M}\gamma^{2\mu M-1}(1+\eta)^{2\mu M}p^{\frac{2\mu M p}{1+p}}}{\bar{\gamma}^{2\mu M}\Gamma(2\mu M)(1+p)^{2\mu M}\eta^{\frac{2\mu M p}{1+p}}}\, {}_1F_1\left(\frac{2\mu M p}{1+p}; 2\mu M; \frac{2\gamma(\eta-p)(1+\eta)\mu}{(1+p)\eta\bar{\gamma}}\right) \\ & \times \exp\left(-\frac{2\gamma(1+\eta)\mu}{(1+p)\bar{\gamma}}\right). \end{aligned} \tag{3.84}$$

Following the same expansion procedure, the MGF for the sum of M identically distributed instantaneous SNR is equated as

$$M_{\Upsilon}(s) = \frac{p^{\frac{2\mu M p}{1+p}}}{\eta^{\frac{2\mu M p}{1+p}}\Gamma\left(\frac{2\mu M p}{1+p}\right)} \sum_{k=0}^{\infty} \left(1-\frac{p}{\eta}\right)^{k} \frac{\Gamma\left(k+\frac{2\mu M p}{1+p}\right)}{k!\Gamma(k+2\mu M)}$$
$$\times G_{1,1}^{1,1}\left(\frac{2(1+\eta)\mu}{(1+p)s\bar{\gamma}} \middle| \begin{array}{c} 1 \\ k+2\mu M \end{array}\right). \tag{3.85}$$

Average Bit Error Rate

For a coherent binary system, the average bit error rate, $P_b(E)$, is expressed as [21]

$$P_b(E) = \frac{1}{\pi}\int_0^{\pi/2} M_{\Upsilon}\left(\frac{g}{\sin^2\theta}\right) \mathrm{d}\theta, \tag{3.86}$$

wherein $g = 1$, $g = 1/2$ and $g = 0.715$ are for BPSK, BFSK and BFSK with minimum correlation, respectively. Replacing (3.82) in (3.86) and rearranging the summation operator, the average bit error rate is found as

$$P_b(E) = \frac{p^{\frac{2\mu p}{1+p}}}{\pi\eta^{\frac{2\mu p}{1+p}}\Gamma\left(\frac{2\mu p}{1+p}\right)} \sum_{k=0}^{\infty} \left(1-\frac{p}{\eta}\right)^{k} \frac{\Gamma\left(k+\frac{2p\mu}{1+p}\right)}{k!\Gamma(k+2\mu)}$$
$$\times \int_0^{\pi/2} G_{1,1}^{1,1}\left(\frac{2(1+\eta)\mu\sin^2\theta}{g(1+p)\bar{\gamma}} \middle| \begin{array}{c} 1 \\ k+2\mu \end{array}\right) \mathrm{d}\theta. \tag{3.87}$$

From (3.87), let us define an auxiliary function D, which is represented by

$$D = \int_0^{\pi/2} G_{1,1}^{1,1}\left(\frac{2\mu(1+\eta)\sin^2\theta}{g(1+p)\bar{\gamma}} \middle| \begin{array}{c} 1 \\ k+2\mu \end{array}\right) \mathrm{d}\theta. \tag{3.88}$$

By making the transformation of variable $u = \cos^2(\theta)$ in (3.88), the following is obtained

$$D = \int_0^{1} u^{-\frac{1}{2}}(1-u)^{-\frac{1}{2}}\, G_{1,1}^{1,1}\left(\frac{2\mu(1+\eta)(1-u)}{g(1+p)\bar{\gamma}} \middle| \begin{array}{c} 1 \\ k+2\mu \end{array}\right) \mathrm{d}u. \tag{3.89}$$

With [2, Eq. (8.3.2.21)], the Meijer G-function in (3.89) can be rewritten in terms of Fox's H-function [2, Eq. (8.3.1.1)], $H_{p,q}^{m,n}(z)$, as given in

$$D = \int_0^{1} u^{-\frac{1}{2}}(1-u)^{-\frac{1}{2}}\, H_{1,1}^{1,1}\left(\frac{2\mu(1+\eta)(1-u)}{g(1+p)\bar{\gamma}} \middle| \begin{array}{c} (1,1) \\ (k+2\mu,1) \end{array}\right) \mathrm{d}u. \tag{3.90}$$

Finally, (3.90) is solved with the help of [2, Eq. (2.25.2.2)], resulting in

$$D = \sqrt{\pi}\, G_{2,2}^{1,2}\left(\frac{2\mu(1+\eta)}{g(1+p)\bar{\gamma}} \middle| \begin{array}{c} \frac{1}{2}, 1 \\ (k+2\mu, 0) \end{array}\right). \tag{3.91}$$

Therefore, the average bit error rate for coherent signals is given as

$$P_b(E) = \frac{\eta^{-\frac{2\mu p}{1+p}} p^{\frac{2\mu p}{1+p}}}{2\sqrt{\pi}\Gamma\left(\frac{2\mu p}{1+p}\right)} \sum_{k=0}^{\infty} \left(1-\frac{p}{\eta}\right)^k \frac{\Gamma\left(k+\frac{2\mu p}{1+p}\right)}{k!\Gamma(k+2\mu)} G_{2,2}^{1,2}\left(\frac{2\mu(1+\eta)}{g(1+p)\bar{\gamma}} \middle| \begin{matrix} \frac{1}{2}, 1 \\ (k+2\mu, 0) \end{matrix} \right). \quad (3.92)$$

For a balanced condition ($p = 1$), (3.92) is numerically equivalent to the average ABER obtained in [57].

In a maximal ratio combining scenario, the ABER of a coherent fading channel is attained in same fashion as (3.92) and is given as

$$\begin{aligned} P_b(E) = & \frac{1}{2\sqrt{\pi}\Gamma\left(\frac{2\mu M}{1+p}\right)} \left(\frac{p}{\eta}\right)^{\frac{2\mu M p}{1+p}} \sum_{k=0}^{\infty} \left(1-\frac{p}{\eta}\right)^k \frac{\Gamma\left(k+\frac{2\mu M p}{1+p}\right)}{k!\Gamma(k+2\mu M)} \\ & \times G_{2,2}^{1,2}\left(\frac{2\mu(1+\eta)}{g(1+p)\bar{\gamma}} \middle| \begin{matrix} \frac{1}{2}, 1 \\ (k+2\mu M, 0) \end{matrix} \right). \end{aligned} \quad (3.93)$$

Figure 3.18 compares the ABER of a coherent BFSK modulation scheme ($g = 1/2$) of both integral and series expansion solutions for $M = 1$. For any given SNR, the closer p is to η, the smaller is the ABER. This clearly reflects the fading conditions as already commented in the envelope PDF and cases. It is noteworthy that the series expansion formulas developed here converge rapidly, but, of course, it depends on the parameters utilized. In particular, for the plots shown, no more than 30 terms were necessary for the required accuracy.

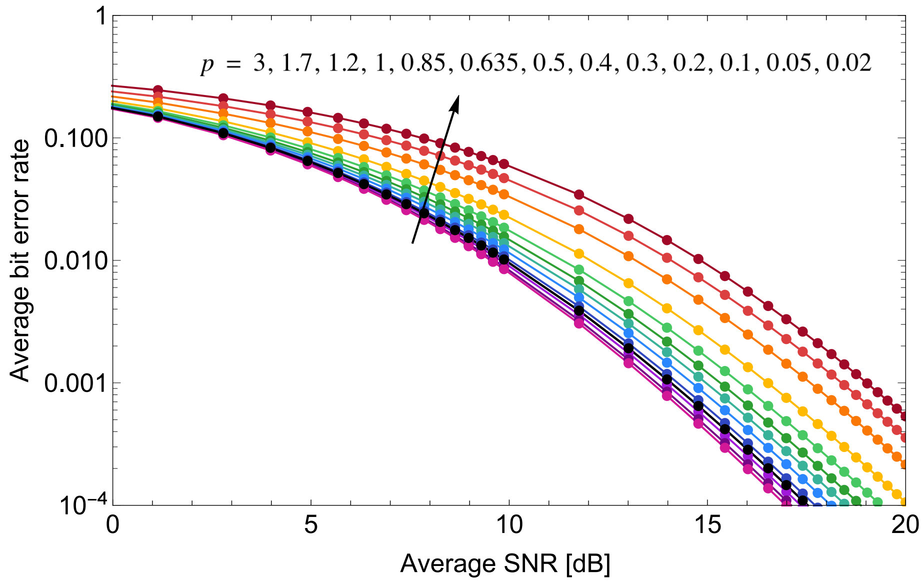

Figure 3.18: ABER of the coherent BFSK modulation ($g = 1/2$) for varying values of p ($\eta = 3.0$ and $\mu = 1.75$). Solid lines indicate integral solution and dot markers indicate series expansion solution.

3.6 Particular Cases

As is already known, the traditional η-μ distribution encompasses a whole set of other fading models. By introducing a new cluster imbalance parameter, the Extended model is susceptible to new particular cases beyond the previously known possibilities. The objective of this section is to explore both the classic and the new particular cases of the Extended η-μ model.

3.6.1 The η-μ Distribution

As mentioned throughout this chapter, the Extended η-μ model encompass the original η-μ distribution. Regardless of the Format used, when $p = 1$ the multipath clusters are balanced; therefore, *all* equations here derived reduce to the original η-μ case.

Surprisingly, the generalized η-μ case can also be attained by replacing $p_e = (1+p_g)/(1-p_g)$ for both Format 1 and 2, in which p_e refers to the Extended η-μ parameter and p_g indicates the generalized η-μ parameter.

3.6.2 Generalized Nakagami-m Distribution

Interestingly, for all equations derived here, the generalized Nakagami-m distribution is obtained in exact manner for $\eta_h = (1 + p_n)/(1 - p_n)$ or $\eta_e = p_h$, $p_h = (1+p_n)/(1-p_n)$ and $\mu = m/2$ in Format 1, and $\eta_h = 0$ and $\mu = m/2$ in Format 2, wherein the h index indicates Extended η-μ and the n index concerns Nakagami-m model, and m is the Nakagami parameter.

More interestingly, when the formulation related only to the envelope (i.e. (3.25)), is submitted to the limits $p \to 0$ or $p \to \infty$, it results in the classic Nakagami-m envelope equations.

3.7 Conclusion

This chapter presented an extension to the original η-μ fading model. This model introduces an imbalance parameter, which quantifies the relative number of multipath clusters in the in-phase and quadrature components of the fading signals. Although the introduction of such a parameter adds flexibility to the model. The mathematical complexity introduced is no greater than that of the original model. Closed-form expressions for the joint phase-envelope and marginal PDFs have been found, as well as closed-form formulations for the moments. The CDF and MGF of the envelope have been found in rapidly convergent infinite series. The phase CDF was wondrously obtained in closed-form equation. In addition, higher order statistics were derived for both envelope and phase distributions and their respective time derivatives. The clustering imbalance parameter has been found to directly affect both envelope and phase related statistics. Interestingly, the envelope statistics are seen to have a symmetry around the ratio relating the power imbalance and phase imbalance parameters. It is observed that the closer to each other the clustering imbalance and power imbalance parameters of in-phase and quadrature components, the better the fading conditions. It is noteworthy that the Extended η-μ fading model is a particular case of the more general α-η-κ-μ fading model, but it bears several closed-form expressions.

Chapter 4

The Extended κ-μ Fading Model

The κ-μ fading complex model was first introduced in [18]. There, joint phase-envelope distributions were derived and an integral-form solution was presented for the phase distribution. Later on, [45] developed a clever method to obtain a tight closed-form approximation for the κ-μ phase PDF. This solution proved to be highly accurate and allowed the authors to derive a very useful and elegant closed-form expressions for its phase statistics. Despite this huge breakthrough, both studies, [18] and [45], never considered parameterizing the cluster imbalance phenomenon. Cluster imbalance was first introduced for the Nakagami-m process in [16], and was later remodeled for the α-η-κ-μ fading model. As observed in both researches, this phenomenon is quite interesting and has great potential to deliver new unexplored fading scenarios. Hence, in order to fill this gap, an extension to the κ-μ fading model is proposed here. Here again, the Extended model is based on the uneven number of multipath cluster between the in-phase and quadrature components. This chapter introduces a complete statistical research for the Extended κ-μ model, and is organized as follows:

- Section 4.1 develops the Extended κ-μ physical model and introduces the joint phase-envelope PDF;
- Section 4.2 presents the envelope and the phase PDFs, and shows novel mathematical identities for the Bessel function;
- Section 4.3 proposes an approximate expression for the phase PDF, accompanied by some plots;
- Section 4.4 introduces new expressions for the Extended κ-μ higher order statistics, and as a consequence, exact and approximate PCR formulations are proposed;

– Finally, in Section 4.5, some particular cases are obtained from the new Extended model.

4.1 Joint Phase-Envelope Statistics

For this extension proposal, the in-phase and quadrature signals follow the general quadrature process described in (2.64). Thus, the general process $-\infty < Z < \infty$ is defined as

$$f_Z(z) = \frac{|z|^{\frac{\mu_z}{2}}}{2\sigma_z^2 |\lambda_z|^{\frac{\mu_z}{2}-1} \cosh\left(\frac{z\lambda_z}{\sigma_z^2}\right)} \exp\left(-\frac{(z-\lambda_z)^2}{2\sigma_z^2}\right) I_{\frac{\mu_z}{2}-1}\left(\frac{|\lambda_z z|}{\sigma_z^2}\right), \tag{4.1}$$

wherein: (i) $\sigma_z^2 > 0$ is the power of one multipath cluster; (ii) λ_z^2 is the power of the dominant components of all multipath clusters, with $-\infty < \lambda_z < \infty$; (iii) $\mu_z > 0$ is the number of multipath clusters; and (iv) $I_\nu(z)$ is the Bessel function of first kind and order ν [1, Eq. 9.6.20].

Now, the complex κ-μ signal is described as

$$S = X + jY, \tag{4.2}$$

in which X and Y are independent processes and correspond, respectively, to the real and to the imaginary parts of S. Their PDFs, namely, $f_X(x)$ and $f_Y(y)$ follow that in (4.1), with respective parameters σ_x, λ_x and μ_x, and σ_y, λ_y and μ_y.

The envelope R is determined as the absolute value of S, i.e. $R = |S|$, and the phase is given as $\Theta = \arg(X + jY)$. With a simple variable transformation, X and Y can be rewritten in terms of R and Θ, as $X = R\cos\Theta$ e $Y = R\sin\Theta$. Thus, the joint phase-envelope PDF can be written as

$$f_{R,\Theta}(r,\theta) = r f_X(r\cos\theta) f_Y(r\sin\theta). \tag{4.3}$$

For the Extended κ-μ fading model, let us define p as the parameter that quantifies the ratio between the number of multipath clusters of in-phase and quadrature components, given as follows

$$p = \frac{\mu_X}{\mu_Y}. \tag{4.4}$$

Here again, the balanced condition is attained for $p = 1$, and the imbalanced case is obtained for any $p > 0$. Then, μ_x and μ_y are related as in

$$\mu_X + \mu_Y = 2\mu, \tag{4.5}$$

with $\mu > 0$ denoting the total number of multipath clusters. After manipulating algebraically (4.4) and (4.5), μ_x and μ_y are found, respectively, as

$$\mu_X = \frac{2\mu p}{1+p} \tag{4.6}$$

and

$$\mu_Y = \frac{2\mu}{1+p}. \tag{4.7}$$

Finally, as specified in [13] and [18], define $\kappa > 0$ as the ratio of the total power of dominant components to the total power of scattered waves, i.e. $\kappa = \left(\lambda_x^2 + \lambda_y^2\right)/(2\mu)$. Solving for λ_x and λ_y, we have that

$$\lambda_x = \sqrt{\frac{pq\kappa}{(1+pq)(1+\kappa)}}\hat{r} \tag{4.8}$$

and

$$\lambda_y = \sqrt{\frac{\kappa}{(1+pq)(1+\kappa)}}\hat{r}, \tag{4.9}$$

wherein: (i) $q > 0$ is ratio of two ratios: the ratio of the power of the dominant components to the power of he scattered waves of the in-phase signal and its counterpart for the quadrature signal, i.e. $q = \lambda_x^2/(\lambda_y^2 p)$; (ii) $\hat{r} = \sqrt{E\left(R^2\right)}$ is the RMS value; and (iii) $E(\cdot)$ is the expectation operator.

Additionally, in a κ-μ signal, the in-phase and quadrature powers are identical, i.e. $\sigma_x^2 = \sigma_y^2 = \sigma^2$, then,

$$\sigma^2 = \frac{\hat{r}^2}{2\mu(1+\kappa)}. \tag{4.10}$$

Having defined all the parameters, the joint phase-envelope PDF of the Extended κ-μ model can be obtained by replacing (4.1), (4.6), (4.7), (4.8), (4.9), (4.10) in (4.3), resulting in

$$\begin{aligned} f_{R,\Theta}(r,\theta) = {} & \mu^2 \kappa^{1-\frac{\mu}{2}} p^{\frac{1}{2}-\frac{\mu p}{2(1+p)}} q^{\frac{1}{2}-\frac{\mu p}{2(1+p)}} (1+\kappa)^{\frac{\mu}{2}+1} (1+pq)^{\frac{\mu}{2}-1} \left|\sin(\theta)\right|^{\frac{\mu}{1+p}} \left|\cos(\theta)\right|^{\frac{\mu p}{1+p}} \frac{r^{\mu+1}}{\hat{r}^{\mu+2}} \\ & \times \exp\left(2\sqrt{\frac{\kappa(1+\kappa)}{1+pq}}\mu\left(\sin\theta + \sqrt{pq}\cos\theta\right)\frac{r}{\hat{r}} - \kappa\mu - (1+\kappa)\mu\frac{r^2}{\hat{r}^2}\right) \\ & \times I_{\frac{\mu}{1+p}-1}\left(2\sqrt{\frac{\kappa(1+\kappa)}{1+pq}}\mu\left|\sin\theta\right|\frac{r}{\hat{r}}\right) \operatorname{sech}\left(2\sqrt{\frac{\kappa(1+\kappa)}{1+pq}}\mu\sin\theta\frac{r}{\hat{r}}\right) \\ & \times I_{\frac{\mu p}{1+p}-1}\left(2\sqrt{\frac{\kappa pq(1+\kappa)}{1+pq}}\mu\left|\cos\theta\right|\frac{r}{\hat{r}}\right) \operatorname{sech}\left(2\sqrt{\frac{\kappa pq(1+\kappa)}{1+pq}}\mu\cos\theta\frac{r}{\hat{r}}\right), \end{aligned} \tag{4.11}$$

with $r > 0$ and $-\pi \leq \theta \leq \pi$. To obtain the original κ-μ model as in (2.48), the following settings must hold: $p = 1$ and $q = \tan^2\phi$, wherein ϕ is the phase parameter as defined earlier for the α-η-κ-μ fading model.

4.2 Envelope and Phase PDF

With (4.11), both envelope and phase PDF, namely $f_R(r)$ and $f_\Theta(\theta)$, can be calculated after integrating with respect to θ and r, respectively. In these cases, however, no closed-form expressions can be found .

For the Extended κ-μ phase distribution, it is anticipated that cluster imbalance has a major role on its overall behavior. Thus, special attention is given for such matter in Section 4.3, wherein plots are depicted for different fading scenarios while comparing exact and approximate phase distribution.

By construction, the envelope PDF of the Extended κ-μ model, for any $p > 0$, was found to yield the same values as the envelope PDF of the traditional model. Hence, it is secure to assert that the Extended κ-μ envelope PDF is defined as

$$f_R(r) = \frac{2\mu(1+\kappa)^{\frac{\mu+1}{2}} r^\mu}{\kappa^{\frac{\mu-1}{2}} \hat{r}^{\mu+1}} \exp\left(-\mu\kappa - \mu(1+\kappa)\left(\frac{r}{\hat{r}}\right)^2\right) I_{\mu-1}\left(2\mu\sqrt{\kappa(1+\kappa)}\frac{r}{\hat{r}}\right). \tag{4.12}$$

More importantly, with

$$f_R(r) = \int_{-\pi}^{\pi} f_{R,\Theta}(r,\theta)\, \mathrm{d}\theta, \tag{4.13}$$

one can easily maintain that the following empirical mathematical identity for the modified Bessel function of first kind is true

$$\begin{aligned} I_{\alpha+\beta-1}(z) = {} & \frac{1}{4} z \frac{a^{\frac{1-\beta}{2}}}{(1+a)^{1-\frac{\alpha+\beta}{2}}} \int_{-\pi}^{\pi} \exp\left(\frac{z}{\sqrt{1+a}}\left(\sin\theta + \sqrt{a}\cos\theta\right)\right) |\sin\theta|^\alpha |\cos\theta|^\beta \\ & \times I_{\alpha-1}\left(\frac{z}{\sqrt{1+a}}|\sin\theta|\right) I_{\beta-1}\left(z\sqrt{\frac{a}{1+a}}|\cos\theta|\right) \\ & \times \operatorname{sech}\left(\frac{z}{\sqrt{1+a}}\sin\theta\right) \operatorname{sech}\left(z\sqrt{\frac{a}{1+a}}\cos\theta\right) \mathrm{d}\theta, \end{aligned} \tag{4.14}$$

with $z > 0$, $a > 0$, $\alpha > 0$ and $\beta > 0$. It is important to mention that (4.14) is new and to the best of the author's knowledge has never been described in the literature. Note also that (4.14) is a more general version of the identity found in [18, Eq. (17)].

In the limits, $q \to 0$ and $q \to \infty$, the identity in (4.14) can be rewritten with the help of [1, Eq. (9.6.7)], wherein for small arguments the relation below is used

$$I_{\nu-1}(z) \approx \left(\frac{z}{2}\right)^{\nu-1} \frac{1}{\Gamma(\nu)}. \tag{4.15}$$

Then, for $q \to 0$ and $q \to \infty$, novel identities arise respectively as,

$$I_{\alpha+\beta-1}(z) = \frac{z^\beta}{2^{\beta+1}\Gamma(\beta)} \int_{-\pi}^{\pi} |\sin\theta|^\alpha |\cos\theta|^{2\beta-1} I_{\alpha-1}(z|\sin\theta|) \operatorname{sech}(z\sin\theta)\, \mathrm{d}\theta \tag{4.16}$$

and

$$I_{\alpha+\beta-1}(z) = \frac{z^{\alpha}}{2^{\alpha+1}\Gamma(\alpha)} \int_{-\pi}^{\pi} |\sin\theta|^{2\alpha-1} |\cos\theta|^{\beta} I_{\beta-1}(z|\cos\theta|) \operatorname{sech}(z\cos\theta)\, \mathrm{d}\theta. \quad (4.17)$$

Again, the identities (4.16) and (4.17) encompass the expressions obtained in [18].

4.3 Phase PDF - An Approximate Solution

As explained earlier, the Extended κ-μ phase distribution is limited to its integral-form, and despite its exactness, when evaluated repeatedly, this procedure can become computationally impaired. In a way, mathematical tractability is often desired, in order to pursue some studies related to fading models. Hence, [45] developed an elegant and clever technique, coming up with a tight closed-form expression for the classic κ-μ phase PDF. This approximation method proved to be highly resourceful in deriving other phase statistics, and by maintaining most of the PDFs properties, delivered excellent and accurate curves. Following this approach, the aim of this section is to propose a tight closed-form approximate solution for the Extended κ-μ phase distribution.

First, let us introduce some concepts. As known, the phase PDF is promptly calculated as

$$f_{\Theta}(\theta) = \int_{0}^{\infty} f_{R,\Theta}(r,\theta)\, \mathrm{d}r, \quad (4.18)$$

wherein $f_{R,\Theta}(r,\theta)$ is (4.11). However, for this direct procedure, no solution was found. Another way of tackling this problem is to obtain the series expansion of some of the transcendental functions available in (4.11) in series. Here again, the results are rather complicated and unpractical; therefore, finding an approximate solution is a better approach.

The authors in [45] proposed to Taylor expand (4.11) in terms of r as shown below

$$f_{R,\Theta}(r,\theta) = f_{R,\Theta}(a,\theta) + (r-a) f'_{R,\Theta}(a,\theta) + (x-a)^2 \frac{f''_{R,\Theta}(a,\theta)}{2!} + \ldots + (x-a)^n \frac{f^{(n)}_{R,\Theta}(a,\theta)}{n!}, \quad (4.19)$$

with a being the expansion point, and n being the n$^{\text{th}}$ term of the series. Note, however, that after performing the integration with respect to r within the interval 0 and infinity, (4.19) does not converge for any r. To overcome this situation, [45] cleverly truncated the integration in two operations with distinct intervals, i.e. from 0 to 1 and from 1 to infinity, before Taylor expanding the joint PDF, i.e.

$$f_\Theta(\theta) = \int_0^1 f_{R,\Theta}(r,\theta)\,\mathrm{d}r + \int_1^\infty f_{R,\Theta}(r,\theta)\,\mathrm{d}r. \tag{4.20}$$

Then, a simple variable transformation is carried out at the second integral, i.e. $r = 1/y$, and the differential term is substituted as $\mathrm{d}r = -\,\mathrm{d}y/y^2$. With this, the intervals are promptly replaced from $r = \infty$ to $y = 0$ and from $r = 1$ to $y = 1$, so that

$$f_\Theta(\theta) = \int_0^1 f_{R,\Theta}(r,\theta)\,\mathrm{d}r + \int_0^1 \frac{f_{R,\Theta}(\frac{1}{y},\theta)}{y^2}\,\mathrm{d}y. \tag{4.21}$$

Finally, by performing the following variable transformation $y = r$, both terms can be grouped under the same interval as

$$f_\Theta(\theta) = \int_0^1 u(r,\theta)\,\mathrm{d}r, \tag{4.22}$$

wherein $u(r,\theta) = f_{R,\Theta}(r,\theta) + f_{R,\Theta}(1/r,\theta)/r^2$.

All these guarantee a proper integral convergence within the proposed interval. We now Taylor expand $u(r,\theta)$ around $a = 1$, with $n = 1$, obtaining

$$\begin{aligned} u(r,\theta) =\ & \mu^2 \kappa^{1-\frac{\mu}{2}} p^{\frac{1}{2}-\frac{\mu p}{2(1+p)}} q^{\frac{1}{2}-\frac{\mu p}{2(1+p)}} (1+\kappa)^{\frac{\mu}{2}+1} (1+pq)^{\frac{\mu}{2}-1} |\sin\theta|^{\frac{\mu}{1+p}} |\cos\theta|^{\frac{\mu p}{1+p}} \frac{(2-r)}{\hat{r}^{\mu+2}} \\ & \times \exp\left(2\sqrt{\frac{\kappa(1+\kappa)}{1+pq}}\mu\left(\sin\theta + \sqrt{pq}\cos\theta\right)\frac{1}{\hat{r}} - \kappa\mu - (1+\kappa)\mu\frac{1}{\hat{r}^2}\right) \\ & \times I_{\frac{\mu}{1+p}-1}\left(2\sqrt{\frac{\kappa(1+\kappa)}{1+pq}}\mu|\sin\theta|\frac{1}{\hat{r}}\right) \operatorname{sech}\left(2\sqrt{\frac{\kappa(1+\kappa)}{1+pq}}\mu\sin\theta\frac{1}{\hat{r}}\right) \\ & \times I_{\frac{\mu p}{1+p}-1}\left(2\sqrt{\frac{\kappa pq(1+\kappa)}{1+pq}}\mu|\cos\theta|\frac{1}{\hat{r}}\right) \operatorname{sech}\left(2\sqrt{\frac{\kappa pq(1+\kappa)}{1+pq}}\mu\cos\theta\frac{1}{\hat{r}}\right). \end{aligned} \tag{4.23}$$

With (4.23), the integral can be solved, resulting in

$$\begin{aligned} U(r,\theta) &= \int_0^1 u(r,\theta)\,\mathrm{d}r \\ &= \mu^2 \kappa^{1-\frac{\mu}{2}} p^{\frac{1}{2}-\frac{\mu p}{2(1+p)}} q^{\frac{1}{2}-\frac{\mu p}{2(1+p)}} (1+\kappa)^{\frac{\mu}{2}+1} (1+pq)^{\frac{\mu}{2}-1} |\sin\theta|^{\frac{\mu}{1+p}} |\cos\theta|^{\frac{\mu p}{1+p}} \frac{3}{\hat{r}^{\mu+2}} \\ &\quad \times \exp\left(2\sqrt{\frac{\kappa(1+\kappa)}{1+pq}}\mu\left(\sin\theta + \sqrt{pq}\cos\theta\right)\frac{1}{\hat{r}} - \kappa\mu - (1+\kappa)\mu\frac{1}{\hat{r}^2}\right) \\ &\quad \times I_{\frac{\mu}{1+p}-1}\left(2\sqrt{\frac{\kappa(1+\kappa)}{1+pq}}\mu|\sin\theta|\frac{1}{\hat{r}}\right) \operatorname{sech}\left(2\sqrt{\frac{\kappa(1+\kappa)}{1+pq}}\mu\sin\theta\frac{1}{\hat{r}}\right) \\ &\quad \times I_{\frac{\mu p}{1+p}-1}\left(2\sqrt{\frac{\kappa pq(1+\kappa)}{1+pq}}\mu|\cos\theta|\frac{1}{\hat{r}}\right) \operatorname{sech}\left(2\sqrt{\frac{\kappa pq(1+\kappa)}{1+pq}}\mu\cos\theta\frac{1}{\hat{r}}\right). \end{aligned} \tag{4.24}$$

In order to obtain a true PDF, (4.24) has to go through a normalization process. First, let us remove all the multiplicative terms that are not related to θ from (4.24), resulting in

$$\begin{aligned} U^*(\theta) = {} & |\sin\theta|^{\frac{\mu}{1+p}} \, |\cos\theta|^{\frac{\mu p}{1+p}} \exp\left(2\sqrt{\frac{\kappa(1+\kappa)}{1+pq}}\mu\left(\sin\theta + \sqrt{pq}\cos\theta\right)\right) \\ & \times I_{\frac{\mu}{1+p}-1}\left(2\sqrt{\frac{\kappa(1+\kappa)}{1+pq}}\mu\,|\sin\theta|\right) \operatorname{sech}\left(2\sqrt{\frac{\kappa(1+\kappa)}{1+pq}}\mu\sin\theta\right) \\ & \times I_{\frac{\mu p}{1+p}-1}\left(2\sqrt{\frac{\kappa pq(1+\kappa)}{1+pq}}\mu\,|\cos\theta|\right) \operatorname{sech}\left(2\sqrt{\frac{\kappa pq(1+\kappa)}{1+pq}}\mu\cos\theta\right). \end{aligned} \tag{4.25}$$

After this procedure, (4.25) must be integrated with respect to θ, leading to its area A. By doing so, the result resembles the first mathematical identity derived in this Chapter given by (4.14). The result of this process is given as follows

$$\begin{aligned} A &= \int_{-\pi}^{\pi} U^*(\theta)\,\mathrm{d}\theta \\ &= \frac{2(1+pq)^{1-\frac{\mu}{2}}}{\sqrt{\kappa(1+\kappa)}\mu(pq)^{\frac{1}{2}-\frac{\mu p}{2(1+p)}}} I_{\mu-1}\left(2\sqrt{\kappa(1+\kappa)}\mu\right). \end{aligned} \tag{4.26}$$

Finally, the approximate phase PDF for the Extended κ-μ model, $f_{\mathbb{O}}(\theta)$, is formalized as

$$f_{\mathbb{O}}(\theta) = \frac{U^*(\theta)}{A}. \tag{4.27}$$

Substituting, (4.25) and (4.26) in (4.27), we have that

$$\begin{aligned} f_{\mathbb{O}}(\theta) = {} & \frac{\sqrt{\kappa(1+\kappa)}\mu(pq)^{\frac{1}{2}-\frac{\mu p}{2(1+p)}}}{2(1+pq)^{1-\frac{\mu}{2}}} |\sin\theta|^{\frac{\mu}{1+p}} \, |\cos\theta|^{\frac{\mu p}{1+p}} \, I_{\mu-1}\left(2\sqrt{\kappa(1+\kappa)}\mu\right) \\ & \times \exp\left(2\sqrt{\frac{\kappa(1+\kappa)}{1+pq}}\mu\left(\sin\theta + \sqrt{pq}\cos\theta\right)\right) \\ & \times I_{\frac{\mu}{1+p}-1}\left(2\sqrt{\frac{\kappa(1+\kappa)}{1+pq}}\mu\,|\sin\theta|\right) \operatorname{sech}\left(2\sqrt{\frac{\kappa(1+\kappa)}{1+pq}}\mu\sin\theta\right) \\ & \times I_{\frac{\mu p}{1+p}-1}\left(2\sqrt{\frac{\kappa pq(1+\kappa)}{1+pq}}\mu\,|\cos\theta|\right) \operatorname{sech}\left(2\sqrt{\frac{\kappa pq(1+\kappa)}{1+pq}}\mu\cos\theta\right). \end{aligned} \tag{4.28}$$

Curiously, in the limits $q \to 0$ and $q \to \infty$, (4.28) reduces to two distinct phase functions, with respective expressions are given as follow,

$$f_\Theta(\theta)_{q\to 0} = \frac{\left(\sqrt{\kappa(1+\kappa)}\mu\right)^{\frac{\mu p}{1+p}}}{2\Gamma\left(\frac{\mu p}{1+p}\right) I_{\mu-1}\left(2\sqrt{\kappa(1+\kappa)}\mu\right)} \left|\sin\theta\right|^{\frac{\mu}{p+1}} \left|\cos\theta\right|^{\frac{2\mu p}{p+1}-1}$$
$$\times I_{\frac{\mu}{p+1}-1}\left(2\sqrt{\kappa(1+\kappa)}\mu\left|\sin\theta\right|\right) \operatorname{sech}\left(2\sqrt{\kappa(1+\kappa)}\mu\sin\theta\right)$$
$$\times \exp\left(2\sqrt{\kappa(1+\kappa)}\mu\sin\theta\right) \tag{4.29}$$

and

$$f_\Theta(\theta)_{q\to \infty} = \frac{\left(\sqrt{\kappa(1+\kappa)}\mu\right)^{\frac{\mu}{1+p}}}{2\Gamma\left(\frac{\mu}{1+p}\right) I_{\mu-1}\left(2\sqrt{\kappa(1+\kappa)}\mu\right)} \left|\sin\theta\right|^{\frac{2\mu}{p+1}-1} \left|\cos\theta\right|^{\frac{\mu p}{p+1}}$$
$$\times I_{\frac{\mu p}{p+1}-1}\left(2\sqrt{\kappa(1+\kappa)}\mu\left|\cos\theta\right|\right) \operatorname{sech}\left(2\sqrt{\kappa(1+\kappa)}\mu\cos\theta\right)$$
$$\times \exp\left(2\sqrt{\kappa(1+\kappa)}\mu\cos\theta\right). \tag{4.30}$$

It is important to emphasize that, when clusters are balanced ($p = 1$), (4.28) reduces strikingly to the approximate phase PDF of the classic κ-μ model represented in (2.53), as expected. Consequently, as already observed in [45], exact Nakagami-m phase PDF and von Mises are also obtained after proper parameter substitution. Wondrously, with $\mu = m$, $\kappa = 1$ and $p_\kappa = (1 + p_n)/(1 - p_n))$, wherein p_κ and p_n indicate, respectively, the parameter p of the Extended κ-μ and Nakagami-m models, (4.28) reduces to the exact generalized Nakagami-m phase distribution as in (2.21). More importantly, due to the normalization procedure, the equation in (4.28) is a true PDF, and henceforth, is considered a new phase distribution model with random variable $\mathbb{O}$.

In order to investigate cluster imbalance and to confront both exact and approximate phase PDFs, some plots are presented considering different fading scenarios. A quick look in Figures 4.1-4.3, shows that the approximate solution maintains all properties of the exact phase PDF like minimum and maximum points, yielding an incredible fit in most cases.

In Figure 4.1, the phase scenario is molded for smaller $\kappa = 0.01$ and varying values of p. First, note the clear influence of cluster imbalance in the phase PDF. Furthermore, observe that in this particular situation, while $p < 0.4$, the PDF grows indefinitely around $\pm\pi/2$, when reaching $p = 0.4$, the PDF assumes a bimodal shape with peaks in $\pm\pi/2$, and finally, as $p > 0.4$, the PDF mass changes to an uneven quadrimodal form. Notice that this pattern repeats itself after a $\pi/2$ shift. This can be explained due to either the in-phase and quadrature components reaches the Gaussian condition, i.e. $2\mu = (1+p)/p$ or $2\mu = 1+p$. Once again, it can be seen that both exact and approximate PDF are quite close to each other.

Figure 4.2 depicts another scenario with $\kappa = 0.5$, and cluster imbalance is still explored. Here again the Gaussian condition is observed, as the PDF mass cycles from an indefinite to a trimodal shape, and then again to an indefinite form. Another scenario is illustrated in Figure 4.3, in which κ assumes different increasing values and the PDF mass follows its growth.

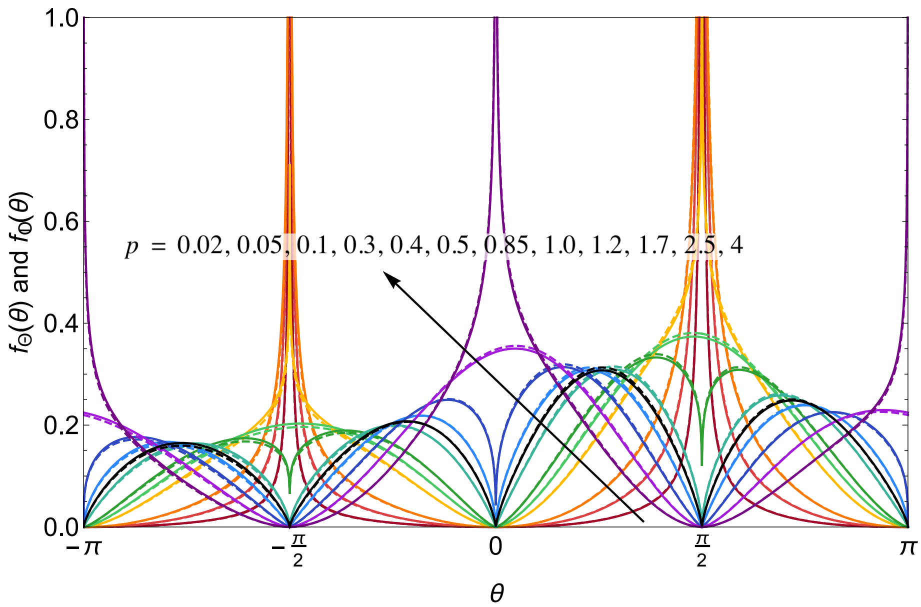

Figure 4.1: Exact (solid lines) and approximate (dashed lines) phase PDF for varying p ($\kappa = 0, 01$, $\mu = 1, 75$ and $q = 0.3$).

4.4 Higher Order Statistics

As already explained, higher order statistics are calculated through temporal derivatives of the signal's components. After properly defining the temporal derivative component, the joint X, $\dot{X}$, Y and $\dot{Y}$ PDF are determined, wherein the dot indicates time derivative. Finally, by means of a variable transformations, the joint PDF of R, $\dot{R}$, Θ and $\dot{\Theta}$ can be obtained, leading the way to other interesting statistics such as phase crossing rate.

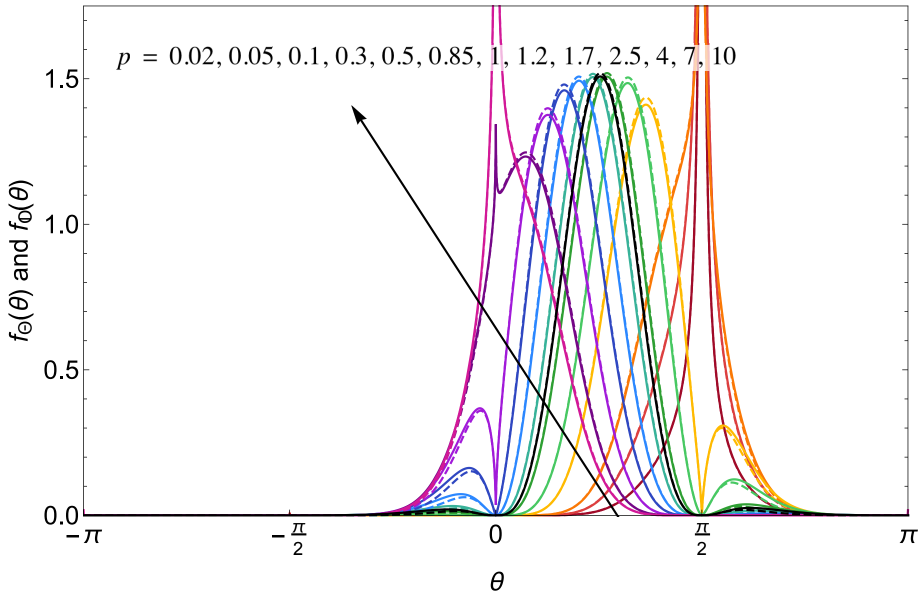

Figure 4.2: Exact (solid lines) and approximate (dashed lines) phase PDF for varying p ($\kappa = 0, 50$, $\mu = 3, 75$ and $q = 0.90$).

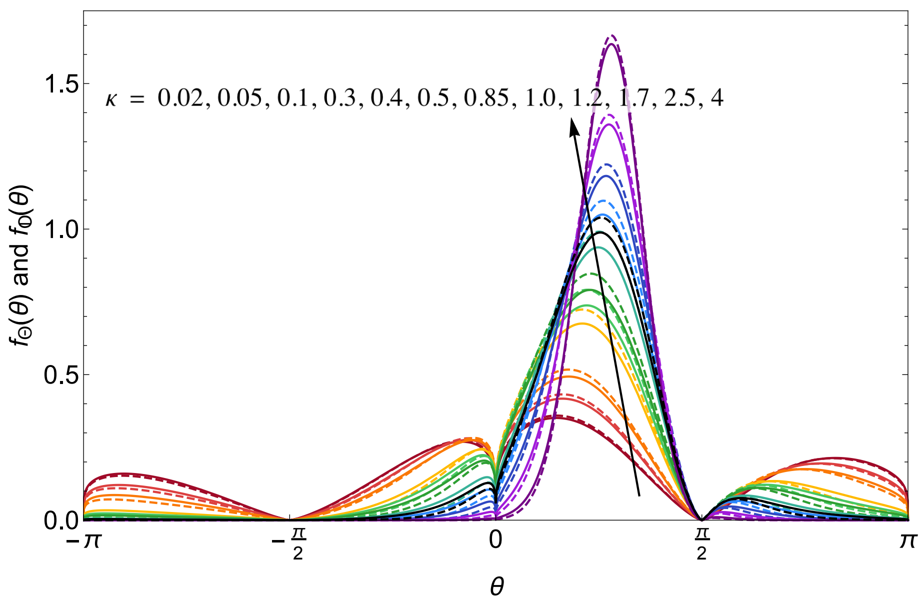

Figure 4.3: Exact (solid lines) and approximate (dashed lines) phase PDF for varying κ ($\mu = 1, 75$, $p = 1.90$ and $q = 0.30$).

4.4.1 Joint PDF of X, $\dot{X}$, Y and $\dot{Y}$

In [45], the authors conducted an extensive study over the time derivative component for the κ-μ signal. In their research, the general variable $\dot{Z}$ is a Gaussian process with zero mean and variance $\dot{\sigma}^2$, and therefore, its PDF can be depicted as

$$f_{\dot{Z}}(\dot{z}) = \frac{1}{\sqrt{2\pi\dot{\sigma}^2}} \exp\left(-\frac{\dot{z}^2}{2\dot{\sigma}^2}\right), \tag{4.31}$$

which for an isotropic environment, its variance is modeled as

$$\dot{\sigma}^2 = 2\pi^2 f_m^2 \sigma^2, \tag{4.32}$$

with f_m denoting maximum Doppler shift in hertz, and σ^2 is represented in (4.10).

Hence, by definition, X and Y are independent processes, and therefore, their time derivative counterpart, namely $\dot{X}$ and $\dot{Y}$ are also independent. Being so, the joint PDF of X, $\dot{X}$, Y and $\dot{Y}$ can be written as in

$$f_{X,\dot{X},Y,\dot{Y}} = f_X(x) f_{\dot{X}}(\dot{x}) f_Y(y) f_{\dot{Y}}(\dot{y}), \tag{4.33}$$

wherein $f_X(x)$ and $f_Y(y)$ follow the general quadrature established in (4.1), and $f_{\dot{X}}(\dot{x})$ and $f_{\dot{Y}}(\dot{y})$ PDFs are indicated in (4.31).

By making the appropriate replacements in (4.33), we have that

$$\begin{aligned} f_{X,\dot{X},Y,\dot{Y}}(x,\dot{x},y,\dot{y}) = {} & \frac{\mu^3 \kappa^{1-\frac{\mu}{2}} (1+\kappa)^{\frac{\mu}{2}+2} (pq)^{\frac{1}{2}-\frac{\mu p}{2(1+p)}} (1+pq)^{\frac{\mu}{2}-1}}{2\pi^3 f_m^2 \hat{r}^{\mu+4}} |x|^{\frac{\mu p}{1+p}} |y|^{\frac{\mu}{1+p}} \\ & \times \exp\left(-\frac{(1+\kappa)\mu}{2\hat{r}^2}\left(\frac{\dot{x}}{\pi^2 f_m^2} + 2\left(x - \hat{r}\sqrt{\frac{\kappa pq}{(1+\kappa)(1+pq)}}\right)^2\right)\right) \\ & \times \exp\left(-\frac{(1+\kappa)\mu}{2\hat{r}^2}\left(\frac{\dot{y}}{\pi^2 f_m^2} + 2\left(y - \hat{r}\sqrt{\frac{\kappa}{(1+\kappa)(1+pq)}}\right)^2\right)\right) \\ & \times I_{\frac{\mu}{1+p}-1}\left(2\sqrt{\frac{\kappa(1+\kappa)}{1+pq}}\mu\frac{|y|}{\hat{r}}\right) \operatorname{sech}\left(2\sqrt{\frac{\kappa(1+\kappa)}{1+pq}}\mu\frac{y}{\hat{r}}\right) \\ & \times I_{\frac{\mu p}{1+p}-1}\left(2\sqrt{\frac{\kappa pq(1+\kappa)}{1+pq}}\mu\frac{|x|}{\hat{r}}\right) \operatorname{sech}\left(2\sqrt{\frac{\kappa pq(1+\kappa)}{1+pq}}\mu\frac{x}{\hat{r}}\right). \end{aligned} \tag{4.34}$$

4.4.2 Joint PDF of R, $\dot{R}$, Θ and $\dot{\Theta}$

By means of transformations of variables, the joint PDF of R, $\dot{R}$, Θ and $\dot{\Theta}$ is calculated through (4.34) with

$$f_{R,\dot{R},\Theta,\dot{\Theta}}(r,\dot{r},\theta,\dot{\theta}) = |J| \times f_{X,\dot{X},Y,\dot{Y}}(x,\dot{x},y,\dot{y}), \tag{4.35}$$

in which $|J| = R^2$ is the Jacobian of the transformation, and $X = R\cos(\Theta)$, $Y = R\sin(\Theta)$, $\dot{X} = \dot{R}\cos(\Theta) - R\dot{\Theta}\sin(\Theta)$ and $\dot{Y} = \dot{R}\sin(\Theta) + R\dot{\Theta}\cos(\Theta)$. With that, the joint PDF is expressed as

$$
\begin{aligned}
f_{R,\dot{R},\Theta,\dot{\Theta}}(r,\dot{r},\theta,\dot{\theta}) = & \frac{\mu^3(1+\kappa)^{\frac{\mu}{2}+2}p^{\frac{1}{2}-\frac{\mu p}{2(1+p)}}q^{\frac{1}{2}-\frac{\mu p}{2(1+p)}}(1+pq)^{\frac{\mu}{2}-1}}{2\pi^3 f_m^2 \kappa^{\frac{\mu}{2}-1}} |\sin\theta|^{\frac{\mu}{1+p}} |\cos\theta|^{\frac{\mu p}{1+p}} \frac{r^{\mu+2}}{\hat{r}^{\mu+4}} \\
& \times \exp\left(2\sqrt{\frac{\kappa(1+\kappa)}{1+pq}}\mu\left(\sin\theta+\sqrt{pq}\cos\theta\right)\frac{r}{\hat{r}}-\kappa\mu\right) \\
& \times \exp\left(-(1+\kappa)\mu\frac{r^2}{\hat{r}^2}-\frac{(1+\kappa)\mu\left(r^2\dot{\theta}^2+\dot{r}^2\right)}{2\pi^2 f_m^2 \hat{r}^2}\right) \\
& \times I_{\frac{\mu}{1+p}-1}\left(2\sqrt{\frac{\kappa(1+\kappa)}{1+pq}}\mu\left|\sin\theta\right|\frac{r}{\hat{r}}\right) I_{\frac{\mu p}{1+p}-1}\left(2\sqrt{\frac{\kappa pq(1+\kappa)}{1+pq}}\mu\left|\cos\theta\right|\frac{r}{\hat{r}}\right) \\
& \times \operatorname{sech}\left(2\sqrt{\frac{\kappa(1+\kappa)}{1+pq}}\mu\sin\theta\frac{r}{\hat{r}}\right)\operatorname{sech}\left(2\sqrt{\frac{\kappa pq(1+\kappa)}{1+pq}}\mu\cos\theta\frac{r}{\hat{r}}\right). \qquad (4.36)
\end{aligned}
$$

4.4.3 Other Joint PDFs

Given (4.36), other joint PDFs can be directly obtained by simple integral procedure. Here again, new closed form expressions emerge for distinct combinations of R, $\dot{R}$, Θ and $\dot{\Theta}$.

The joint PDF of R, $\dot{R}$, and $\dot{\Theta}$ can be calculated by integrating (4.36) with respect to Θ, and with the help of the mathematical identity derived in (4.14) leading to

$$
\begin{aligned}
f_{R,\dot{R},\dot{\Theta}}(r,\dot{r},\dot{\theta}) = & \frac{\mu^2\kappa^{\frac{1-\mu}{2}}(1+\kappa)^{\frac{\mu+3}{2}}r^{\mu+1}}{\pi^3 f_m^2 \hat{r}^{\mu+3}} \exp\left(-\frac{(1+\kappa)\mu}{2\pi^2 f_m^2 \hat{r}^2}\left(\dot{\theta}^2 r^2+\dot{r}^2\right)-(1+\kappa)\mu\frac{r^2}{\hat{r}^2}-\kappa\mu\right) \\
& \times I_{\mu-1}\left(2\sqrt{\kappa(1+\kappa)}\mu\frac{r}{\hat{r}}\right). \qquad (4.37)
\end{aligned}
$$

Interestingly, (4.37) is identical to the expression found in [45, Eq. (30)], proving once more that cluster imbalance does not affect envelope statistics.

The joint PDF of R, $\dot{R}$, and Θ is derived by integrating (4.36) in terms of $\dot{\Theta}$, that is

$$
\begin{aligned}
f_{R,\dot{R},\Theta}(r,\dot{r},\theta) = & \frac{\mu^{\frac{5}{2}}\kappa^{1-\frac{\mu}{2}}(1+\kappa)^{\frac{\mu+3}{2}}(pq)^{\frac{1}{2}-\frac{\mu p}{2(1+p)}}}{\sqrt{2}\pi^{\frac{3}{2}} f_m (1+pq)^{1-\frac{\mu}{2}}} |\sin\theta|^{\frac{\mu}{p+1}} |\cos\theta|^{\frac{\mu p}{p+1}} \frac{r^{\mu+1}}{\hat{r}^{\mu+3}} \\
& \times I_{\frac{\mu}{p+1}-1}\left(2\sqrt{\frac{\kappa(1+\kappa)}{1+pq}}\mu\left|\sin\theta\right|\frac{r}{\hat{r}}\right) I_{\frac{\mu p}{p+1}-1}\left(2\sqrt{\frac{\kappa pq(1+\kappa)}{1+pq}}\mu\left|\cos\theta\right|\frac{r}{\hat{r}}\right) \\
& \times \operatorname{sech}\left(2\sqrt{\frac{\kappa(1+\kappa)}{1+pq}}\mu\sin\theta\frac{r}{\hat{r}}\right)\operatorname{sech}\left(2\sqrt{\frac{\kappa pq(1+\kappa)}{1+pq}}\mu\cos\theta\frac{r}{\hat{r}}\right) \\
& \times \exp\left(2\sqrt{\frac{\kappa(1+\kappa)}{1+pq}}\mu\left(\sin\theta+\sqrt{pq}\cos\theta\right)\frac{r}{\hat{r}}-(1+\kappa)\mu\frac{r^2}{\hat{r}^2}\right) \\
& \times \exp\left(-\frac{(1+\kappa)\mu\dot{r}^2}{2\pi^2 f_d^2 \hat{r}^2}-\kappa\mu\right). \qquad (4.38)
\end{aligned}
$$

Similarly, the joint PDF of R, Θ and $\dot{\Theta}$ is obtained from the integration of (4.36) with respect to $\dot{R}$,

$$
\begin{aligned}
f_{R,\Theta,\dot{\Theta}}(r,\theta,\dot{\theta}) = {} & \frac{\mu^{\frac{5}{2}}\kappa^{1-\frac{\mu}{2}}(1+\kappa)^{\frac{\mu+3}{2}}(pq)^{\frac{1}{2}-\frac{\mu p}{2(1+p)}}}{\sqrt{2}\pi^{\frac{3}{2}}f_m(1+pq)^{1-\frac{\mu}{2}}}\left|\sin\theta\right|^{\frac{\mu}{p+1}}\left|\cos\theta\right|^{\frac{\mu p}{p+1}}\frac{r^{\mu+2}}{\hat{r}^{\mu+3}} \\
& \times I_{\frac{\mu}{p+1}-1}\left(2\sqrt{\frac{\kappa(1+\kappa)}{1+pq}}\mu\left|\sin\theta\right|\frac{r}{\hat{r}}\right) I_{\frac{\mu p}{p+1}-1}\left(2\sqrt{\frac{\kappa pq(1+\kappa)}{1+pq}}\mu\left|\cos\theta\right|\frac{r}{\hat{r}}\right) \\
& \times \operatorname{sech}\left(2\sqrt{\frac{\kappa(1+\kappa)}{1+pq}}\mu\sin\theta\frac{r}{\hat{r}}\right)\operatorname{sech}\left(2\sqrt{\frac{\kappa pq(1+\kappa)}{1+pq}}\mu\cos\theta\frac{r}{\hat{r}}\right) \\
& \times \exp\left(2\sqrt{\frac{\kappa(1+\kappa)}{1+pq}}\mu\left(\sin\theta+\sqrt{pq}\cos\theta\right)\frac{r}{\hat{r}}-(1+\kappa)\mu\frac{r^2}{\hat{r}^2}\right) \\
& \times \exp\left(-\frac{(1+\kappa)\mu\dot{\theta}^2r^2}{2\pi^2f_m^2\hat{r}^2}-\kappa\mu\right). \qquad (4.39)
\end{aligned}
$$

Now, by integrating (4.37) or (4.38) in terms of $\dot{\Theta}$ or Θ, respectively, the joint PDF of R and $\dot{R}$, mapped in [60], is determined as

$$
\begin{aligned}
f_{R,\dot{R}}(r,\dot{r}) = {} & \frac{\sqrt{2}\mu^{\frac{3}{2}}\kappa^{\frac{1-\mu}{2}}(1+\kappa)^{1+\frac{\mu}{2}}r^{\mu}}{\pi^{\frac{3}{2}}f_m\hat{r}^{\mu+2}}\exp\left(-\frac{(1+\kappa)\mu\dot{r}^2}{2\pi^2f_m^2\hat{r}^2}-(1+\kappa)\mu\frac{r^2}{\hat{r}^2}-\kappa\mu\right) \\
& \times I_{\mu-1}\left(2\sqrt{\kappa(1+\kappa)}\mu\frac{r}{\hat{r}}\right). \qquad (4.40)
\end{aligned}
$$

Also, with either (4.37) or (4.39), the joint PDF of R and $\dot{\Theta}$ can be calculated as observed in [45, Eq. (35)],

$$
\begin{aligned}
f_{R,\dot{\Theta}}(r,\dot{\theta}) = {} & \frac{\sqrt{2}\mu^{\frac{3}{2}}\kappa^{\frac{1-\mu}{2}}(1+\kappa)^{1+\frac{\mu}{2}}r^{\mu+1}}{\pi^{\frac{3}{2}}f_m\hat{r}^{\mu+2}}\exp\left(-\frac{(1+\kappa)\mu\dot{\theta}^2r^2}{2\pi^2f_m^2\hat{r}^2}-(1+\kappa)\mu\frac{r^2}{\hat{r}^2}-\kappa\mu\right) \\
& \times I_{\mu-1}\left(2\sqrt{\kappa(1+\kappa)}\mu\frac{r}{\hat{r}}\right). \qquad (4.41)
\end{aligned}
$$

Another interesting outcome is observed with the integration of either (4.38) or (4.39), in terms of $\dot{R}$ and $\dot{\Theta}$, respectively, which result exactly in the joint phase-envelope PDF derived earlier in (4.11).

4.4.4 Phase Crossing Rate - Exact Solution

As defined in the previous chapter, phase crossing rate characterizes random variations of the phase of the faded signal. The PCR is calculated through the following expression,

$$
N_\Theta(\theta) = \int_0^\infty \dot{\theta} f_{\Theta,\dot{\Theta}}(\theta,\dot{\theta})\,\mathrm{d}\dot{\theta}, \qquad (4.42)
$$

in which $f_{\Theta,\dot{\Theta}}(\theta,\dot{\theta})$ denotes the joint PDF of the phase and its corresponding time derivative. Theoretically, this PDF is obtained after integrating (4.39). However, no closed-form expression is found for $f_{\Theta,\dot{\Theta}}(\theta,\dot{\theta})$. Thus, with (4.39), the PCR is formulated as follows

$$N_\Theta(\theta) = \int_0^\infty \dot{\theta} \int_0^\infty f_{R,\Theta,\dot{\Theta}}(r,\theta,\dot{\theta})\,\mathrm{d}r\,\mathrm{d}\dot{\theta}. \tag{4.43}$$

In order to reduce computational strain, the integration sequence in (4.43) can be switched, rewriting the PCR as

$$N_\Theta(\theta) = \int_0^\infty \int_0^\infty \dot{\theta} f_{R,\Theta,\dot{\Theta}}(r,\theta,\dot{\theta})\,\mathrm{d}\dot{\theta}\,\mathrm{d}r. \tag{4.44}$$

From (4.44), let us define an auxiliary function given below as

$$\begin{aligned}
N_{R,\Theta}(r,\theta) &= \int_0^\infty \dot{\theta} f_{R,\Theta,\dot{\Theta}}(r,\theta,\dot{\theta})\,\mathrm{d}\dot{\theta} \\
&= \frac{\sqrt{\pi} f_m \mu^{\frac{3}{2}} \kappa^{1-\frac{\mu}{2}} (1+\kappa)^{\frac{\mu+1}{2}} (pq)^{\frac{1}{2}-\frac{\mu p}{2(1+p)}}}{\sqrt{2}(1+pq)^{1-\frac{\mu}{2}}} |\sin\theta|^{\frac{\mu}{p+1}} |\cos\theta|^{\frac{\mu p}{p+1}} \frac{r^\mu}{\hat{r}^{\mu+1}} \\
&\quad \times I_{\frac{\mu}{p+1}-1}\left(2\sqrt{\frac{\kappa(1+\kappa)}{1+pq}}\mu\,|\sin\theta|\,\frac{r}{\hat{r}}\right) I_{\frac{\mu p}{p+1}-1}\left(2\sqrt{\frac{\kappa pq(1+\kappa)}{1+pq}}\mu\,|\cos\theta|\,\frac{r}{\hat{r}}\right) \\
&\quad \times \operatorname{sech}\left(2\sqrt{\frac{\kappa(1+\kappa)}{1+pq}}\mu\sin\theta\frac{r}{\hat{r}}\right) \operatorname{sech}\left(2\sqrt{\frac{\kappa pq(1+\kappa)}{1+pq}}\mu\cos\theta\frac{r}{\hat{r}}\right) \\
&\quad \times \exp\left(2\sqrt{\frac{\kappa(1+\kappa)}{1+pq}}\mu\left(\sin\theta+\sqrt{pq}\cos\theta\right)\frac{r}{\hat{r}} - (1+\kappa)\mu\frac{r^2}{\hat{r}^2} - \kappa\mu\right).
\end{aligned} \tag{4.45}$$

Hence, replacing (4.45) in (4.44), the Extended κ-μ PCR is solved as

$$\begin{aligned}
N_\Theta(\theta) &= \int_0^\infty N_{R,\Theta}(r,\theta)\,\mathrm{d}r \\
&= \frac{\sqrt{\pi} f_m \mu^{\frac{3}{2}} \kappa^{1-\frac{\mu}{2}} (1+\kappa)^{\frac{\mu+1}{2}} (pq)^{\frac{1}{2}-\frac{\mu p}{2(1+p)}}}{\sqrt{2}(1+pq)^{1-\frac{\mu}{2}} \hat{r}^{\mu+1} \exp(\kappa\mu)} |\sin\theta|^{\frac{\mu}{p+1}} |\cos\theta|^{\frac{\mu p}{p+1}} \\
&\quad \times \int_0^\infty r^\mu I_{\frac{\mu}{p+1}-1}\left(2\sqrt{\frac{\kappa(1+\kappa)}{1+pq}}\mu\,|\sin\theta|\,\frac{r}{\hat{r}}\right) I_{\frac{\mu p}{p+1}-1}\left(2\sqrt{\frac{\kappa pq(1+\kappa)}{1+pq}}\mu\,|\cos\theta|\,\frac{r}{\hat{r}}\right) \\
&\quad \times \operatorname{sech}\left(2\sqrt{\frac{\kappa(1+\kappa)}{1+pq}}\mu\sin\theta\frac{r}{\hat{r}}\right) \operatorname{sech}\left(2\sqrt{\frac{\kappa pq(1+\kappa)}{1+pq}}\mu\cos\theta\frac{r}{\hat{r}}\right) \\
&\quad \times \exp\left(2\sqrt{\frac{\kappa(1+\kappa)}{1+pq}}\mu\left(\sin\theta+\sqrt{pq}\cos\theta\right)\frac{r}{\hat{r}} - (1+\kappa)\mu\frac{r^2}{\hat{r}^2}\right)\mathrm{d}r.
\end{aligned} \tag{4.46}$$

As expected, when $p = 1$, (4.46) reduce to the balanced case presented in [45, Eq. (44)].

Here again, the limits of q can be explored for (4.45) wherein for $q \to 0$ and

$q \to \infty$ the following equations are calculated

$$
\begin{aligned}
N_{R,\Theta}(r,\theta)_{q\to 0} = {} & \frac{\sqrt{\pi} f_m \mu^{\frac{1}{2}+\frac{\mu p}{1+p}} \kappa^{\frac{1}{2}-\frac{\mu}{2(1+p)}} (1+\kappa)^{\frac{\mu}{2}+\frac{\mu p}{2(1+p)}}}{\sqrt{2}\Gamma\left(\frac{\mu p}{1+p}\right)} |\sin\theta|^{\frac{\mu}{p+1}} |\cos\theta|^{\frac{2\mu p}{p+1}-1} \frac{r^{\mu+\frac{\mu p}{1+p}-1}}{\hat{r}^{\mu+\frac{\mu p}{1+p}}} \\
& \times I_{\frac{\mu}{p+1}-1}\left(2\sqrt{\kappa(1+\kappa)}\mu\,|\sin\theta|\,\frac{r}{\hat{r}}\right) \operatorname{sech}\left(2\sqrt{\kappa(1+\kappa)}\mu\sin\theta\frac{r}{\hat{r}}\right) \\
& \times \exp\left(2\sqrt{\kappa(1+\kappa)}\mu\sin\theta\frac{r}{\hat{r}} - (1+\kappa)\mu\frac{r^2}{\hat{r}^2} - \kappa\mu\right)
\end{aligned} \tag{4.47}
$$

and

$$
\begin{aligned}
N_{R,\Theta}(r,\theta)_{q\to \infty} = {} & \frac{\sqrt{\pi} f_m \mu^{\frac{1}{2}+\frac{\mu}{1+p}} \kappa^{\frac{1}{2}-\frac{\mu p}{2(1+p)}} (1+\kappa)^{\frac{\mu}{2}+\frac{\mu}{2(1+p)}}}{\sqrt{2}\Gamma\left(\frac{\mu}{1+p}\right)} |\sin\theta|^{\frac{2\mu}{p+1}-1} |\cos\theta|^{\frac{\mu p}{p+1}} \frac{r^{\mu+\frac{\mu}{1+p}-1}}{\hat{r}^{\mu+\frac{\mu}{1+p}}} \\
& \times I_{\frac{\mu p}{p+1}-1}\left(2\sqrt{\kappa(1+\kappa)}\mu\,|\cos\theta|\,\frac{r}{\hat{r}}\right) \operatorname{sech}\left(2\sqrt{\kappa(1+\kappa)}\mu\cos\theta\frac{r}{\hat{r}}\right) \\
& \times \exp\left(2\sqrt{\kappa(1+\kappa)}\mu\cos\theta\frac{r}{\hat{r}} - (1+\kappa)\mu\frac{r^2}{\hat{r}^2} - \kappa\mu\right).
\end{aligned} \tag{4.48}
$$

4.4.5 Phase Crossing Rate - Approximate Solution

The method employed earlier to approximate the phase distribution is really interesting and with proper handling can be used to explore an uncountable number of different cases. As can be seen, both (4.11) and (4.45) are quite similar, which turns the latter an excellent candidate for the approximation procedure developed in [45].

For comprehensiveness, a concise explanation of the approximation method is here given. From (4.46), the integral can be divided in two intervals, i.e. 0 to 1, and 1 to infinity, as in (4.49a). Next, by applying $r = 1/y$ at the second integrand, the interval is replaced from 1 to 1, and from infinity to 0, as observed in (4.49b). Finally, switching back $y = r$, the whole integral can be grouped under the same interval as the auxiliary function $v(r,\theta)$, in (4.49c).

$$
\begin{aligned}
N_\Theta(\theta) &= \int_0^1 N_{R,\Theta}(r,\theta)\,\mathrm{d}r + \int_1^\infty N_{R,\Theta}(r,\theta)\,\mathrm{d}r && \text{(4.49a)} \\
&= \int_0^1 N_{R,\Theta}(r,\theta)\,\mathrm{d}r + \int_0^1 \frac{N_{R,\Theta}(\frac{1}{y},\theta)}{y^2}\,\mathrm{d}y && \text{(4.49b)} \\
&= \int_0^1 v(r,\theta)\,\mathrm{d}r && \text{(4.49c)}
\end{aligned}
$$

Then, we Taylor expand (4.49c) around $a = 1$ and for $n = 1$, resulting in

$$\begin{aligned} v(r,\theta) = {} & \frac{\sqrt{\pi} f_m \mu^{\frac{3}{2}} \kappa^{1-\frac{\mu}{2}} (1+\kappa)^{\frac{\mu+1}{2}} (pq)^{\frac{1}{2}-\frac{\mu p}{2(1+p)}}}{\sqrt{2}(1+pq)^{1-\frac{\mu}{2}}} |\sin\theta|^{\frac{\mu}{p+1}} |\cos\theta|^{\frac{\mu p}{p+1}} \frac{(2-r)}{\hat{r}^{\mu+1}} \\ & \times I_{\frac{\mu}{p+1}-1}\left(2\sqrt{\frac{\kappa(1+\kappa)}{1+pq}}\mu|\sin\theta|\frac{1}{\hat{r}}\right) I_{\frac{\mu p}{p+1}-1}\left(2\sqrt{\frac{\kappa pq(1+\kappa)}{1+pq}}\mu|\cos\theta|\frac{1}{\hat{r}}\right) \\ & \times \operatorname{sech}\left(2\sqrt{\frac{\kappa(1+\kappa)}{1+pq}}\mu\sin\theta\frac{1}{\hat{r}}\right) \operatorname{sech}\left(2\sqrt{\frac{\kappa pq(1+\kappa)}{1+pq}}\mu\cos\theta\frac{1}{\hat{r}}\right) \\ & \times \exp\left(2\sqrt{\frac{\kappa(1+\kappa)}{1+pq}}\mu\left(\sin\theta+\sqrt{pq}\cos\theta\right)\frac{1}{\hat{r}} - (1+\kappa)\mu\frac{1}{\hat{r}^2} - \kappa\mu\right). \end{aligned} \tag{4.50}$$

By solving the integral of (4.50) with respect to R leads to $V(\theta)$ as in

$$\begin{aligned} V(\theta) = {} & \frac{3\sqrt{\pi} f_m \mu^{\frac{3}{2}} \kappa^{1-\frac{\mu}{2}} (1+\kappa)^{\frac{\mu+1}{2}} (pq)^{\frac{1}{2}-\frac{\mu p}{2(1+p)}}}{\sqrt{2}(1+pq)^{1-\frac{\mu}{2}}} |\sin\theta|^{\frac{\mu}{p+1}} |\cos\theta|^{\frac{\mu p}{p+1}} \frac{1}{\hat{r}^{\mu+1}} \\ & \times I_{\frac{\mu}{p+1}-1}\left(2\sqrt{\frac{\kappa(1+\kappa)}{1+pq}}\mu|\sin\theta|\frac{1}{\hat{r}}\right) I_{\frac{\mu p}{p+1}-1}\left(2\sqrt{\frac{\kappa pq(1+\kappa)}{1+pq}}\mu|\cos\theta|\frac{1}{\hat{r}}\right) \\ & \times \operatorname{sech}\left(2\sqrt{\frac{\kappa(1+\kappa)}{1+pq}}\mu\sin\theta\frac{1}{\hat{r}}\right) \operatorname{sech}\left(2\sqrt{\frac{\kappa pq(1+\kappa)}{1+pq}}\mu\cos\theta\frac{1}{\hat{r}}\right) \\ & \times \exp\left(2\sqrt{\frac{\kappa(1+\kappa)}{1+pq}}\mu\left(\sin\theta+\sqrt{pq}\cos\theta\right)\frac{1}{\hat{r}} - (1+\kappa)\mu\frac{1}{\hat{r}^2} - \kappa\mu\right). \end{aligned} \tag{4.51}$$

Still, for normalization purposes, all terms not related to θ are removed from (4.51), leading to

$$\begin{aligned} V^*(\theta) = {} & |\sin\theta|^{\frac{\mu}{p+1}} |\cos\theta|^{\frac{\mu p}{p+1}} \\ & \times I_{\frac{\mu}{p+1}-1}\left(2\sqrt{\frac{\kappa(1+\kappa)}{1+pq}}\mu|\sin\theta|\right) I_{\frac{\mu p}{p+1}-1}\left(2\sqrt{\frac{\kappa pq(1+\kappa)}{1+pq}}\mu|\cos\theta|\right) \\ & \times \operatorname{sech}\left(2\sqrt{\frac{\kappa(1+\kappa)}{1+pq}}\mu\sin\theta\right) \operatorname{sech}\left(2\sqrt{\frac{\kappa pq(1+\kappa)}{1+pq}}\mu\cos\theta\right) \\ & \times \exp\left(2\sqrt{\frac{\kappa(1+\kappa)}{1+pq}}\mu\left(\sin\theta+\sqrt{pq}\cos\theta\right)\right). \end{aligned} \tag{4.52}$$

Now, as before, the normalization has to match the same area under the exact PCR and $V^*(\theta)$. For such, both (4.46) and (4.52) have to be integrated over the interval $-\pi$ and π. The latter has been previously calculated in (4.26), and the former shall be carried out as follows. First, let the area of the exact PDF be defined as

$$\begin{aligned} A_{PCR} &= \int_{-\pi}^{\pi} N_\Theta(\theta)\,\mathrm{d}\theta \\ &= \int_{-\pi}^{\pi}\int_0^\infty N_{R,\Theta}(r,\theta)\,\mathrm{d}r\,\mathrm{d}\theta, \end{aligned} \tag{4.53}$$

wherein $N_{R,\Theta}(r,\theta)$ is represented by (4.45). Then, by switching the integrals, (4.53) can be rewritten as

$$A_{PCR} = \int_0^\infty \int_{-\pi}^{\pi} N_{R,\Theta}(r,\theta)\,\mathrm{d}\theta\,\mathrm{d}r. \tag{4.54}$$

Solving the inner integral of (4.54) with the mathematical identity in (4.14), we have that

$$\begin{aligned}\int_{-\pi}^{\pi} N_{R,\Theta}(r,\theta)\,\mathrm{d}\theta = \sqrt{2\pi} f_m \mu^{\frac{1}{2}} \kappa^{\frac{1-\mu}{2}} (1+\kappa)^{\frac{\mu}{2}} \frac{r^{\mu-1}}{\hat{r}^{\mu}} \exp\left(-(1+\kappa)\mu\frac{r^2}{\hat{r}^2} - \kappa\mu\right) \\ \times I_{\mu-1}\left(2\sqrt{\kappa(1+\kappa)}\mu\frac{r}{\hat{r}}\right). \end{aligned} \tag{4.55}$$

Having (4.55), the area of the exact PCR is expressed in

$$A_{PCR} = \sqrt{\frac{\pi}{2}} f_m \Gamma\left(\mu - \frac{1}{2}\right) {}_1\tilde{F}_1\left(\frac{1}{2}; \mu; -\kappa\mu\right), \tag{4.56}$$

with $\mu > 1/2$, and with ${}_1\tilde{F}_1\left(a;b;z\right) = {}_1F_1(a;b;z)/\Gamma\left(b\right)$ indicating the regularized notation of the Kummer confluent hypergeometric function [1, Eq. (13.1.2)].

Finally, the approximate PCR, namely $N_{\mathbb{O}}(\theta)$, is formalized as

$$N_{\mathbb{O}}(\theta) = \frac{A_{PCR}}{A} V^*(\theta). \tag{4.57}$$

Replacing (4.26), (4.52) and (4.56) in (4.57), we have the Extended κ-μ approximate PCR given as

$$\begin{aligned} N_{\mathbb{O}}(\theta) = & \frac{\sqrt{\pi} f_d \sqrt{\kappa(1+\kappa)}\mu\Gamma\left(\mu-\frac{1}{2}\right)(pq)^{\frac{1}{2}-\frac{\mu p}{2(1+p)}}}{\sqrt{2}(1+pq)^{1-\frac{\mu}{2}} I_{\mu-1}\left(2\sqrt{\kappa(1+\kappa)}\mu\right)} \left|\sin\theta\right|^{\frac{\mu}{p+1}} \left|\cos\theta\right|^{\frac{\mu p}{p+1}} \\ & \times I_{\frac{\mu}{p+1}-1}\left(2\sqrt{\frac{\kappa(1+\kappa)}{1+pq}}\mu\left|\sin\theta\right|\right) I_{\frac{\mu p}{p+1}-1}\left(2\sqrt{\frac{\kappa pq(1+\kappa)}{1+pq}}\mu\left|\cos\theta\right|\right) \\ & \times \ \mathrm{sech}\left(2\sqrt{\frac{\kappa(1+\kappa)}{1+pq}}\mu\sin\theta\right) \mathrm{sech}\left(2\sqrt{\frac{\kappa pq(1+\kappa)}{1+pq}}\mu\cos\theta\right) \\ & \times \ \exp\left(2\sqrt{\frac{\kappa(1+\kappa)}{1+pq}}\mu\left(\sin\theta + \sqrt{pq}\cos\theta\right)\right) {}_1\tilde{F}_1\left(\frac{1}{2};\mu;-\kappa\mu\right). \end{aligned} \tag{4.58}$$

As observed earlier, in the limits $q \to 0$ and $q \to \infty$, the approximate PCR can be evaluated, respectively, as

$$\begin{aligned} N_{\mathbb{O}}(\theta)_{q\to 0} = & \frac{\sqrt{\pi} f_m \Gamma\left(\mu - \frac{1}{2}\right)\left(\sqrt{\kappa(1+\kappa)}\mu\right)^{\frac{\mu p}{p+1}}}{\sqrt{2}\Gamma\left(\frac{\mu p}{p+1}\right)} \left|\sin\theta\right|^{\frac{\mu}{p+1}} \left|\cos\theta\right|^{\frac{2\mu p}{p+1}-1} \\ & \times \ \mathrm{sech}\left(2\sqrt{\kappa(1+\kappa)}\mu\sin\theta\right)\exp\left(2\sqrt{\kappa(1+\kappa)}\mu\sin\theta\right) \\ & \times \frac{I_{\frac{\mu}{p+1}-1}\left(2\sqrt{\kappa(1+\kappa)}\mu\left|\sin\theta\right|\right) {}_1\tilde{F}_1\left(\frac{1}{2};\mu;-\kappa\mu\right)}{I_{\mu-1}\left(2\sqrt{\kappa(1+\kappa)}\mu\right)} \end{aligned} \tag{4.59}$$

and

$$N_{\mathbb{O}}(\theta)_{q\to\infty} = \frac{\sqrt{\pi} f_m \left(\sqrt{\kappa(1+\kappa)}\right)^{\frac{\mu}{p+1}} \mu\Gamma\left(\mu-\frac{1}{2}\right)}{\sqrt{2}\Gamma\left(\frac{\mu}{p+1}\right)} |\sin\theta|^{\frac{2\mu}{p+1}-1} |\cos\theta|^{\frac{\mu p}{p+1}}$$
$$\times \operatorname{sech}(2\sqrt{\kappa(1+\kappa)}\mu\cos\theta)\exp\left(2\sqrt{\kappa(1+\kappa)}\mu\cos\theta\right)$$
$$\times \frac{I_{\frac{\mu p}{p+1}-1}\left(2\sqrt{\kappa(1+\kappa)}\mu\,|\cos\theta|\right)\, {}_1\tilde{F}_1\left(\frac{1}{2};\mu;-\kappa\mu\right)}{I_{\mu-1}\left(2\sqrt{\kappa(1+\kappa)}\mu\right)}. \tag{4.60}$$

Figure 4.4 compares different cluster imbalance scenarios for the exact and approximate PCR of the Extended κ-μ model. As observed earlier, p affects directly the behavior of the PCR, promoting new exploitable settings. As far as the comparison goes, the closeness between both exact and approximate solution is a bit larger, if confronted with the PDF cases. However, when analyzing the whole, the closed-form approximation is still an excellent asset to portray Extended κ-μ PCR statistics.

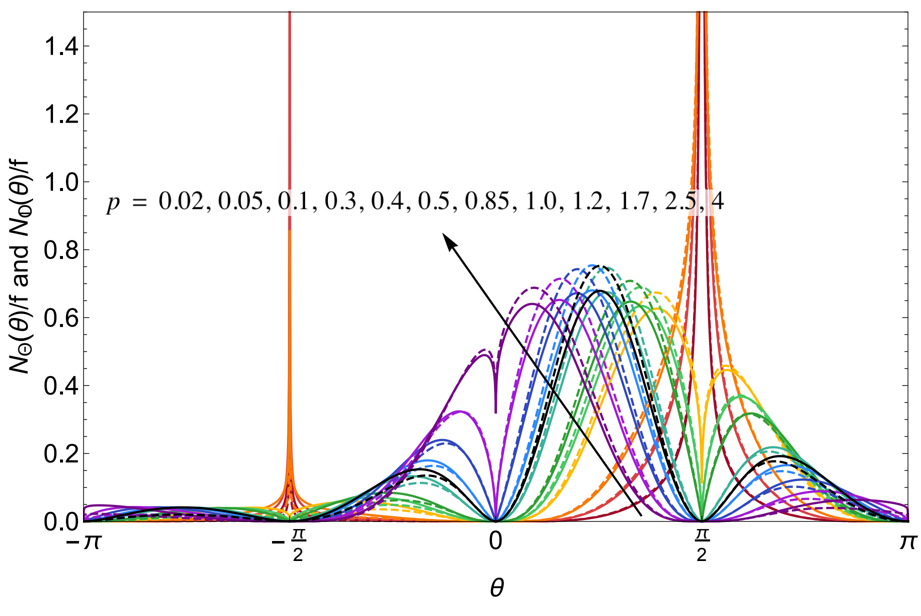

Figure 4.4: Exact (solid lines) and approximate (dashed lines) phase PDF for varying p ($\kappa = 0.1$, $\mu = 2,75$ and $q = 0.70$).

4.5 Particular Cases

This section summarizes some particular case observed throughout the chapter for the Extended κ-μ model.

4.5.1 The κ-μ Distribution

From *all* equations here obtained for the Extended κ-μ model, when $p = 1$ and $q = 1/\tan^2\phi$, the traditional κ-μ statistics arise as in [18] and [45].

4.5.2 Generalized Nakagami-m Distribution

Surprisingly, the Nakagami-m model emerge as an exact particular case of the Extended κ-μ model. Such a feature is attained when $\kappa \to 0$ and $p_\kappa = (1 + p_n)/(1 - p_n)$, wherein p_κ and p_n stand for the p parameter for either κ-μ and Nakagami-m processes. Astoundingly, these conditions are also valid for both approximate phase PDF and PCR. Bear in mind that $\kappa \to 0$ is dependable of the relation given in (4.15) for small values of the modified Bessel function.

4.5.3 Other Distributions

When it comes to the approximate phase distribution, as reported in [45], by setting $\mu = 1$ and $p = 1$, the exact von Mises distribution is obtained, which works as very close approximation of the Rice phase distribution.

4.5.4 New Phase Distribution

As remarked earlier, the approximate solution here derived is a true phase PDF, with random variable $\mathbb{O}$. Hence, its special cases include the generalized Nakagami-m process and the Von Mises distribution. Also, when $q \to 0$ or $q \to \infty$, two new phase PDF arise, as described before.

4.6 Conclusion

In this chapter, an extension to the original κ-μ fading model is introduced. For this, a new parameter is defined as the quantification of the number of multipath clusters in both in-phase and quadrature signals. Unlike the Extended η-μ model, the phase distribution was the only statistic affected by such parameter. Therefore, using the original κ-μ envelope PDF, new mathematical identities emerged from this process. In order to favour further phase studies, an approximate formulation for its statistics were also proposed. The method behind the expression was developed by [45], and its use lead to an incredible accuracy as compared to the exact phase PDF. Furthermore, higher order statistics were derived, which includes several new formulations and an exact approach for the phase crossing rate. Here as well, an approximate solution was carried out, leading to an excellent expression which holds most properties of the exact PCR. Finally, the approximate phase distribution of the Extended κ-μ model was derived to behave as a true PDF and, hence, it was identified as a new phase distribution with random variable $\mathbb{O}$. It is indisputable that the Extended κ-μ is a particular case of the very general α-η-κ-μ model.

Chapter 5

Some Miscellaneous Statistics for the α-η-κ-μ Model

The α-η-κ-μ fading model was recently introduced in [19]. It is a very general distribution and was designed to embrace all fading phenomena described in the literature. As a result, the α-η-κ-μ model presents itself with complicated formulations, sometimes only found in integral-form. Due to its flexible nature, the α-η-κ-μ model comprises all established fading distributions, such as Beckmann, Hoyt, Rice, and Nakagami-m.

In [19], the author introduced expressions for the joint phase-envelope PDF, and for the envelope PDF. The former was found in closed-form. For the latter, the author had to resort to an envelope-based approach, leading to a recursive series formulation. Recursive functions are not very handy, and despite its achievable convergence, they are greatly dependent on the parameters. Hence, it is convenient to find new formulations that render the use of such a flexible model simpler. The phase PDF, on the other hand, was only presented in its integral-form, which hinders any further studies.

In this chapter, an approximate phase PDF is derived by following the same method developed by [45]. For this, a simpler representation of the envelope PDF had to be developed[1].

5.1 Envelope PDF - Series Representation

To implement the new series representation for the envelope PDF, let us first, reconsider its integral-form expression given in (2.70). By taking into account Parametrization-2 and by appropriately substituting (2.65) for either $f_U(u)$ and $f_V(v)$ in (2.70), the

[1]The same result has been obtained independently in da Silva's Ph.D thesis [63].

envelope PDF can be formatted as

$$
\begin{aligned}
f_R(r) =&\ \frac{\alpha\mu^2 p(1+\eta)^2(1+\kappa)^{\frac{\mu}{2}+1}(1+q\eta)^{\frac{\mu}{2}-1}}{\kappa^{\frac{\mu}{2}-1}q^{\frac{\mu p}{2(1+p)}-\frac{1}{2}}\eta^{\frac{\mu p}{2(1+p)}+\frac{1}{2}}(1+p)^2}\exp\left(-\frac{\kappa\mu(1+\eta)(1+pq)}{(1+p)(1+q\eta)}\right) \\
&\times\exp\left(-\frac{\mu p(1+\eta)(1+\kappa)r^\alpha}{\eta(1+p)\hat{r}^\alpha}\right)\frac{r^{\alpha-1}}{\hat{r}^{\alpha\left(\frac{\mu}{2}+1\right)}}\int_0^{r^\alpha} v^{\frac{1}{2}\left(\frac{\mu}{1+p}-1\right)}\left(r^\alpha-v\right)^{\frac{1}{2}\left(\frac{p\mu}{1+p}-1\right)} \\
&\times I_{\frac{\mu}{1+p}-1}\left(\frac{2\mu(1+\eta)}{(1+p)}\sqrt{\frac{\kappa(1+\kappa)v}{(1+q\eta)\hat{r}^\alpha}}\right)I_{\frac{\mu p}{1+p}-1}\left(\frac{2\mu p(1+\eta)}{(1+p)}\sqrt{\frac{\kappa q(1+\kappa)\left(r^\alpha-v\right)}{\eta(1+q\eta)\hat{r}^\alpha}}\right) \\
&\times\exp\left(-\frac{\mu(\eta-p)(1+\eta)(1+\kappa)v}{\eta(1+p)\hat{r}^\alpha}\right)\mathrm{d}v. \qquad (5.1)
\end{aligned}
$$

Now, the Bessel functions in (5.1) can be expanded as in [1, Eq. (9.6.10)], leading to the double summation equation, i.e.

$$
\begin{aligned}
f_R(r) =&\ \frac{\alpha\mu^2 p(1+\eta)^2(1+\kappa)^{\frac{\mu}{2}+1}(1+q\eta)^{\frac{\mu}{2}-1}}{\kappa^{\frac{\mu}{2}-1}q^{\frac{\mu p}{2(1+p)}-\frac{1}{2}}\eta^{\frac{\mu p}{2(1+p)}+\frac{1}{2}}(1+p)^2}\exp\left(-\frac{\kappa\mu(1+\eta)(1+pq)}{(1+p)(1+q\eta)}\right) \\
&\times\exp\left(-\frac{\mu p(1+\eta)(1+\kappa)r^\alpha}{\eta(1+p)\hat{r}^\alpha}\right)\frac{r^{\alpha-1}}{\hat{r}^{\alpha\left(\frac{\mu}{2}+1\right)}}\int_0^{r^\alpha} v^{\frac{1}{2}\left(\frac{\mu}{1+p}-1\right)}\left(r^\alpha-v\right)^{\frac{1}{2}\left(\frac{p\mu}{1+p}-1\right)} \\
&\times\sum_{i=0}^{\infty}\frac{1}{i!\Gamma\left(\frac{\mu}{1+p}+i\right)}\left(\frac{\mu(1+\eta)}{(1+p)}\sqrt{\frac{\kappa(1+\kappa)v}{(1+q\eta)\hat{r}^\alpha}}\right)^{2i+\frac{\mu}{1+p}-1} \\
&\times\sum_{j=0}^{\infty}\frac{1}{j!\Gamma\left(\frac{\mu p}{1+p}+j\right)}\left(\frac{\mu p(1+\eta)}{(1+p)}\sqrt{\frac{\kappa q(1+\kappa)\left(r^\alpha-v\right)}{\eta(1+q\eta)\hat{r}^\alpha}}\right)^{2j+\frac{\mu p}{1+p}-1} \\
&\times\exp\left(-\frac{\mu(\eta-p)(1+\eta)(1+\kappa)v}{\eta(1+p)\hat{r}^\alpha}\right)\mathrm{d}v. \qquad (5.2)
\end{aligned}
$$

Then, by switching the order of the integration with both summation operators, the equation is rearranged as

$$
\begin{aligned}
f_R(r) =&\ \frac{\alpha\mu^\mu p^{\frac{\mu p}{1+p}}(1+\eta)^\mu(1+\kappa)^\mu}{\eta^{\frac{\mu p}{1+p}}(1+p)^\mu}\exp\left(-\frac{\kappa\mu(1+\eta)(1+pq)}{(1+p)(1+q\eta)}-\frac{\mu p(1+\eta)(1+\kappa)r^\alpha}{\eta(1+p)\hat{r}^\alpha}\right) \\
&\times\frac{r^{\alpha-1}}{\hat{r}^{\alpha\mu}}\sum_{i=0}^{\infty}\sum_{j=0}^{\infty}\frac{\left(\frac{p^2 q}{\eta}\right)^j}{i!j!\Gamma\left(\frac{\mu}{1+p}+i\right)\Gamma\left(\frac{\mu p}{1+p}+j\right)}\left(\frac{\kappa\mu^2(1+\eta)^2(1+\kappa)}{(1+p)^2(1+q\eta)\hat{r}^\alpha}\right)^{i+j} \\
&\times\int_0^{r^\alpha} v^{i+\frac{\mu}{1+p}-1}\left(r^\alpha-v\right)^{j+\frac{p\mu}{1+p}-1}\exp\left(-\frac{\mu(\eta-p)(1+\eta)(1+\kappa)v}{\eta(1+p)\hat{r}^\alpha}\right)\mathrm{d}v. \qquad (5.3)
\end{aligned}
$$

The integral can now be solved, resulting in

$$
\begin{aligned}
f_R(r) =&\ \frac{\alpha\mu^\mu p^{\frac{\mu p}{1+p}}(1+\eta)^\mu(1+\kappa)^\mu}{\eta^{\frac{\mu p}{1+p}}(1+p)^\mu}\exp\left(-\frac{\kappa\mu(1+\eta)(1+pq)}{(1+p)(1+q\eta)}-\frac{\mu p(1+\eta)(1+\kappa)r^\alpha}{\eta(1+p)\hat{r}^\alpha}\right) \\
&\times\frac{r^{\alpha\mu-1}}{\hat{r}^{\alpha\mu}}\sum_{i=0}^{\infty}\sum_{j=0}^{\infty}\frac{1}{i!j!}\left(\frac{p^2 q}{\eta}\right)^j\left(\frac{\kappa\mu^2(1+\eta)^2(1+\kappa)r^\alpha}{(1+p)^2(1+q\eta)\hat{r}^\alpha}\right)^{i+j} \\
&\times{}_1\tilde{F}_1\left(k+\frac{\mu}{1+p};\mu+i+j;\frac{\mu(p-\eta)(1+\eta)(1+\kappa)r^\alpha}{\eta(1+p)\hat{r}^\alpha}\right), \qquad (5.4)
\end{aligned}
$$

wherein ${}_1\tilde{F}_1(a;b;z) = {}_1F_1(a;b;z)/\Gamma(b)$ is the regularized notation of the Kummer confluent hypergeometric function [1, Eq. (13.1.2)].

To enhance comprehensiveness, from (5.4), let us define S as an auxiliary function which contains all the elements involved by the double summation operators, expressed below in

$$S = \sum_{i=0}^{\infty}\sum_{j=0}^{\infty}\frac{1}{i!j!}\left(\frac{p^2q}{\eta}\right)^j\left(\frac{\kappa\mu^2(1+\eta)^2(1+\kappa)r^\alpha}{(1+p)^2(1+q\eta)\hat{r}^\alpha}\right)^{i+j} \times {}_1\tilde{F}_1\left(\frac{\mu}{1+p}+i;\mu+i+j;\frac{\mu(p-\eta)(1+\eta)(1+\kappa)r^\alpha}{\eta(1+p)\hat{r}^\alpha}\right). \tag{5.5}$$

By expanding, the regularized confluent hypergeometric function with [1, Eq. (13.1.2)], (5.5) is rewritten as

$$S = \sum_{i=0}^{\infty}\sum_{j=0}^{\infty}\sum_{l=0}^{\infty}\frac{1}{i!j!}\left(\frac{p^2q}{\eta}\right)^j\left(\frac{\kappa\mu^2(1+\eta)^2(1+\kappa)r^\alpha}{(1+p)^2(1+q\eta)\hat{r}^\alpha}\right)^{i+j} \times\frac{\left(\frac{\mu}{1+p}+i\right)_l}{\Gamma(\mu+i+j+l)\,l!}\left(\frac{\mu(p-\eta)(1+\eta)(1+\kappa)r^\alpha}{\eta(1+p)\hat{r}^\alpha}\right)^l, \tag{5.6}$$

with $(z)_k$ being the Pochhammer symbol [1, Eq. (6.1.22)].

Equation (5.6) can be reorganized by swapping the summation operators of index j and l, and by introducing ${}_0\tilde{F}_1(;b;z) = {}_0F_1(;b;z)/\Gamma(b)$, indicating the regularized notation for one particular case of the generalized hypergeometric function [2, Eq. (7.2.3.1)], leading to

$$S = \sum_{i=0}^{\infty}\sum_{l=0}^{\infty}\frac{\left(\frac{\mu}{1+p}+i\right)_l}{i!l!}\left(\frac{\kappa\mu^2(1+\eta)^2(1+\kappa)r^\alpha}{(1+p)^2(1+q\eta)\hat{r}^\alpha}\right)^i\left(\frac{\mu(p-\eta)(1+\eta)(1+\kappa)r^\alpha}{\eta(1+p)\hat{r}^\alpha}\right)^l \times {}_0\tilde{F}_1\left(;\mu+i+l;\frac{\kappa\mu^2p^2q(1+\eta)^2(1+\kappa)r^\alpha}{\eta\left(1+p\right)^2(1+q\eta)\hat{r}^\alpha}\right). \tag{5.7}$$

Then, the Cauchy product of two infinite series, [3, Eq. (0.316)], is applied in (5.7) wherein the original summation indexes are replaced by $i = m$ and $l = n-m$, leading to

$$S = \sum_{n=0}^{\infty}\sum_{m=0}^{n}\frac{\Gamma\left(n+\frac{\mu}{1+p}\right)}{m!(n-m)!\Gamma\left(m+\frac{\mu}{1+p}\right)}\left(\frac{\eta\kappa\mu(1+\eta)}{(1+p)(1+q\eta)(p-\eta)}\right)^m \times\left(\frac{\mu(p-\eta)(1+\eta)(1+\kappa)r^\alpha}{\eta(1+p)\hat{r}^\alpha}\right)^n {}_0\tilde{F}_1\left(;\mu+n;\frac{\kappa\mu^2p^2q(1+\eta)^2(1+\kappa)r^\alpha}{\eta\left(1+p\right)^2(1+q\eta)\hat{r}^\alpha}\right). \tag{5.8}$$

After some algebraic manipulations and with the relation $(-1)^m = (-n)_m/(n-$

$m+1)_m$ [64, Eq. (9)], (5.8) is expressed as

$$S = \sum_{n=0}^{\infty}\sum_{m=0}^{n} \frac{\Gamma\left(n+\frac{\mu}{1+p}\right)(-n)_m}{n!m!\Gamma\left(m+\frac{\mu}{1+p}\right)} \left(\frac{\eta\kappa\mu(1+\eta)}{(1+p)(1+q\eta)(\eta-p)}\right)^m$$
$$\times \left(\frac{\mu(p-\eta)(1+\eta)(1+\kappa)r^{\alpha}}{\eta(1+p)\hat{r}^{\alpha}}\right)^n {}_0\tilde{F}_1\left(;\mu+n;\frac{\kappa\mu^2p^2q(1+\eta)^2(1+\kappa)r^{\alpha}}{\eta\left(1+p\right)^2(1+q\eta)\hat{r}^{\alpha}}\right). \quad (5.9)$$

Finally, by using the definition of the generalized Laguerre polynomial, $L_n^{\lambda}(z)$ [1, Eq. (22.3.9)], (5.9) is given as

$$S = \sum_{n=0}^{\infty} L_n^{\frac{\mu}{1+p}-1}\left(\frac{\eta\kappa\mu(1+\eta)}{(1+p)(1+q\eta)(\eta-p)}\right)\left(\frac{\mu(p-\eta)(1+\eta)(1+\kappa)r^{\alpha}}{\eta(1+p)\hat{r}^{\alpha}}\right)^n$$
$$\times {}_0\tilde{F}_1\left(;\mu+n;\frac{\kappa\mu^2p^2q(1+\eta)^2(1+\kappa)r^{\alpha}}{\eta\left(1+p\right)^2(1+q\eta)\hat{r}^{\alpha}}\right). \quad (5.10)$$

Then, substituting (5.10) back into (5.4), the envelope PDF is elegantly given as follows

$$f_R(r) = \frac{\alpha\mu^{\mu}p^{\frac{\mu p}{1+p}}(1+\eta)^{\mu}(1+\kappa)^{\mu}}{\eta^{\frac{\mu p}{1+p}}(1+p)^{\mu}} \exp\left(-\frac{\kappa\mu(1+\eta)(1+pq)}{(1+p)(1+q\eta)} - \frac{\mu p(1+\eta)(1+\kappa)r^{\alpha}}{\eta(1+p)\hat{r}^{\alpha}}\right)$$
$$\times \frac{r^{\alpha\mu-1}}{\hat{r}^{\alpha\mu}} \sum_{n=0}^{\infty} L_n^{\frac{\mu}{1+p}-1}\left(\frac{\eta\kappa\mu(1+\eta)}{(1+p)(1+q\eta)(\eta-p)}\right)\left(\frac{\mu(p-\eta)(1+\eta)(1+\kappa)r^{\alpha}}{\eta(1+p)\hat{r}^{\alpha}}\right)^n$$
$$\times {}_0\tilde{F}_1\left(;\mu+n;\frac{\kappa\mu^2p^2q(1+\eta)^2(1+\kappa)r^{\alpha}}{\eta\left(1+p\right)^2(1+q\eta)\hat{r}^{\alpha}}\right). \quad (5.11)$$

Curiously, from (5.4), by expanding the regularized hypergeometric function into Bessel functions, the PDF of the α-η-κ-μ fading model can be viewed as the PDF of an α-κ-μ distribution with a linear combination of Bessel functions. Thus, the statistics of the α-η-κ-μ fading model are conjectured to be a linear combination of those of the α-κ-μ distribution.

Analyzing (5.11), it can be seen that the envelope PDF features an indeterminacy when $p=\eta$, and surprisingly, when this condition is met, the series reduces exactly to the PDF of the α-κ-μ fading model, as reported in [19]. In addition, it is important to note that this new equation evaluates substantially faster than any of the formulations presented in [19], and, in general, needs no more than 20 terms for high numerical precision.

Note that from (2.69) and (5.11), a new mathematical identity can be obtained empirically for the sum of generalized Laguerre polynomials and regularized hypergeometric function ${}_0\tilde{F}_1(;b;z)$, given as

$$\int_{-\pi}^{\pi} \exp\left(2a\sqrt{bc}\left(\sin\theta + \sqrt{de}\cos\theta\right) - ab\left(\sin^2\theta + d\cos^2\theta\right)\right)|\sin\theta|^{\alpha}|\cos\theta|^{\beta}$$
$$\times \frac{I_{\alpha-1}\left(2a\sqrt{bc}\,|\sin\theta|\right) I_{\beta-1}\left(2a\sqrt{bcde}\,|\cos\theta|\right)}{\cosh\left(2a\sqrt{bc}\,|\sin\theta|\right)\cosh\left(2a\sqrt{bcde}\,|\cos\theta|\right)}\mathrm{d}\theta = 2\exp\left(-abd\right)a^{\alpha+\beta-2}(bc)^{\frac{\alpha+\beta}{2}-1}$$
$$\times (de)^{\frac{\beta-1}{2}}\sum_{n=0}^{\infty}\left(ab(d-1)\right)^n L_n^{\alpha-1}\left(\frac{ac}{(1-d)}\right) {}_0\tilde{F}_1\left(;\alpha+\beta+n;a^2bcde\right), \quad (5.12)$$

wherein $a > 0$, $b > 0$, $c > 0$, $d > 0$, $e > 0$, $\alpha > 0$ and $\beta > 0$ are Real. To the best of the author's knowledge, the identity in (5.12) is new and encompass the identities derived previously in Chapter 4 (Eq. (4.14), (4.16) and (4.17)).

5.2 Special Cases

As reported in Chapter 1, the α-η-κ-μ model has a long list of well-known distributions as special cases. It is also acquainted that a number of other fading scenarios are comprised by α-η-κ-μ that are not yet known in the literature. Here, some new relations are obtained. For this section, let the indexes k and h stand, respectively, for the Extended κ-μ and Extended η-μ parameters.

5.2.1 Extended η-μ and κ-μ Distributions

By setting $\alpha = 2$, $\mu = 2\mu_h$, $\kappa \to 0$, $\eta = \eta_h$, $p = p_h$ and $\hat{r} = \hat{r_h}$, and after cumbersome algebraic manipulations the Extended η-μ model is obtained.

For the Extended κ-μ distribution, the following α-η-κ-μ parameters have to be configured: $\alpha = 2$, $\mu = \mu_k$, $\kappa = \kappa_k$, $\eta = p$, $p = p_k$, $q = q_k$ and $\hat{r} = \hat{r_k}$.

5.2.2 New Distributions

Two new distributions can be obtained by setting $q = 0$ or $q \to \infty$. With $q = 0$, the hypergeometric function disappears leading to an infinite sum of Laguerre polynomials, which can also be rewritten in terms of a confluent double Gaussian series as

$$f_R(r) = \frac{\alpha\exp\left(-\frac{\mu(1+\eta)(1+\kappa)r^{\alpha}}{(1+p)\hat{r}^{\alpha}}\right)}{\exp\left(\frac{\kappa\mu(1+\eta)}{(1+p)}\right)\Gamma(\mu)}\left(\frac{\mu(1+\eta)(1+\kappa)}{1+p}\right)^{\mu}\left(\frac{p}{\eta}\right)^{\frac{\mu p}{(1+p)}}\frac{r^{\alpha\mu-1}}{\hat{r}^{\alpha\mu}}$$
$$\times\phi_3\left(\frac{\mu p}{1+p};\mu;\frac{\mu(1+\eta)(1+\kappa)(\eta-p)r^{\alpha}}{\eta(1+p)\hat{r}^{\alpha}},\frac{\kappa\mu^2(1+\eta)^2(1+\kappa)r^{\alpha}}{(1+p)^2\hat{r}^{\alpha}}\right), \quad (5.13)$$

in which $\phi_3(b;c;w,z)$ is a confluent form of the Appell function [2, Eq. (7.2.4.7)]. This particular function can be computed using

$$\phi_3(\beta;\gamma;x,y) = \lim_{\sigma\to 0}\lim_{\epsilon\to 0} F_1\left(\frac{1}{\epsilon};\beta,\frac{1}{\sigma};\gamma;\epsilon x,\epsilon\sigma y\right), \tag{5.14}$$

in which F_1 is one of the Appell hypergeometric series [2, Eq. (7.2.4.1)]. In Mathematica, the evaluation of (5.14) can render an incorrect outcome, and hence, to overcome this situation, ϵ and σ must be manually set to as close to zero as possible.

A similar approach can be done for $q\to\infty$, resulting in

$$\begin{aligned} f_R(r) = {} & \frac{\alpha \exp\left(-\frac{\mu p(1+\eta)(1+\kappa)r^\alpha}{\eta(1+p)\hat{r}^\alpha}\right)}{\exp\left(\frac{\kappa\mu p(1+\eta)}{\eta(1+p)}\right)\Gamma(\mu)}\left(\frac{\mu(1+\eta)(1+\kappa)}{1+p}\right)^{\mu}\left(\frac{p}{\eta}\right)^{\frac{\mu p}{1+p}}\frac{r^{\alpha\mu-1}}{\hat{r}^{\alpha\mu}} \\ & \times\phi_3\left(\frac{\mu}{1+p};\mu;\frac{\mu(1+\eta)(1+\kappa)(p-\eta)r^\alpha}{\eta(1+p)\hat{r}^\alpha},\frac{\kappa\mu^2p^2(1+\eta)^2(1+\kappa)r^\alpha}{\eta^2(1+p)^2\hat{r}^\alpha}\right). \end{aligned} \tag{5.15}$$

5.3 Phase PDF Approximation

Differently from the envelope PDF, which was already found in series expansion forms, the phase PDF for the α-η-κ-μ fading model was only provided in an integral form. Hence, most phase statistics applications are limited to integral-form formulations, which can be computationally restrictive if performed repeatedly. In [45], the authors developed a clever method to obtain tight closed-form approximation for κ-μ phase distribution. This solution proved to be highly accurate and allowed the authors to derive a very useful and elegant closed-form expression for its phase statistics. Following the approach of [45], a tight approximate solution for the α-η-κ-μ phase PDF is here proposed.

By definition, the phase distribution for the α-η-κ-μ model is given as

$$f_\Theta = \int_0^\infty f_{R,\Theta}(r,\theta)\,\mathrm{d}r, \tag{5.16}$$

with $f_{R,\Theta}(r,\theta)$ being indicated by (2.69).

Now, as before, let us conveniently split the interval of integration in (5.16) as in

$$f_\Theta(\theta) = \int_0^1 f_{R,\Theta}(r,\theta)\,\mathrm{d}r + \int_1^\infty f_{R,\Theta}(r,\theta)\,\mathrm{d}r. \tag{5.17}$$

A change of variable as $r = 1/y$ for the second integral is used, so that $y = 0$ when $r\to\infty$ and $y = 1$ when $r = 1$. Now, y is changed back to r and both integrands are regrouped under the same interval as $h(r,\theta)$,

$$\begin{aligned} f_\Theta(\theta) &= \int_0^1 f_{R,\Theta}(r,\theta) + \frac{f_{R,\Theta}(\frac{1}{r},\theta)}{r^2}\,\mathrm{d}r \\ &= \int_0^1 h(r,\theta)\,\mathrm{d}r. \end{aligned} \tag{5.18}$$

This first set of steps guarantees that after Taylor expanding $h(r,\theta)$ over r, the integral will converge for every truncated versions of the expansion, which is crucial for this method to work. Now, a Taylor expansion of $h(r,\theta)$ about the point $r_0 = 1$ is performed leading to

$$\begin{aligned} h(r,\theta) &= h(1,\theta) + (r-1)h'(1,\theta) \\ &= \frac{\alpha\mu^2 p(1+\eta)^2(1+\kappa)^{\frac{\mu}{2}+1}(1+q\eta)^{\frac{\mu}{2}-1}}{\eta(1+p)^2(q\eta)^{\frac{\mu p}{2(1+p)}-\frac{1}{2}}\kappa^{\frac{\mu}{2}-1}} |\sin\theta|^{\frac{\mu}{1+p}} |\cos\theta|^{\frac{\mu p}{1+p}} \frac{(2-r)}{\hat{r}^{\frac{\alpha}{2}(\mu+2)}} \\ &\quad \times \exp\left(-\frac{(1+\eta)\kappa\mu(1+pq)}{(1+p)(1+q\eta)} - \frac{(1+\eta)(1+\kappa)\mu\left(\eta\sin^2\theta + p\cos^2\theta\right)}{\eta(1+p)}\frac{1}{\hat{r}^\alpha}\right) \\ &\quad \times \exp\left(\frac{2(1+\eta)\mu\cos(\theta-\phi)}{\eta(1+p)}\sqrt{\frac{\eta\kappa(1+\kappa)\left(\eta+p^2q\right)}{1+q\eta}}\frac{1}{\hat{r}^{\frac{\alpha}{2}}}\right) \\ &\quad \times \frac{I_{\frac{\mu}{1+p}-1}\left(\frac{2\mu(1+\eta)|\sin\theta|}{1+p}\sqrt{\frac{\kappa(1+\kappa)}{1+q\eta}}\frac{1}{\hat{r}^{\frac{\alpha}{2}}}\right) I_{\frac{\mu p}{1+p}-1}\left(\frac{2(1+\eta)\mu p|\cos\theta|}{\eta(1+p)}\sqrt{\frac{\eta\kappa q(1+\kappa)}{1+q\eta}}\frac{1}{\hat{r}^{\frac{\alpha}{2}}}\right)}{\cosh\left(\frac{2(1+\eta)\mu|\sin\theta|}{1+p}\sqrt{\frac{\kappa(1+\kappa)}{1+q\eta}}\frac{1}{\hat{r}^{\frac{\alpha}{2}}}\right)\cosh\left(\frac{2\mu p(1+\eta)|\cos\theta|}{\eta(1+p)}\sqrt{\frac{\eta\kappa q(1+\kappa)}{1+q\eta}}\frac{1}{\hat{r}^{\frac{\alpha}{2}}}\right)}. \end{aligned} \tag{5.19}$$

The integral of (5.19) from $r=0$ to $r=1$ is found as

$$\begin{aligned} H(\theta) &= \int_0^1 h(r,\theta)\,\mathrm{d}r \\ &= \frac{3\alpha\mu^2 p(1+\eta)^2(1+\kappa)^{\frac{\mu}{2}+1}(1+q\eta)^{\frac{\mu}{2}-1}}{2\eta(1+p)^2(q\eta)^{\frac{\mu p}{2(1+p)}-\frac{1}{2}}\kappa^{\frac{\mu}{2}-1}} |\sin\theta|^{\frac{\mu}{1+p}} |\cos\theta|^{\frac{\mu p}{1+p}} \frac{1}{\hat{r}^{\frac{\alpha}{2}(\mu+2)}} \\ &\quad \times \exp\left(-\frac{(1+\eta)\kappa\mu(1+pq)}{(1+p)(1+q\eta)} - \frac{(1+\eta)(1+\kappa)\mu\left(\eta\sin^2\theta + p\cos^2\theta\right)}{\eta(1+p)}\frac{1}{\hat{r}^\alpha}\right) \\ &\quad \times \exp\left(\frac{2(1+\eta)\mu\cos(\theta-\phi)}{\eta(1+p)}\sqrt{\frac{\eta\kappa(1+\kappa)\left(\eta+p^2q\right)}{1+q\eta}}\frac{1}{\hat{r}^{\frac{\alpha}{2}}}\right) \\ &\quad \times \frac{I_{\frac{\mu}{1+p}-1}\left(\frac{2\mu(1+\eta)|\sin\theta|}{1+p}\sqrt{\frac{\kappa(1+\kappa)}{1+q\eta}}\frac{1}{\hat{r}^{\frac{\alpha}{2}}}\right) I_{\frac{\mu p}{1+p}-1}\left(\frac{2(1+\eta)\mu p|\cos\theta|}{\eta(1+p)}\sqrt{\frac{\eta\kappa q(1+\kappa)}{1+q\eta}}\frac{1}{\hat{r}^{\frac{\alpha}{2}}}\right)}{\cosh\left(\frac{2(1+\eta)\mu|\sin\theta|}{1+p}\sqrt{\frac{\kappa(1+\kappa)}{1+q\eta}}\frac{1}{\hat{r}^{\frac{\alpha}{2}}}\right)\cosh\left(\frac{2\mu p(1+\eta)|\cos\theta|}{\eta(1+p)}\sqrt{\frac{\eta\kappa q(1+\kappa)}{1+q\eta}}\frac{1}{\hat{r}^{\frac{\alpha}{2}}}\right)}. \end{aligned} \tag{5.20}$$

To obtain a true PDF, (5.20) has to be normalized, thus, it is important to remove the multiplicative terms that are not function of θ and ϕ, leading to $H^*(\theta)$ found as

$$H^{*}(\theta) = |\sin\theta|^{\frac{\mu}{1+p}} |\cos\theta|^{\frac{\mu p}{1+p}} \exp\left(-\frac{\mu(1+\eta)}{\eta(1+p)}\left((1+\kappa)\left(\eta\sin^2\theta + p\cos^2\theta\right)\right)\right)$$
$$\times\exp\left(\frac{\mu(1+\eta)}{\eta(1+p)}\left(2\sqrt{\frac{\eta\kappa(1+\kappa)\left(\eta+p^2q\right)}{1+q\eta}}\cos(\theta-\phi)\right)\right)$$
$$\times\frac{I_{\frac{\mu}{1+p}-1}\left(\frac{2\mu(1+\eta)}{(1+p)}\sqrt{\frac{\kappa(1+\kappa)}{1+q\eta}}|\sin\theta|\right) I_{\frac{\mu p}{1+p}-1}\left(\frac{2\mu p(1+\eta)}{\eta(1+p)}\sqrt{\frac{\eta\kappa q(1+\kappa)}{1+q\eta}}|\cos\theta|\right)}{\cosh\left(\frac{2\mu(1+\eta)}{(1+p)}\sqrt{\frac{\kappa(1+\kappa)}{1+q\eta}}|\sin\theta|\right)\cosh\left(\frac{2\mu p(1+\eta)}{\eta(1+p)\rho^{\alpha/2}}\sqrt{\frac{\eta\kappa q(1+\kappa)}{1+q\eta}}|\cos\theta|\right)}. \tag{5.21}$$

Therefore, the area A of $H^{*}(\theta)$ is defined as

$$A = \int_{-\pi}^{\pi} H^{*}(\theta)\,\mathrm{d}\theta, \tag{5.22}$$

which can be solved with the help of (5.12), leading to

$$A = 2\left(\frac{\mu(1+\eta)}{1+p}\right)^{\mu-2}\left(\frac{\kappa(1+\kappa)}{1+q\eta}\right)^{\frac{\mu}{2}-1}\left(\frac{\eta}{p^2q}\right)^{\frac{1}{2}-\frac{\mu p}{2(1+p)}}\exp\left(-\frac{\mu p(1+\eta)(1+\kappa)}{\eta(1+p)}\right)$$
$$\times\sum_{n=0}^{\infty}\left(\frac{\mu(1+\eta)(1+\kappa)(p-\eta)}{(1+p)\eta}\right)^{n} {}_0\tilde{F}_1\left(;n+\mu;\frac{\kappa\mu^2p^2q(1+\eta)^2(1+\kappa)}{\eta(1+p)^2(1+q\eta)}\right)$$
$$\times L_n^{\frac{\mu}{1+p}-1}\left(\frac{\eta\kappa\mu(1+\eta)}{(1+p)(1+q\eta)(\eta-p)}\right). \tag{5.23}$$

Finally, the approximation for the phase PDF $f_{\tilde{\mathbb{O}}}(\theta)$ is given by $H^{*}(\theta)/A$, or (5.21) divided by (5.23), leading to

$$f_{\tilde{\mathbb{O}}}(\theta) = \frac{2|\sin\theta|^{\frac{2\mu}{1+p}-1}|\cos\theta|^{\frac{2\mu p}{1+p}-1}}{\Gamma\left(\frac{\mu}{1+p}\right)\Gamma\left(\frac{p\mu}{1+p}\right)\left(\exp\left(\frac{4\mu(1+\eta)}{1+p}\sqrt{\frac{\kappa(1+\kappa)}{1+q\eta}}|\sin\theta|\right)+1\right)}$$
$$\times\frac{\exp\left(\frac{\mu(1+\eta)}{\eta(1+p)}\left(2\sqrt{\frac{\eta\kappa(1+\kappa)(\eta+p^2q)}{1+q\eta}}\cos(\theta-\phi)-(1+\kappa)(p-\eta)\cos^2\theta\right)\right)}{\left(\exp\left(\frac{4\mu p(1+\eta)}{\eta(1+p)}\sqrt{\frac{\eta\kappa q(1+\kappa)}{1+q\eta}}|\cos\theta|\right)+1\right)}$$
$$\times\frac{{}_1F_1\left(\frac{\mu}{1+p}-\frac{1}{2};\frac{2\mu}{1+p}-1;\frac{4\mu(1+\eta)}{1+p}\sqrt{\frac{\kappa(1+\kappa)}{1+q\eta}}|\sin\theta|\right)}{\sum_{n=0}^{\infty}\left(\frac{(1+\eta)(1+\kappa)(p-\eta)\mu}{\eta(1+p)}\right)^{n}{}_0\tilde{F}_1\left(;n+\mu;\frac{\kappa\mu^2p^2q(1+\eta)^2(1+\kappa)}{\eta(1+p)^2(1+q\eta)}\right)L_n^{\frac{\mu}{1+p}-1}\left(\frac{\eta\kappa\mu(1+\eta)}{(1+p)(1+q\eta)(\eta-p)}\right)}$$
$$\times{}_1F_1\left(\frac{\mu p}{1+p}-\frac{1}{2};\frac{2\mu p}{1+p}-1;\frac{4\mu p(1+\eta)}{\eta(1+p)}\sqrt{\frac{\eta\kappa q(1+\kappa)}{1+q\eta}}|\cos\theta|\right), \tag{5.24}$$

in which the modified Bessel functions in (5.21) have been replaced by their equivalent Kummer confluent hypergeometric functions, ${}_1F_1(a;b;z)$ [1, Eq. (9.6.47)]. It is important to note that (5.24) maintains all the properties of the exact phase PDF, i.e. minimum and maximum values, even at close values of θ. Also, as indicated previously, (5.24) has unitary area and is non-negative, and therefore, its expression can be used to describe a new PDF of a random variable $\tilde{\mathbb{O}}$.

5.3.1 Special Cases

Interestingly, with proper parameter manipulations, a variety of exact an approximate phase statistics can be obtained from (5.24). From now on, assume that the indexes k, h and n indicate, respectively, the Extended κ-μ, η-μ, and generalized Nakagami-m parameters.

When $\eta \to p_k$ and $p = p_k$, (5.24) reduces in an exact manner to the approximation here derived for the Extended κ-μ phase distribution (4.28). In addition, by making $\kappa \to 0$, $p = (1 + p_n)/(1 - p_n)$, and $\mu = m$, the exact phase distribution for the generalized Nakagami-m model is obtained. Also, for $\eta \to 0$, $\kappa = k$, $\mu = 1$ and $p = 1$, the exact von Mises (Tikhonov) distribution is derived, a strikingly amazing result, already reported in [45].

On the other hand, with $\kappa \to 0$, the generalized Laguerre polynomials reduce to a binomial function [1, Eq. (24.1.1)] with respective coefficients $n + \frac{\mu}{1+p} - 1$ and n, and both hypergeometric functions ${}_1F_1$ and ${}_0\tilde{F}_1$ vanish from (5.24). After proper algebraic manipulation and with $\mu = 2\mu_h$, the Extended η-μ approximate phase PDF is given as

$$f_{\tilde{\Theta}}(\theta) = \frac{\Gamma(2\mu)\exp\left(\frac{2\mu(1+\eta)(p-\eta)}{\eta(1+p)}\sin^2\theta\right)}{2\Gamma\left(\frac{2\mu}{1+p}\right)\Gamma\left(\frac{2\mu p}{1+p}\right)\ {}_1F_1\left(\frac{2\mu}{1+p}; 2\mu; \frac{2\mu(p-\eta)(1+\eta)}{(1+p)\eta}\right)} \left|\sin\theta\right|^{\frac{4\mu}{1+p}-1} \left|\cos\theta\right|^{\frac{4\mu p}{1+p}-1}. \tag{5.25}$$

Impressively, (5.25) renders the exact generalized Nakagami-m phase distribution with $\mu = m/2$, $\eta = (1 + p_n)/(1 - p_n)$ and $p = (1 + p_n)/(1 - p_n)$. Also, by setting $\mu = 0.5$ and $p = 1$, an approximate Hoyt phase distribution can be calculated from (5.25). This incredible outcome is presented below as

$$f_{\tilde{\Theta}}(\theta) = \frac{\exp\left(\frac{(\eta^2-1)}{4\eta}\cos(2\theta)\right)}{2\pi I_0\left(\frac{\eta^2-1}{4\eta}\right)}. \tag{5.26}$$

With no doubt, the formulation in (5.26) is the exact von Mises distribution [65] where $b = (\eta^2 - 1)/(4\eta)$ and $a = -\theta$. This result indicates that both Rice and Hoyt phase PDFs can be approximated by the von Mises model, which is unprecedented in the literature.

Other interesting particular cases arise in the limits where $q \to 0$ and $q \to \infty$. In this scenario, either one of the hypergeometric function ${}_1F_1$ disappears, and as for the generalized Laguerre polynomials and the hypergeometric function ${}_0\tilde{F}_1$, the same procedure proposed in (5.13) or (5.15) is done, leading, respectively, to the equations below

$$\begin{aligned} f_{\tilde{\Theta}}(\theta)_{q\to 0} =& \frac{\Gamma(\mu)}{\Gamma\left(\frac{\mu}{1+p}\right)\Gamma\left(\frac{p\mu}{1+p}\right)} |\sin\theta|^{\frac{2\mu}{1+p}-1} |\cos\theta|^{\frac{2\mu p}{1+p}-1} \exp\left(\frac{\mu(1+\eta)(1+\kappa)(\eta-p)}{\eta(1+p)}\right) \\ &\times \frac{\exp\left(\frac{\mu(1+\eta)}{\eta(1+p)}\left(2\eta\sqrt{\kappa(1+\kappa)}\sin\theta + (1+\kappa)(p-\eta)\sin^2\theta\right)\right)}{\left(\exp\left(\frac{4\mu(1+\eta)}{(1+p)}\sqrt{\kappa(1+\kappa)}\,|\sin\theta|\right)+1\right)} \\ &\times \frac{{}_1F_1\left(\frac{\mu}{1+p}-\frac{1}{2}; \frac{2\mu}{1+p}-1; \frac{4(1+\eta)\mu}{(1+p)}\sqrt{\kappa(1+\kappa)}\,|\sin\theta|\right)}{\phi_3\left(\frac{\mu p}{1+p}; \mu; \frac{\mu(1+\eta)(1+\kappa)(\eta-p)}{\eta(1+p)}, \frac{\kappa\mu^2(1+\eta)^2(1+\kappa)}{(1+p)^2}\right)} \end{aligned} \tag{5.27}$$

and

$$\begin{aligned} f_{\tilde{\Theta}}(\theta)_{q\to \infty} =& \frac{\Gamma(\mu)}{\Gamma\left(\frac{\mu}{1+p}\right)\Gamma\left(\frac{p\mu}{1+p}\right)} |\sin\theta|^{\frac{2\mu}{1+p}-1} |\cos\theta|^{\frac{2\mu p}{1+p}-1} \\ &\times \frac{\exp\left(\frac{\mu(1+\eta)}{\eta(1+p)}\left(2p\sqrt{\kappa(1+\kappa)}\cos\theta + (1+\kappa)(p-\eta)\sin^2\theta\right)\right)}{\left(\exp\left(\frac{4\mu p(1+\eta)}{(1+p)\eta}\sqrt{\kappa(1+\kappa)}\,|\cos\theta|\right)+1\right)} \\ &\times \frac{{}_1F_1\left(\frac{\mu p}{1+p}-\frac{1}{2}; \frac{2\mu p}{1+p}-1; \frac{4p(1+\eta)\mu}{(1+p)\eta}\sqrt{\kappa(1+\kappa)}\,|\cos\theta|\right)}{\phi_3\left(\frac{\mu}{1+p}; \mu; \frac{\mu(1+\eta)(1+\kappa)(p-\eta)}{\eta(1+p)}, \frac{\kappa\mu^2p^2(1+\eta)^2(1+\kappa)}{\eta^2(1+p)^2}\right)}. \end{aligned} \tag{5.28}$$

5.3.2 Some Plots

Among the distinct scenarios offered by the α-η-κ-μ model, those presenting cluster imbalance, dominant components and number of multipath clusters will be used as examples to confront both exact and approximate phase PDF. Obviously, the approximation here derived can be promptly used for a myriad of parameters combinations. In Figures 5.1 to 5.3, the exact (solid line) and approximate (dashed line) phase PDF are compared for different values of p, κ and μ. Note the closeness between both exact and approximate curves. In some situations, they are almost indistinct one from the other. Impressively, the approximate phase PDF has evaluated an, or even some, order(s) of magnitude faster than the exact integral solution.

5.4 Conclusion

In this Chapter, two new essential statistics concerning the α-η-κ-μ model were presented. In the first, a novel series formulation of the envelope PDF was elegantly derived in terms of acquainted and easily implementable functions, wherein no recursion is needed. With proper algebraic manipulation, this new expression renders the Extended η-μ envelope PDF, and two new envelope PDFs wherein $q \to 0$ and $q \to \infty$. In addition,

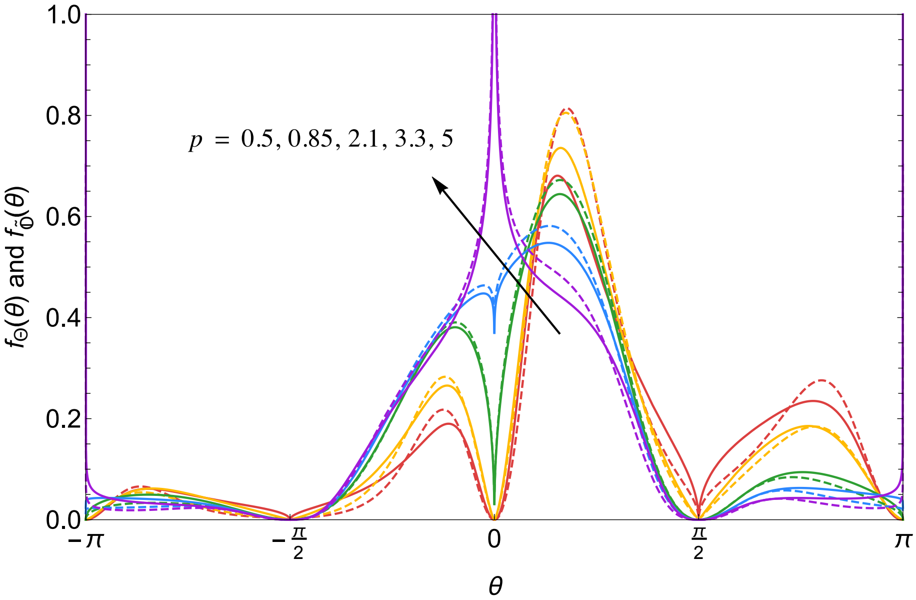

Figure 5.1: Exact (solid line) and approximate (dashed line) phase PDF for different values of p, and $\eta = 2.0$, $\kappa = 0.1$, $\mu = 2.25$ and $q = 1.6$.

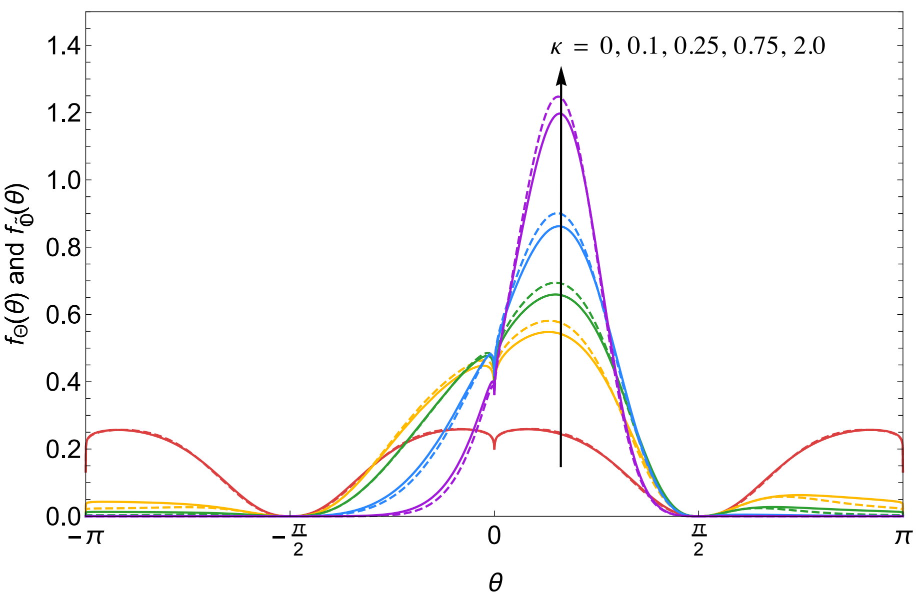

Figure 5.2: Exact (solid line) and approximate (dashed line) phase PDF for different values of κ, and $\eta = 2.0$, $\mu = 2.25$, $p = 3.3$ and $q = 1.6$.

a new mathematical identity was proposed for the sum of generalized Laguerre polynomials and regularized hypergeometric function. With the envelope PDF, an approximate formulation for the phase PDF was derived in a series representation and yields results almost indistinguishable from the intricate exact formula. Furthermore, a thorough analysis shown that the approximate solution encompass a variety of both approximate and exact distributions, which includes: (i) a new exact phase distribution with random variable $\tilde{\mathbb{O}}$; (ii) the approximate Extended κ-μ phase PDF; (iii) the approximate Extended η-μ phase

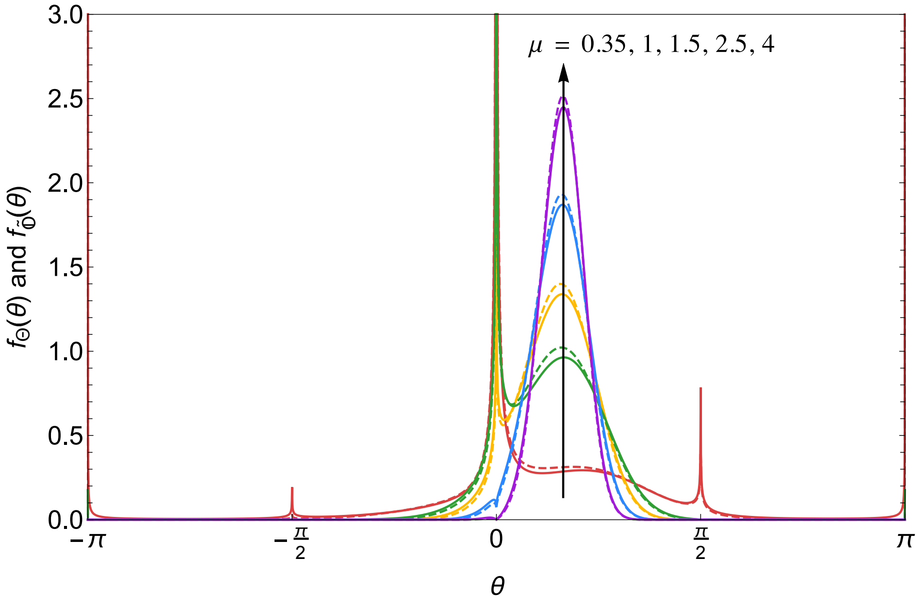

Figure 5.3: Exact (solid line) and approximate (dashed line) phase PDF for different values of μ, and $\eta = 2.0$, $\mu = 2.25$, $p = 3.3$ and $q = 1.6$.

PDF; (iv) the exact generalized Nakagami-m phase PDF; (v) the exact von Mises distribution, which approximates both Rice and Hoyt phase PDFs; and (vi) the exact phase PDF for $q \to 0$ and $q \to \infty$.

Chapter 6

Conclusions and Future Work

The main objective of this work was to only propose a new extended versions of the η-μ and κ-μ fading models. However, as the research progressed, new possibilities emerged, leading to other scenarios and very prospective work. It is empowering to realize that some of the presented work was obtained independently, which led to new outstanding results of the α-η-κ-μ fading model.

The thesis was mainly divided in four distinct chapters. Chapter 2 is a quick reference guide for interested readers about relevant fading models statistics. Chapter 3 proposed an extension to the η-μ fading model, which introduced a new parameter that quantifies the clustering imbalance between in-phase and quadrature components. Furthermore, in order to demonstrate the effects of this new parameter, a complete statistical analysis of the model was performed, which led to: (i) the exact closed-form expressions for both envelope and phase PDF and CDF; (ii) the higher order moments and the amount of fading of the envelope; (iii) the exact formulations of different joint distribution of the envelope and phase components and their respective time derivatives; (iv) the exact closed-form of the LCR, AFD and PCR; and (v) the exact MGF with diversity scheme, and applications. Chapter 4 introduced an Extended version of the κ-μ model by inserting the same imbalance parameter. This time, its effects were only limited to the phase distribution, wherein an approximate solution was also proposed. More importantly, this analytic expression corresponds to a new phase random variable $\mathbb{O}$. Moreover, higher order joint distributions and a tight approximation for the PCR was calculated. The final Chapter took advantage of the approximation method to derive a novel closed-form solution for the phase PDF of the α-η-κ-μ model and to obtain a new exact phase distribution with random variable $\tilde{\mathbb{O}}$. Such procedure was only accessible after developing a new series representation for the envelope PDF of the α-η-κ-μ distribution.

In analytic terms, future work should feature other possible distributions available through the α-η-κ-μ fading model. Also with the proposal of two new random variables, $\mathbb{O}$ and $\tilde{\mathbb{O}}$, new fading scenarios are up for further modeling. It is noteworthy that all the results presented here for the Extended η-μ and Extended κ-μ fading models can be straightforwardly applied to the α-η-μ and α-κ-μ fading models. These would then lead to the Extended α-η-μ and Extended α-κ-μ fading models. Besides, after developing such theoretical mathematical models, practical application analysis, data fitting performance and simulation methods are always interesting subjects to pursue as future works.

References

[1] M. Abramowitz and I. A. Stegun, *Handbook of Mathematical Functions: With Formulars, Graphs, and Mathematical Tables.* New York: Dover Publications, Incorporated, 1972.

[2] A. Prudnikov, *Integrals and Series: Volume 3: More Special Functions.* Gordon & Breach Science Publishers, 1990.

[3] I. S. Gradshteyn and I. M. Ryzhik, *Table of integrals, series, and products*, 7th ed. Elsevier/Academic Press, Amsterdam, 2007, translated from the Russian, Translation edited and with a preface by Alan Jeffrey and Daniel Zwillinger, With one CD-ROM (Windows, Macintosh and UNIX).

[4] "Popular internet of things forecast of 50 billion devices by 2020 is outdated," https://spectrum.ieee.org/tech-talk/telecom/internet/popular-internet-of-things-forecast-of-50-billion-devices-by-2020-is-outdated, accessed: 2018-07-04.

[5] "Ieee 5g and beyond technology roadmap white paper," https://5g.ieee.org/images/files/pdf/ieee-5g-roadmap-white-paper.pdf, accessed: 2018-07-04.

[6] M. D. Yacoub, *Foundations of Mobile Radio Engineering.* Taylor & Francis, 1993.

[7] T. S. Rappaport, *Wireless Communications: Principles and Practice*, ser. Prentice Hall Communications Engineering and Emerging Technologies Series. Dorling Kindersley, 2009.

[8] L. Rayleigh, "Xii. on the resultant of a large number of vibrations of the same pitch and of arbitrary phase," *The London, Edinburgh, and Dublin Philosophical Magazine and Journal of Science*, vol. 10, no. 60, pp. 73–78, 1880.

[9] S. O. Rice, "Mathematical analysis of random noise," *The Bell System Technical Journal*, vol. 24, no. 1, pp. 46–156, Jan 1945.

[10] R. S. Hoyt, "Probability functions for the modulus and angle of the normal complex variate," *Bell System Technical Journal*, vol. 26, no. 2, pp. 318–359, 1947.

[11] M. Nakagami, "The m-distribution – a general formula of intensity distribution of rapid fading," *Statistical Methods in Radio Wave Propagation: Proceedings of a Symposium hel June 18-20*, pp. 3–36, 1960.

[12] M. D. Yacoub, "The α-μ distribution: A physical fading model for the stacy distribution," *IEEE Transactions on Vehicular Technology*, vol. 56, no. 1, pp. 27–34, January 2007.

[13] ——, "The κ-μ; distribution and the η-μ distribution," *IEEE Antennas and Propagation Magazine*, vol. 49, no. 1, pp. 68–81, February 2007.

[14] G. Fraidenraich and M. D. Yacoub, "The α-η-μ and α-κ-μ fading distributions," in *2006 IEEE Ninth International Symposium on Spread Spectrum Techniques and Applications*, Aug 2006, pp. 16–20.

[15] M. D. Yacoub, G. Fraidenraich, and J. C. S. Santos Filho, "Nakagami-m phase-envelope joint distribution," *Electronics Letters*, vol. 41, no. 5, pp. 259–261, 2005.

[16] M. D. Yacoub, "Nakagami-m phase-envelope joint distribution: A new model," *IEEE Transactions on Vehicular Technology*, vol. 59, no. 3, pp. 1552–1557, 2010.

[17] D. B. Costa and M. D. Yacoub, "The η-μ joint phase-envelope distribution," *Antennas and Wireless Propagation Letters, IEEE*, vol. 6, pp. 195–198, 2007.

[18] U. S. Dias and M. D. Yacoub, "The κ-μ phase-envelope joint distribution," *IEEE Transactions on Communications*, vol. 58, no. 1, pp. 40–45, 2010.

[19] M. D. Yacoub, "The α-η-κ-μ fading model," *IEEE Transactions on Antennas and Propagation*, vol. 64, no. 8, pp. 3597–3610, Aug 2016.

[20] P. Beckmann, *Probability in Communication Engineering.* New York: Harcourt, Brace & World, 1967.

[21] M. K. Simon and M.-S. Alouini, *Digital communication over fading channels.* John Wiley & Sons, 2005, vol. 95.

[22] S. Tsai, "Markov characterization of the hf channel," *Communication Technology, IEEE Transactions on*, vol. 17, no. 1, pp. 24–32, 1969.

[23] J. Marcum, "A statistical theory of target detection by pulsed radar," *IRE Transactions on Information Theory*, vol. 6, no. 2, pp. 59–267, 1960.

[24] J. G. Proakis, *Digital Communications.* New York: McGraw-Hill Higher Education, 2001.

[25] S. O. Rice, "Statistical properties of a sine wave plus random noise," *Bell System Technical Journal*, vol. 27, no. 1, pp. 109–157, January 1948.

[26] D. T. Hess, "Cycle slipping in a first-order phase-locked loop," *Communication Technology, IEEE Transactions on*, vol. 16, no. 2, pp. 255–260, 1968.

[27] S. O. Rice, "Noise in fm receivers," *Time series analysis*, pp. 395–422, 1963.

[28] I. Bar-David and S. Shamai, "On the rice model of noise in fm receivers," *Information Theory, IEEE Transactions on*, vol. 34, no. 6, pp. 1406–1419, 1988.

[29] J. C. S. Santos Filho and M. D. Yacoub, "Highly accurate η-μ; approximation to the sum of m independent nonidentical hoyt variates," *IEEE Antennas and Wireless Propagation Letters*, vol. 4, pp. 436–438, 2005.

[30] L. Yang, M. O. Hasna, and I. S. Ansari, "Unified performance analysis for multiuser mixed η - μ and $\mathcal{M}$ - distribution dual-hop rf/fso systems," *IEEE Transactions on Communications*, vol. 65, no. 8, pp. 3601–3613, Aug 2017.

[31] H. Al-Hmood and H. S. Al-Raweshidy, "Unified modeling of composite *kappa-mu* /gamma, *eta-mu*/gamma, and *alpha-mu*/gamma fading channels using a mixture gamma distribution with applications to energy detection," *IEEE Antennas and Wireless Propagation Letters*, vol. 16, pp. 104–108, 2017.

[32] J. Yang, L. Chen, X. Lei, K. P. Peppas, and T. Q. Duong, "Dual-hop cognitive amplify-and-forward relaying networks over $\eta - \mu$ fading channels," *IEEE Transactions on Vehicular Technology*, vol. 65, no. 8, pp. 6290–6300, Aug 2016.

[33] O. S. Badarneh and R. Mesleh, "Cooperative dual-hop wireless communication systems with beamforming over η-μ fading channels," *IEEE Transactions on Vehicular Technology*, vol. 65, no. 1, pp. 37–46, Jan 2016.

[34] J. P. P. na Martín, J. M. Romero-Jerez, and C. Tellez-Labao, "Performance of selection combining diversity in $\eta-\mu$ fading channels with integer values of μ," *IEEE Transactions on Vehicular Technology*, vol. 64, no. 2, pp. 834–839, Feb 2015.

[35] R. Mesleh, O. S. Badarneh, A. Younis, and H. Haas, "Performance analysis of spatial modulation and space-shift keying with imperfect channel estimation over generalized $eta-mu$ fading channels," *IEEE Transactions on Vehicular Technology*, vol. 64, no. 1, pp. 88–96, Jan 2015.

[36] C. B. Issaid, M. S. Alouini, and R. Tempone, "On the fast and precise evaluation of the outage probability of diversity receivers over α-μ , κ-μ, and η-μ fading channels," *IEEE Transactions on Wireless Communications*, vol. 17, no. 2, pp. 1255–1268, Feb 2018.

[37] N. Bhargav, C. R. N. da Silva, Y. J. Chun, S. L. Cotton, and M. D. Yacoub, "Co-channel interference and background noise in κ-μ fading channels," *IEEE Communications Letters*, vol. 21, no. 5, pp. 1215–1218, May 2017.

[38] N. Bhargav, S. L. Cotton, and D. B. Smith, "An experimental-based analysis of inter-ban co-channel interference using the κ - μ fading model," *IEEE Transactions on Antennas and Propagation*, vol. 65, no. 2, pp. 983–988, Feb 2017.

[39] J. Zhang, X. Chen, K. P. Peppas, X. Li, and Y. Liu, "On high-order capacity statistics of spectrum aggregation systems over κ-μ and κ-μ shadowed fading channels," *IEEE Transactions on Communications*, vol. 65, no. 2, pp. 935–944, Feb 2017.

[40] P. Kumar and P. R. Sahu, "Analysis of m-psk with mrc receiver over κ-μ fading channels with outdated csi," *IEEE Wireless Communications Letters*, vol. 3, no. 6, pp. 557–560, Dec 2014.

[41] P. C. Sofotasios, E. Rebeiz, L. Zhang, T. A. Tsiftsis, D. Cabric, and S. Freear, "Energy detection based spectrum sensing over κ-μ and κ-μ extreme fading channels," *IEEE Transactions on Vehicular Technology*, vol. 62, no. 3, pp. 1031–1040, March 2013.

[42] A. A. dos Anjos, T. R. R. Marins, R. A. A. de Souza, and M. D. Yacoub, "Higher order statistics for the α-η-κ-μ fading model," *IEEE Transactions on Antennas and Propagation*, pp. 1–1, 2018.

[43] X. Li, X. Chen, J. Zhang, Y. Liang, and Y. Liu, "Capacity analysis of α - η - κ - μ fading channels," *IEEE Communications Letters*, vol. 21, no. 6, pp. 1449–1452, June 2017.

[44] V. M. Rennó, R. A. A. de Souza, and M. D. Yacoub, "On the generation of α-η-κ-μ samples with applications," in *2017 IEEE 28th Annual International Symposium on Personal, Indoor, and Mobile Radio Communications (PIMRC)*, Oct 2017, pp. 1–5.

[45] I. B. G. Pôrto and M. D. Yacoub, "On the phase statistics of the κ-μ process," *IEEE Transactions on Wireless Communications*, vol. 15, no. 7, pp. 4732–4744, July 2016.

[46] N. Youssef, C.-X. Wang, and M. Patzold, "A study on the second order statistics of nakagami-hoyt mobile fading channels," *IEEE Transactions on Vehicular Technology*, vol. 54, no. 4, pp. 1259–1265, July 2005.

[47] N. Youssef, W. Elbahri, M. Patzold, and S. Elasmi, "On the crossing statistics of phase processes and random fm noise in nakagami-q mobile fading channels," *Wireless Communications, IEEE Transactions on*, vol. 4, no. 1, pp. 24–29, 2005.

[48] B. Chytil, "The distribution of amplitude scintillation and the conversion of scintillation indices," *Journal of Atmospheric and Terrestrial Physics*, vol. 29, no. 9, pp. 1175–1177, 1967.

[49] K. Bischoff and B. Chytil, "A note on scintillation indices," *Planetary and Space Science*, vol. 17, no. 5, pp. 1059–1066, 1969.

[50] M. K. Simon and M.-S. Alouini, "A unified approach to the performance analysis of digital communication over generalized fading channels," *Proceedings of the IEEE*, vol. 86, no. 9, pp. 1860–1877, 1998.

[51] A. Mehrnia and H. Hashemi, "Mobile satellite propagation channel. part ii-a new model and its performance," in *Vehicular Technology Conference, 1999. VTC 1999-Fall. IEEE VTS 50th*, vol. 5. IEEE, 1999, pp. 2780–2784.

[52] C.-X. Wang, N. Youssef, and M. Patzold, “Level-crossing rate and average duration of fades of deterministic simulation models for nakagami-hoyt fading channels,” in *Wireless Personal Multimedia Communications, 2002. The 5th International Symposium on*, vol. 1. IEEE, 2002, pp. 272–276.

[53] K. T. Hemachandra and N. C. Beaulieu, “Simple expressions for the ser of dual mrc in correlated nakagami-q (hoyt) fading,” *Communications Letters, IEEE*, vol. 14, no. 8, pp. 743–745, 2010.

[54] N. Hajri, N. Youssef, T. Kawabata, M. Pätzold, and W. Dahech, “Statistical properties of double hoyt fading with applications to the performance analysis of wireless communication systems,” *IEEE Access*, vol. 6, pp. 19 597–19 609, 2018.

[55] M. D. Yacoub, J. E. V. Bautista, and L. G. R. Guedes, “On higher order statistics of the nakagami-m distribution,” *Vehicular Technology, IEEE Transactions on*, vol. 48, no. 3, pp. 790–794, 1999.

[56] M. D. Yacoub, “Nakagami-m phase-envelope joint distribution: A new model,” *IEEE Transactions on Vehicular Technology*, vol. 59, no. 3, pp. 1552–1557, 2010.

[57] D. B. Costa, J. C. S. S. Filho, M. D. Yacoub, and G. Fraidenraich, “Second-order statistics of η-μ fading channels: Theory and applications,” *Wireless Communications, IEEE Transactions on*, vol. 7, no. 3, pp. 819–824, 2008.

[58] G. R. L. Tejerina and M. D. Yacoub, “Distribuição conjunta de fase-envoltória η-μ: uma nova abordagem,” in *XXXI Simpósio Brasileiro de Telecomunicações, (SBrT2013)*, vol. 1, Sept 2013, pp. 1–5.

[59] ——, “Efeito do desbalanceamento de clusters no modelo η-μ,” in *XXXIII Simpósio Brasileiro de Telecomunicações, (SBrT2015)*, vol. 1, Sept 2015, pp. 1–5.

[60] S. L. Cotton and W. G. Scanlon, “Higher-order statistics for κ-μ distribution,” *Electronics Letters*, vol. 43, no. 22, Oct 2007.

[61] A. Prudnikov, *Integrals and Series: Volume 1: Elementary Functions.* Gordon & Breach Science Publishers, 1986.

[62] I. B. G. Porto, M. D. Yacoub, J. C. S. S. Filho, S. L. Cotton, and W. G. Scanlon, "Nakagami-m phase model: Further results and validation," *IEEE Wireless Communications Letters*, vol. 2, no. 5, pp. 523–526, October 2013.

[63] C. R. N. da Silva, "On the statistics of the product and the ratio of fading envelopes taken from α-μ, η-μ and κ-μ distributions," Ph.D. dissertation, State University of Campinas, 2018.

[64] E. W. Weisstein, "Pochhamer symbol. From MathWorld—A Wolfram Web Resource," http://mathworld.wolfram.com/PochhammerSymbol.html, accessed: 2018-06-30.

[65] ——, "von mises distribution. From MathWorld—A Wolfram Web Resource," http://mathworld.wolfram.com/PochhammerSymbol.html, accessed: 2018-06-30.